

2015

Dispersant Effects on Zinc Dialkyldithiophosphate (ZDDP) Tribofilm Structure and Composition

Makaye Tabibi
tabibim@gmail.com

Follow this and additional works at: <http://scholarscompass.vcu.edu/etd>

 Part of the [Physical Chemistry Commons](#)

© The Author

Downloaded from

<http://scholarscompass.vcu.edu/etd/4059>

This Thesis is brought to you for free and open access by the Graduate School at VCU Scholars Compass. It has been accepted for inclusion in Theses and Dissertations by an authorized administrator of VCU Scholars Compass. For more information, please contact libcompass@vcu.edu.

©Makaye Tabibi _____ 2015

All Rights Reserved

DISPERSANT EFFECTS ON ZINC DIALKYLDITHIOPHOSPHATE (ZDDP)
TRIBOFILM STRUCTURE AND COMPOSITION

A thesis submitted in partial fulfillment of the requirements for the degree of Master of Science
at Virginia Commonwealth University.

by

Makaye Tabibi

Bachelor of Science in Chemistry, Virginia Commonwealth University, 2008

Director: Dr. B. Frank Gupton

Research Professor and Chair, Department of Chemical and Life Science Engineering

Virginia Commonwealth University

Richmond, Virginia

December 2015

Acknowledgement

My BIGGEST thanks go to my advisors, Dr. B. Frank Gupton at VCU and Dr. Mark T. Devlin at Afton Chemical Corporation. This would not have been possible without their constant guidance, support, and positivity. I thank them for their motivation, inspiration, and continuous support.

I would like to thank Afton Chemical Corporation for funding this project. I would also like to thank my committee members Dr. M. Samy El-Shall, Dr. Hani El-Kaderi, Dr. Everett Carpenter, Dr. Nastassja Lewinski, and Dr. Katherine Belecki for their help and support along the way. Many thanks to my colleagues who have been a part of this project – Dr. Jeffery Guevremont, Ken Garelick, Grant Pollard, and Jeff Soden. I would also like to thank all my fellow group members for their help over the years!

A special thanks to my mentor of all trades, Dr. William J. Colucci, for his ongoing teachings and support. Another special thanks to Dr. Chelsea Coffey and Dr. Charles Shanahan, who both helped me along many steps of the way. I thank all of my family and friends for their support and motivation.

Most importantly, my greatest appreciation goes to my father, Dr. Bagher M. Tabibi. I thank him for constantly pushing me to my full potential. His passion for Physics and accomplishments in life have been the biggest inspiration of all.

Table of Contents

Acknowledgement	ii
List of Tables	v
List of Figures	vi
List of Schemes	xii
List of Abbreviations	xiii
Abstract	xiv
Chapter 1 - Introduction	1
1.1 Background	2
1.2 Tribology in the Engine	5
1.3 Lubricant Additives	7
1.4 Zinc Dialkyldithiophosphate (ZDDP).....	9
1.4 Dispersants	12
Chapter 2 – Project Rationale	14
Chapter 3 – Dispersant Effects on ZDDP Tribofilms	17
3.1 Method Development.....	18
3.1.1 ZDDP Tribofilm Formation	18
3.1.2 ZDDP Tribofilm Analysis.....	23
3.2 Dispersant Effects on ZDDP Tribofilms.....	27
3.2.1 Dispersant Chemistries	27
3.2.2 Dispersant A.....	29
3.2.3 Effects of Dispersant A Structure	34
3.2.4 Dispersant B	38
3.2.5 Dispersant C	43
3.2.6 Dispersant D.....	48
3.2.7 Dispersant E	53
3.2.8 Summary of Dispersant Effects on ZDDP Tribofilms	58
3.3 Dispersant Precursor Effects on ZDDP Tribofilms	64
3.3.1 PIB	64

3.3.2 PIBSA	66
3.3.3 PIB Di-acid	70
3.4 Dispersant Effects on Tribofilm Removal	71
3.5 Discussion of Results.....	73
3.5.1 Surface and Bulk Fluid Interactions.....	75
Chapter 4 - Conclusion.....	84
Chapter 5 – Experimental.....	90
5.1 Sample Preparation	91
5.2 Instrumentation	91
5.2.1 Mini Traction Machine with Spacer Layer Image Mapping (MTM-SLIM).....	91
5.2.2 Scanning Electron Microscopy – Energy Dispersive X-ray – SEM-EDX.....	92
5.2.3 Quartz Crystal Microbalance with Dissipation (QCM-D)	92
5.2.4 ³¹ Phosphorus Nuclear Magnetic Resonance Spectroscopy (³¹ P-NMR)	93
5.2.5 Fourier Transform Infrared (FTIR) Spectroscopy (FTIR)	93
References	95
Appendices.....	99

List of Tables

Table 1 - 1 Global fuel economy standards up to 2025, normalized to the CAFE MPG.	4
Table 3 - 1 Elemental composition of ZDDP tribofilms from SEM-EDX spectra including normalized values.	25
Table 3 - 2 Dispersant chemistries selected for evaluation of their effects on ZDDP tribofilms.	29
Table 3 - 3 Samples of ZDDP with varying PIBSA concentrations in isooctane for QCM-D evaluation.	79

List of Figures

Figure 1 - 1 Minimum MPG required by CAFE standards for passenger cars since 1978.	3
Figure 1 - 2 The regimes of friction, boundary, mixed, and hydrodynamic, represented by the Stribeck Curve	6
Figure 1 - 3 The thickness of the separating lubricant layer during different friction regimes	7
Figure 1 - 4 Generic lubricant additive package formulation.	9
Figure 1 - 5 Zinc dialkyldithiophosphate (ZDDP) structure.....	10
Figure 1 - 6 Dispersant's role in engine oil additive packs.....	12
Figure 3 - 1 MTM-SLIM test set up and spacer layer imaging technique.....	19
Figure 3 - 2 MTM-SLIM interference imaging (A) is converted to a colored thickness image (B), which is then plotted as a thickness distribution (C).	20
Figure 3 - 3 MTM-SLIM analysis of ZDDP tribofilm growth over a one hour period with interference images that were used to convert to thickness.....	21
Figure 3 - 4 Average roughness of ZDDP tribofilm throughout film formation process over one hour.	22
Figure 3 - 5 The coefficient of friction of ZDDP tribofilms forming over one hour.....	23
Figure 3 - 6 SEM-EDX images and spectra for two ZDDP tribofilm runs.	24
Figure 3 - 7 Elemental analysis of ZDDP tribofilms and reproducibility.....	26

Figure 3 - 8 Dispersant A structure and polymerization upon aging.....	30
Figure 3 - 9 Concentration dependence of Dispersant A on ZDDP tribofilm growth in the MTM-SLIM over one hour.....	31
Figure 3 - 10 End-of-test images of ZDDP tribofilms formed in presence of Dispersant A.....	31
Figure 3 - 11 Concentration dependence of Dispersant A on ZDDP tribofilm roughness.....	32
Figure 3 - 12 Concentration dependence of Dispersant A on friction throughout tribofilm growth.....	33
Figure 3 - 13 (A) Phosphorus to sulfur ratios of ZDDP tribofilms formed with varying concentrations of Dispersant A. (B) Zinc to phosphorus ratios of ZDDP tribofilms formed with varying concentrations of Dispersant A.....	34
Figure 3 - 14 Dispersant A structure effects on ZDDP tribofilm growth in the MTM-SLIM over one hour.....	35
Figure 3 - 15 Dispersant A structure effects on ZDDP tribofilm roughness.....	36
Figure 3 - 16 Dispersant A structure effects on friction during ZDDP tribofilm growth.....	37
Figure 3 - 17 Dispersant B structures of mixed mono-succinimide and bis-succinimide.....	38
Figure 3 - 18 Concentration dependence of Dispersant B on ZDDP tribofilm growth in the MTM-SLIM over one hour.....	39
Figure 3 - 19 End-of-test interference image of ZDDP tribofilms formed in presence of Dispersant B.....	39

Figure 3 - 20 Concentration dependence of Dispersant B on ZDDP tribofilm roughness.	40
Figure 3 - 21 Concentration dependence of Dispersant B on friction throughout tribofilm growth.	41
Figure 3 - 22 (A) Phosphorus to sulfur ratios of ZDDP tribofilms formed with varying concentrations of Dispersant B. (B) Zinc to phosphorus ratios of ZDDP tribofilms formed with varying concentrations of Dispersant B.	42
Figure 3 - 23 Dispersant C bis-succinimide structure.....	43
Figure 3 - 24 Concentration dependence of Dispersant C on ZDDP tribofilm growth in the MTM-SLIM over one hour.....	44
Figure 3 - 25 End-of-test images of ZDDP tribofilms formed with Dispersant C present.	44
Figure 3 - 26 Concentration dependence of Dispersant C on ZDDP tribofilm roughness.	45
Figure 3 - 27 Concentration dependence of Dispersant C on friction throughout tribofilm growth.	46
Figure 3 - 28 (A) Phosphorus to sulfur ratios of ZDDP tribofilms formed with varying concentrations of Dispersant C. (B) Zinc to phosphorus ratios of ZDDP tribofilms formed with varying concentrations of Dispersant C.	47
Figure 3 - 29 Dispersant D structure.....	48
Figure 3 - 30 Concentration dependence of Dispersant D on ZDDP tribofilm growth in the MTM-SLIM over one hour.....	49
Figure 3 - 31 End-of-test images of ZDDP tribofilms formed in presence of Dispersant D.	49

Figure 3 - 32 Concentration dependence of Dispersant D on ZDDP tribofilm roughness.	50
Figure 3 - 33 Concentration dependence of Dispersant D on friction throughout tribofilm growth.	51
Figure 3 - 34 (A) Phosphorus to sulfur ratios of ZDDP tribofilms formed with varying concentrations of Dispersant D. (B) Zinc to phosphorus ratios of ZDDP tribofilms formed with varying concentrations of Dispersant D.....	52
Figure 3 - 35 Dispersant E structure.	53
Figure 3 - 36 Concentration dependence of Dispersant E on ZDDP tribofilm growth in the MTM-SLIM over one hour.....	54
Figure 3 - 37 End-of-test images of ZDDP tribofilms formed in presence of Dispersant E.	54
Figure 3 - 38 Concentration dependence of Dispersant E on ZDDP tribofilm roughness.	55
Figure 3 - 39 Concentration dependence of Dispersant E on friction throughout tribofilm growth.	56
Figure 3 - 40 (A) Phosphorus to sulfur ratios of ZDDP tribofilms formed with varying concentrations of Dispersant E. (B) Zinc to phosphorus ratios of ZDDP tribofilms formed with varying concentrations of Dispersant E.	57
Figure 3 - 41 Dispersant effect on ZDDP tribofilm growth at a 1:1 ratio of ZDDP and dispersant.	58
Figure 3 - 42 Dispersant effect on ZDDP tribofilm growth at a 1:0.5 ratio of ZDDP and dispersant.	59
Figure 3 - 43 Dispersant effect on friction during ZDDP tribofilm growth at a 1:0.5 ratio of ZDDP and dispersant.	60

Figure 3 - 44 SEM-EDX phosphorus and sulfur analysis of ZDDP tribofilms formed in presence of dispersants.	61
Figure 3 - 45 SEM-EDX zinc and phosphorus analysis of ZDDP tribofilms formed in presence of dispersant	62
Figure 3 - 46 Phosphorus to sulfur ratio in relation to PIBSA to amine ratio in dispersant.	63
Figure 3 - 47 Concentration dependence of PIB on ZDDP tribofilm growth in the MTM-SLIM over one hour.	65
Figure 3 - 48 Concentration dependence of PIB on friction throughout tribofilm growth.	66
Figure 3 - 49 Concentration dependence of PIBSA on ZDDP tribofilm growth in the MTM-SLIM over one hour.	67
Figure 3 - 50 End-of-test images of ZDDP tribofilms formed in presence of varying concentrations of PIBSA.	67
Figure 3 - 51 Concentration dependence of PIBSA on friction throughout tribofilm growth.	68
Figure 3 - 52 SEM-EDX phosphorus to sulfur and zinc to phosphorus ratios for ZDDP films formed with varying concentrations of PIBSA.	69
Figure 3 - 53 Conversion of PIBSA to di-acid form.	70
Figure 3 - 54 Concentration dependence of PIB di-acid on ZDDP tribofilm growth in the MTM-SLIM over one hour.	71
Figure 3 - 55 ZDDP tribofilm removal by dispersants after one hour of rubbing time.	72

Figure 3 - 56 SEM-EDX analysis of ZDDP tribofilms after removal by dispersants.	73
Figure 3 - 57 QCM-D evaluation of 1.00 wt.% ZDDP in isooctane.	77
Figure 3 - 58 QCM-D evaluation of 1.00 wt.% PIBSA in isooctane.....	78
Figure 3 - 59 QCM-D evaluation of samples with ZDDP and varying concentrations of PIBSA.	79
Figure 3 - 60 QCM-D frequency change of varying concentrations of PIBSA and ZDDP after initial adsorption.	80
Figure 3 - 61 ³¹ P-NMR spectrum of ZDDP.	82

List of Schemes

Scheme 3 - 1 Generic PIBSI dispersant synthesis.	28
---	----

List of Abbreviations

³¹P-NMR	Phosphorus-31 Nuclear Magnetic Resonance
AFM	Atomic Force Microscopy
CAFE	Corporate Average Fuel Economy
FTIR	Fourier Transform Infrared
HATR	Horizontal Attenuated Total Reflectance
IFM	Interfacial Force Microscopy
MPG	Miles Per Gallon
MTM-SLIM	Mini Traction Machine with Spacer Layer Image Mapping
PEHA	Pentaethylenehexamine
PIB	Polyisobutylene
PIBSA	Polyisobutylene Succinic Anhydride
PIBSI	Polyisobutenyl Succinimide
QCM-D	Quartz Crystal Microbalance with Dissipation
SEM-EDX	Scanning Electron Microscopy – Energy Dispersive X-ray
TEPA	Tetraethylenepentamine
US DOE	United States Department of Energy
XANES	X-ray absorption near-edge spectroscopy
ZDDP	Zinc Dialkyldithiophosphate

Abstract

DISPERSANT EFFECTS ON ZINC DIALKYLDITHIOPHOSPHATE (ZDDP) TRIBOFILM STRUCTURE AND COMPOSITION

By Makaye Tabibi

A thesis submitted in partial fulfillment of the requirements for the degree of Master of Science at Virginia Commonwealth University.

Virginia Commonwealth University, 2015

Director: Dr. B. Frank Gupton

Department of Chemistry

For decades, global regulations and government mandates have driven technological developments to improve vehicle fuel economy. Tribological components found in all automotive engines contain metal-on-metal contact zones that may result in increased friction and wear, reducing overall engine efficiency. Lubricant additives such as antiwear and friction modifying components are added to motor oils to prevent some of the damages that may occur at contact zones and improve friction. The effects of other additive components, such as dispersants, that are prevalent in a lubricant additive package on the anti-wear layer remain relatively unknown. Polyisobutenyl Succinimide (PIBSI) dispersants were evaluated for their interactions with the ZDDP antiwear component. The physical and chemical properties and friction of the tribofilms formed in presence of dispersants were defined revealing a previously unknown structure-activity relationship. Further analysis of ZDDP and dispersants revealed surface and bulk fluid interactions.

Chapter 1 - Introduction

1.1 Background

In 2014, the United States Department of Energy (U.S. DOE) invested over \$55 million in research that advances the development of new vehicle technologies to improve fuel consumption.¹ Prior to the US government's investment, in 1999 the U.S. DOE held a workshop focusing on reducing friction and wear in vehicles. As a result of this workshop, it was estimated an astonishing \$120 billion a year could be saved by reducing friction and wear in automotive engines.² Automotive engine tribology, the study of wear, friction, and lubrication, has been at the forefront of a global shift towards reducing fuel consumption and emissions by improving engine efficiency.³

The investment by the United States government follows decades of global emphasis on increasing fuel economy in vehicles. The United States introduced the Corporate Average Fuel Economy (CAFE) program in 1975 to improve fuel efficiency in vehicles in an effort to reduce dependence on foreign oil. Since then, the mission of the program has shifted to reducing fuel consumption in vehicles in order to protect natural resources, and emissions control for environmental purposes.⁴ Each year, the CAFE rules have become more stringent and span over a wider range of vehicles.

The CAFE program sets a fuel economy standard for passenger cars and light trucks, domestic and imported, in an average Miles Per Gallon (MPG) for each vehicle model year. The standard began with a minimum fuel economy requirement of 20 MPG and slowly increased to almost 30 MPG by 1990, where it remained constant for two decades. With the global shift towards improving fuel efficiency in vehicles, the CAFE standard began to rapidly rise in 2011.

The CAFE standards for passenger cars since program inception are displayed in Figure 1 - 1, with the proposed standard of 56.2 MPG by 2025 represented in red.^{5,6,7}

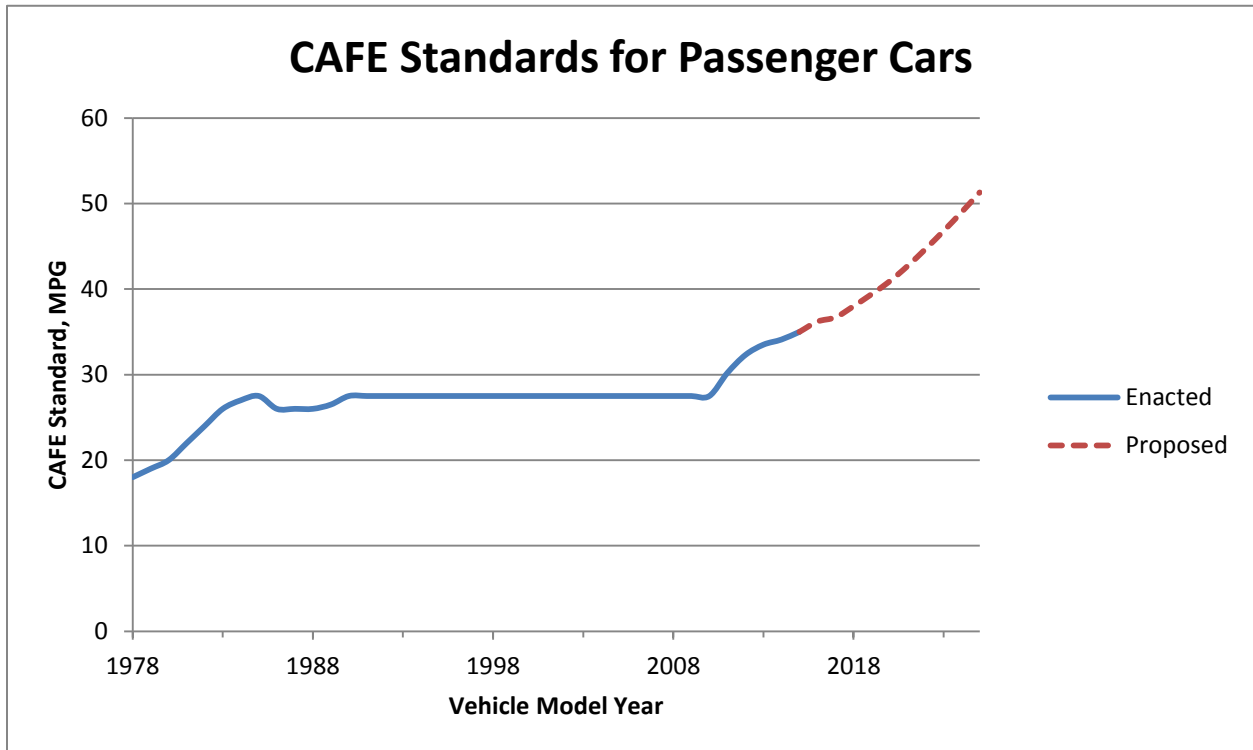


Figure 1 - 1 Minimum MPG required by CAFE standards for passenger cars since 1978.

Failure to meet the CAFE standard has resulted in millions of dollars in fines for automakers. Manufacturers are required to report their fleet average for each model year for passenger cars and light trucks. A \$55 penalty is charged for every 1 MPG that is under the minimum CAFE standard, for every vehicle for the given model year.⁶ Mercedes-Benz and BMW have each paid over \$200 million in CAFE fines to date since beginning of the program.⁸ While the CAFE standard only regulates fuel economy for vehicles driven in the United States, it has triggered a global effort in reducing fuel consumption in other countries. Similarly to the proposed 56.2 MPG by 2025 in the United States, many other countries have proposed efforts to

reach 40 MPG to 50 MPG in the next decade, shown in Table 1 - 1.⁹ With the increasing global interest towards improved fuel economy and less emissions, the automotive industry has shifted towards highly fuel efficient vehicles while the lubricant industry has been developing energy efficient fuels and motor oils.

Table 1 - 1 Global fuel economy standards up to 2025, normalized to the CAFE MPG.

Location	Year	Average MPG
US	2025	56.2
Canada	2025	56.2
EU	2021	56.9
Japan	2020	45.9
China	2020	47.7
South Korea	2020	56.7
India	2021	49.4
Mexico	2016	39.3
Brazil	2017	40.9

In the last 15 years, many research groups dedicated to studying automotive tribology have highlighted the areas in an engine that consume the most energy. Holmberg et. al. completed an in-depth analysis on the total energy loss in an engine and defined areas that result in the most inefficiencies. They calculated that 33% of total fuel energy loss in passenger cars is a result of overcoming friction. To emphasize the magnitude of this amount, they estimated 208 million liters of gasoline and diesel fuel were used worldwide to overcome friction in passenger cars in 2009. Studies have shown that reducing friction in tribological components in an engine by low friction coatings and modifying surface topography has resulted in a 25-30% reduction of

energy loss. Furthermore, studies have shown advanced lubrication systems have resulted in up to 50% improved friction.¹⁰

1.2 Tribology in the Engine

The reciprocating engine is the most common engine design used in the automotive industry today, for both gasoline and diesel powered engines. The engine is powered by one or more pistons reciprocating inside a cylinder and constantly converts fuel into energy at extreme pressures and temperatures. Although this engine design has run faultlessly for decades, the increased attention on energy loss has underscored the inefficiencies of the engine. Several conditions inside the engine such as high speeds and loads impacting all the metal parts can result into increased friction and wear on the parts due to the metal-on-metal contact.² Understanding the impacts of the tribological components in the engine has been leading the research on improving engine efficiency without changing the design of the engine.

Friction arises any time two surfaces are in moving contact with one another. The viscosity of the lubricant and speeds and loads between the moving metal surfaces are factors that result in energy loss due to friction in an automotive engine. Friction is represented by the Stribeck curve, Figure 1 - 2, and is measured by a coefficient of friction, μ . Friction is classified into three regimes; boundary, mixed, and hydrodynamic lubrication regimes. The three regimes are separated by their film thickness ratio called the Sommerfeld number, λ , which is represented by (viscosity x speed) / load. The highest friction occurs in the boundary regime, where the lubricant layer is the thinnest at low speeds and high loads, and the two surfaces may have direct metal on metal contact with one another. As the thickness of the lubricant layer between two surfaces increases, friction is reduced in the hydrodynamic regime, represented by

high speeds and low loads. The movement of different parts in the engine, such as the piston rings, engine bearings, and valve train can all be classified into the different regimes of friction in order to quantify energy loss due to friction in the engine, and improve it with new technologies added to the lubricant.^{2,10,11,12}

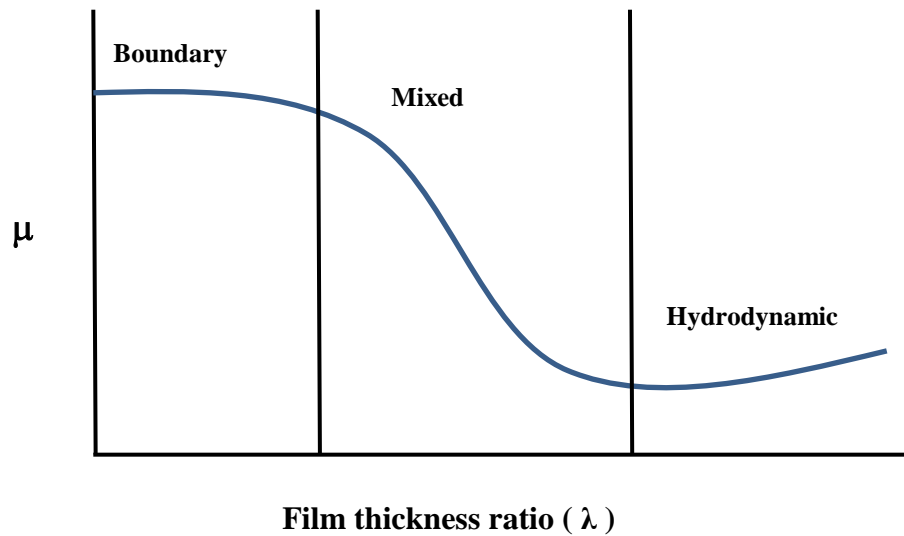


Figure 1 - 2 The regimes of friction, boundary, mixed, and hydrodynamic, represented by the Stribeck Curve

The metal surfaces in an engine may visually appear to be smooth, but at the microscopic level they are rough surfaces with imperfections called asperities. The regimes of friction in relation to the thickness of the separating lubricating layer are shown in Figure 1 - 3. The lubricating layer may be thick enough to separate the surfaces, but not thick enough to separate all the asperities between the two surfaces, resulting in a higher load at the contact areas and an increased potential for wear and friction in this regime. In order to help improve friction and

prevent wear between all the surfaces in contact under the high stresses of an engine, lubricant additives are added to engine oils to prevent damage and improve performance of the engine.^{3,13}

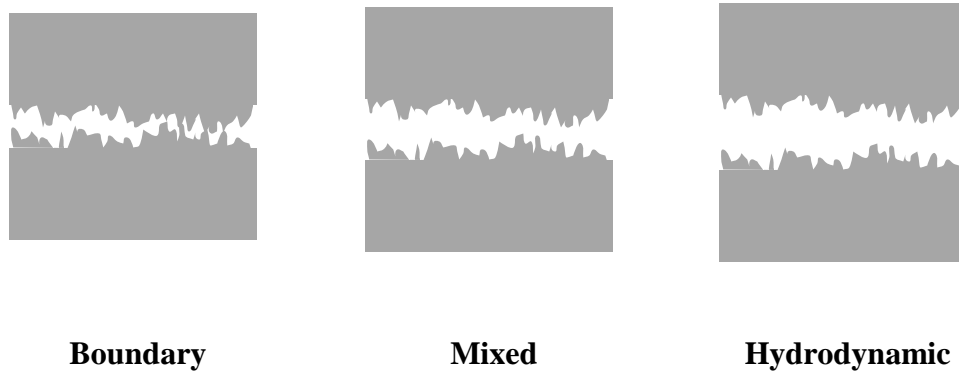


Figure 1 - 3 The thickness of the separating lubricant layer during different friction regimes

1.3 Lubricant Additives

The use of petroleum lubricants as the main source of lubrication in an engine dates back to the 1920s when crude oil distillation was becoming more prominent creating different classes of base oils. Base oils are mixtures of paraffinic or naphthenic hydrocarbons, including some aromatics. It was quickly recognized that base oils without additives could not withstand the extreme conditions in a reciprocating engine. At high temperatures and pressures the hydrocarbon species of the base oil oxidize and degrade, creating unwanted byproducts in the oil that result in a loss of engine functionality and in extreme cases, engine failure.^{14,15} The lubricant additives industry was created to develop additives that prevented harm in the engine as well as improved engine performance.

The core classes of lubricant additives that are used today were mostly identified in the 1930s and were adopted as a mainstay in motor oil technology. Lubricant additives were designed for functions including preventing degradation of the oil, protecting the metal surfaces from wear, improving friction, and keeping the engine clean. Over the past 80 years of lubricant additive development, research within the core classes of lubricant additives continues with new technologies to meet global regulations, such as the current focus on fuel economy.¹⁶

A lubricant additive package is composed of several components with various functions that are designed to perform independently or synergistically with other additive package components. The components are combined into the additive package that is blended into a base oil resulting in an engine oil designed to deliver optimum performance. An example of the types of additives that compose an engine oil additive package at their respective concentrations is shown in Figure 1 - 4. Most engine oil additive packages today contain the components shown below, but are not limited to these additive classes.

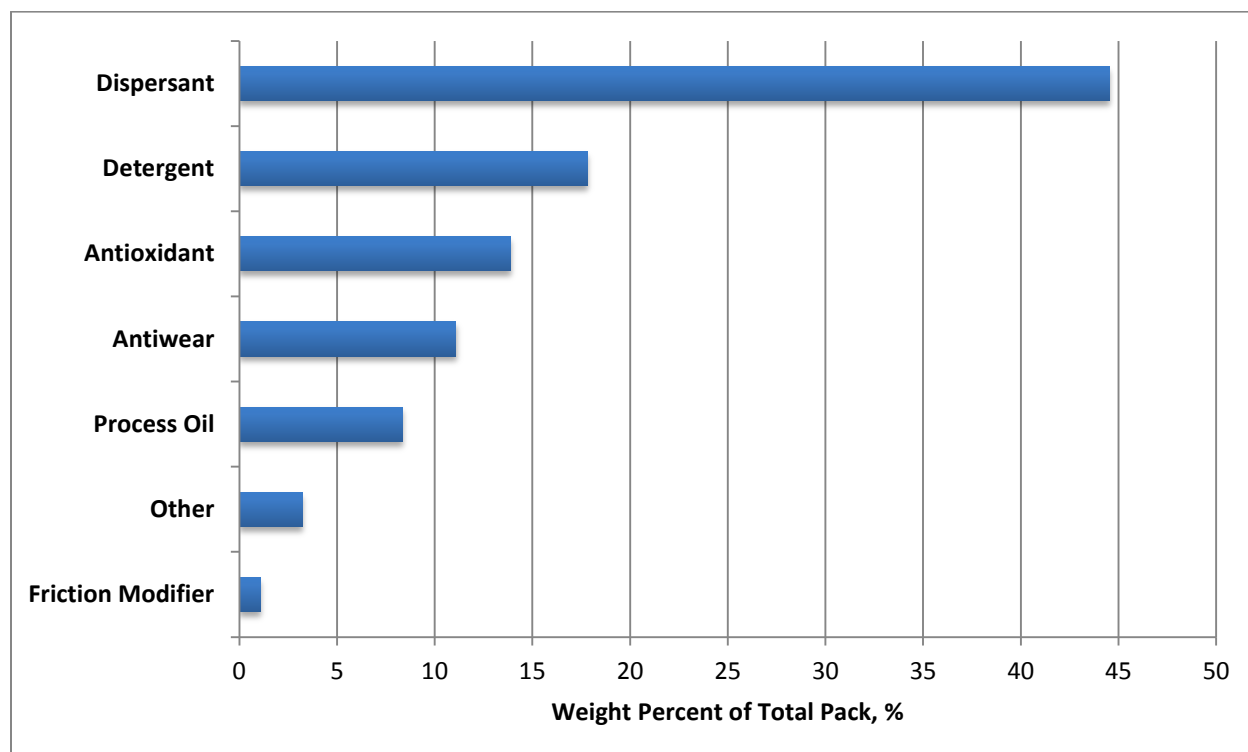


Figure 1 - 4 Generic lubricant additive package formulation.

1.4 Zinc Dialkyldithiophosphate (ZDDP)

One of the main classes of lubricant additives are anti-wear additives, which have been added to engine oils for decades in order to prevent wear on the metal surfaces in an engine. Anti-wear additives work by forming a chemical film on metal surfaces that protects the surface from damage upon sliding contact with another surface. The most common and most effective anti-wear additive used in the automotive industry is zinc dialkyldithiophosphate (ZDDP), Figure 1 - 5. ZDDP was first introduced to the additive industry as an anti-corrosion and antioxidant additive, with its anti-wear properties discovered shortly after.¹⁶ Although ZDDP was adopted as the best anti-wear additive, the complexity of the molecule resulted in decades of research in order to uncover its mechanism of action and properties of the protective film.^{17,18,19}

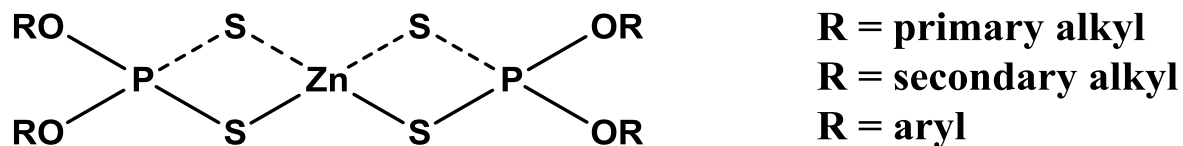


Figure 1 - 5 Zinc dialkyldithiophosphate (ZDDP) structure.

Early studies revealed that ZDDP formed resilient protective chemical films over 100 nm thick on rubbed surfaces called tribofilms. These films did not form on unrubbed surfaces, indicating contact between two surfaces is necessary for ZDDP to form a tribofilm. ^{32}P and ^{35}S radiotracing techniques uncovered that the ratio of P:S shifted from 1:2 in the ZDDP molecule, to 8:1 in the anti-wear film. This discovery showed that the ZDDP structure was different as it formed a protective film on surfaces.¹⁶ After the basic understanding of ZDDP tribofilms was determined, the discovery of new analytical techniques revealed in-depth information on ZDDP tribofilm structure and composition.

Fuller et. al. discovered that even without rubbing, ZDDP forms a thermal film on a surface at temperatures up to 100°C. They studied the differences in film composition between the thermal film and tribofilm by using X-ray absorption near-edge spectroscopy (XANES), which revealed the thermal film composition was similar to the ZDDP structure, whereas tribofilms resembled short chain poly-phosphates. The difference in structure of the two types of films confirmed the ZDDP molecule undergoes degradation to form anti-wear films.²⁰ Topological and mechanical information of the tribofilms became available by the use of atomic force microscopy (AFM) and interfacial force microscopy (IFM).²¹ Other techniques that gave

elemental composition and bonding information of the films were scanning electron microscopy – energy dispersive X-ray (SEM-EDX) and XANES.^{21,22}

More significant advancements in ZDDP research occurred in the early 2000s after the development of the Mini Traction Machine with Spacer Layer Image Mapping (MTM-SLIM).^{23,24} The MTM-SLIM was the first tool with the ability to form ZDDP tribofilms and study the growth of the film and other film properties *in-situ*. The tool overcame many limitations in studying ZDDP anti-wear films by incorporating several analysis techniques in one instrument, and eliminating any disturbance of the ZDDP tribofilm throughout the formation and analysis process. Using the MTM-SLIM, tribofilm thickness, roughness, and friction data is available throughout the entire tribofilm growth process.^{16,25,26,27}

Afton Chemical Corporation has been researching ZDDP using the MTM-SLIM for the past decade. Studies have revealed the desirable properties of ZDDP tribofilms that result in an ideal low friction tribofilm with both wear protection and an improvement in friction.²⁸ Elemental analysis of ZDDP tribofilms using SEM-EDX discovered the ideal tribofilm composition is composed of high phosphorus content and lower sulfur, as well as high amounts of metal. Favorable tribofilm properties included a smooth surface and thinner films that were able to be achieved by ZDDPs interaction with other additive package chemistries.²⁹ While much of the research involved exploring ZDDP degradation and film formation behaviors, more recent research has focused on the interaction of ZDDP with other additive package chemistries in order to manipulate the tribofilm to the desired properties. The most obvious components to study were friction modifiers and their impact on ZDDP tribofilm formation. Now that a better understanding of different friction modifier chemistries impacts on ZDDP tribofilms exists,

research to evaluate the impact of other surface active additive package components, such as dispersants has increased.

1.4 Dispersants

Dispersants are a class of engine oil additives that compose up to 50 wt.% of an engine oil additive package. Dispersants are used to improve the solubility of potentially harmful byproducts that are present in the engine oil through aging of the oil or enter the oil through fuel combustion. These byproducts can form as soot, deposits, or sludge and have the ability to agglomerate, growing in size and resulting in phase separation from the oil. Any insoluble materials in the oil can lead to a loss of engine efficiency, or in more severe cases catastrophic damage to the engine. Dispersant molecules contain an active polar head group attached to a long hydrocarbon tail. The polar group associates with the insoluble polar molecules, with the long hydrocarbon tail keeping them suspended in solution, Figure 1 - 6.³⁰

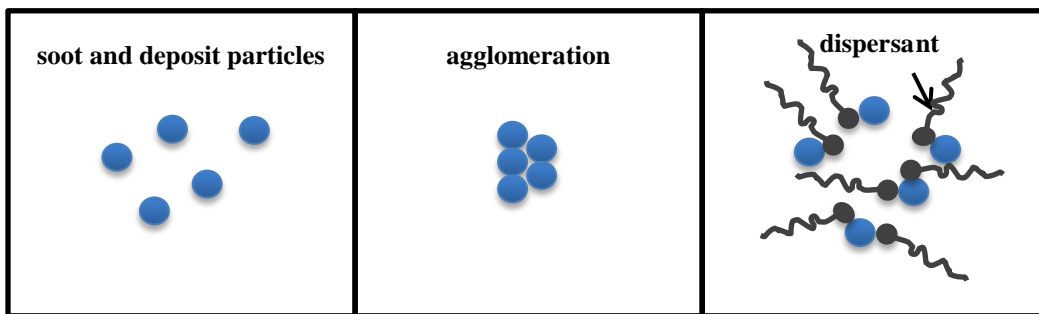


Figure 1 - 6 Dispersant's role in engine oil additive packs.

The evolution of research on ZDDP tribofilms in the last few decades and the ongoing emphasis on improving engine efficiency by understanding tribological contacts in the engine has led to continuing research on ZDDP antiwear films. Along with the pressing global fuel economy regulations, there have been limits to phosphorus and sulfur use in engine oils resulting in the need for the same performance at lower concentrations of ZDDP. Current research has shifted towards evaluating ZDDPs interactions with other additive package chemistries in order to form a desired low friction tribofilm that offers both anti-wear protection and a friction benefit. Any additive that may have a synergistic effect with ZDDP that helps it form a favorable low friction tribofilm may significantly enhance the ZDDP anti-wear additives capabilities. Our motivation was to explore interactions between lower cost additive package components such as dispersants and ZDDPs in hopes to form favorable tribofilms.³¹

Chapter 2 – Project Rationale

ZDDP's structure, properties, and mechanism have become well known after decades of research. The current global shifts towards understanding engine tribology for improved friction and wear control have led to ongoing research on modification of the anti-wear layer. Afton Chemical Corporation has been studying ZDDP tribofilms while in presence of other additive pack chemistries, and evaluating modification of the anti-wear layer into forming a favorable low friction tribofilm.³² Some literature has suggested dispersants interact with ZDDP tribofilms, however the area remained unexplored at Afton Chemical Corporation. Our goal with this project was to evaluate various dispersant chemistries' effects on ZDDP tribofilms in hopes to achieving favorable tribofilm properties by using lower cost components such as dispersants rather than costly friction modifiers.

Studies involving the other additive package component's effects on ZDDP anti-wear films were published as early as the mid-1970s. Without the availability of the techniques we have today, minimal information on additive package component effects on tribofilms was available.^{33,34} By the 2000's more information on ZDDP's mechanism and structure of the tribofilm was beginning to surface.^{35,36} In 2014, Zhang et. al. studied succinimide dispersant effects on ZDDP antiwear films and concluded that dispersants had an antagonistic effect on ZDDP tribofilms. Their studies only evaluated three dispersant chemistries and focused more on concentration effects.³⁷

The objectives of this project were to define various Afton Chemical Corporation dispersant chemistries and their effects on ZDDP tribofilms. We were interested in learning about any dispersant modification of the ZDDP tribofilm structure and any impacts on friction. We evaluated the growth process, physical properties, and composition of the tribofilms. Once

we defined the dispersant's effects on ZDDP tribofilms, we evaluated surface and bulk fluid interactions of ZDDP and dispersants.

We selected one ZDDP that remained constant throughout all testing and varied dispersant chemistries in order to focus on the dispersant's effect on ZDDP tribofilms. All testing was completed in the same base oil without other additive package components present. The dispersant evaluation included changing the structure, concentration, molecular weight, or stoichiometric ratio of starting materials. Standard testing conditions to form ZDDP tribofilms were selected and are described in the experimental section.

Understanding the dispersants effect on ZDDP tribofilms allows us to control ZDDP tribofilm structure and morphology in hopes to achieve better formulation models by understanding component interactions. A dual function additive such as a dispersant would be a major advantage in formulating engine oil packs to meet new standards and specifications. As regulations become more stringent over time, it is essential to optimize formulations with advantages such as synergistic effects between additive package components. The dispersant effects on ZDDP tribofilms were evaluated in hopes to gain a benefit as a dual function additive.

Chapter 3 – Dispersant Effects on ZDDP Tribofilms

3.1 Method Development

3.1.1 ZDDP Tribofilm Formation

ZDDP tribofilms are formed during rolling-sliding contacts between a steel ball and a steel disc in the MTM-SLIM. The disc and ball are made from 52100 steel which are polished to produce a mirrored surface. The contact area of the ball and disc is fully submerged in a lubricant containing ZDDP, while the ball and disc are driven at speeds independent of one another. While the test temperature can vary, we selected 120°C for all our experiments and ran under standard testing conditions specified in the experimental section. ZDDP tribofilms are formed in the MTM-SLIM as the ball and disc are independently driven to slide and roll while an applied load creates contact between the ball and disc. As the ZDDP degrades in the oil solution at the high temperature, the tribofilm forms along the rubbing track of the ball and disc.

As the tribofilm forms on the rubbing track of the steel ball and disc, the MTM-SLIM has the capability to periodically pause the test and take an image of the film using its spacer layer image mapping (SLIM) technique. As the test is stopped, the ball is unloaded off the steel disc and rises up against a glass disc attached to a microscope and camera. This glass disc is coated with a chromium and silica layer that partially reflects light that is shined through it. As a white light source illuminates down through the microscope and glass disc, some of the light is reflected off of the chromium layer, while some of the light continues through the silica layer and anti-wear film, and reflects off of the steel ball, shown in Figure 3 - 1.³⁸

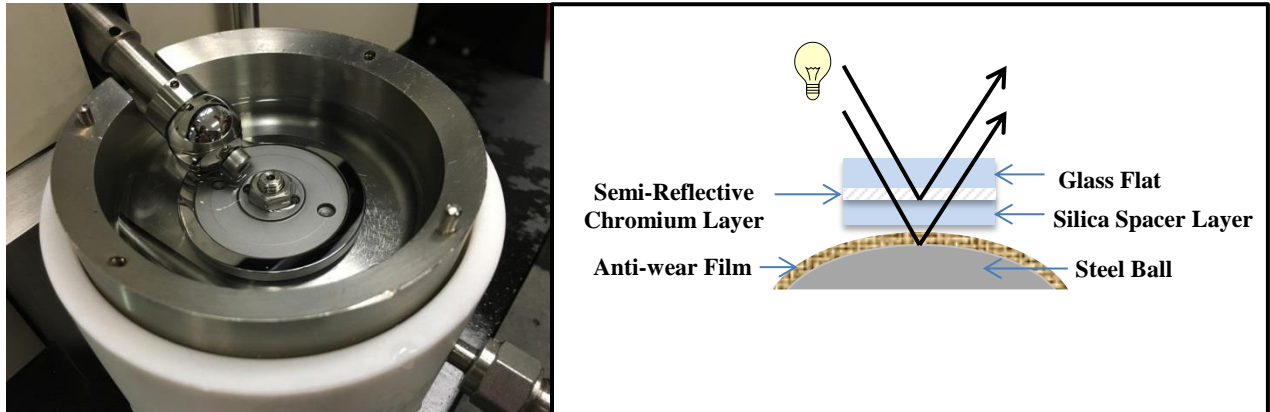


Figure 3 - 1 MTM-SLIM test set up and spacer layer imaging technique.

Interference images are captured using a high resolution RGB color camera. The camera delivers three basic color components, red, green, and blue that combine to form an array of colors. The recombining light paths that are reflected off the glass and steel ball create an interference image, Figure 3 - 1 (A). The color camera can convert the interference image into a thickness distribution shown in Figure 3 - 1 (B). The thickness distribution can be plotted, Figure 3 - 1 (C), and an average thickness for each tribofilm image can be obtained. The SLIM technique offers the ability to gather film thickness information throughout the film formation process, resulting in film growth information.³⁸

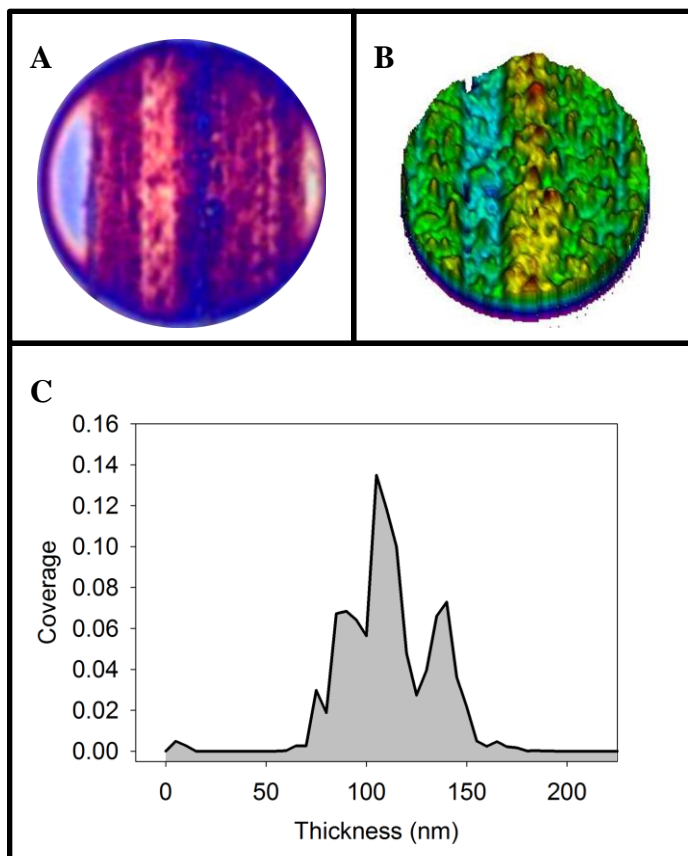


Figure 3 - 2 MTM-SLIM interference imaging (A) is converted to a colored thickness image (B), which is then plotted as a thickness distribution (C).

One ZDDP was selected for all of our work for consistency throughout the project, and to maintain focus on the dispersants. We selected a mixed primary and secondary ZDDP made with a 60:40 molar ratio isobutyl alcohol (primary), isopropyl alcohol (secondary), and 2-ethylhexyl alcohol (primary) starters. The ZDDP was blended in a base oil, that also remained constant throughout all testing, at a concentration of 1.00 wt.%. The test oil was run in the MTM-SLIM for one hour, which is a standard test time for ZDDP to develop a full film. The average tribofilm growth for ZDDP is shown in Figure 3 - 3 along with the interference images that were converted to average thickness.

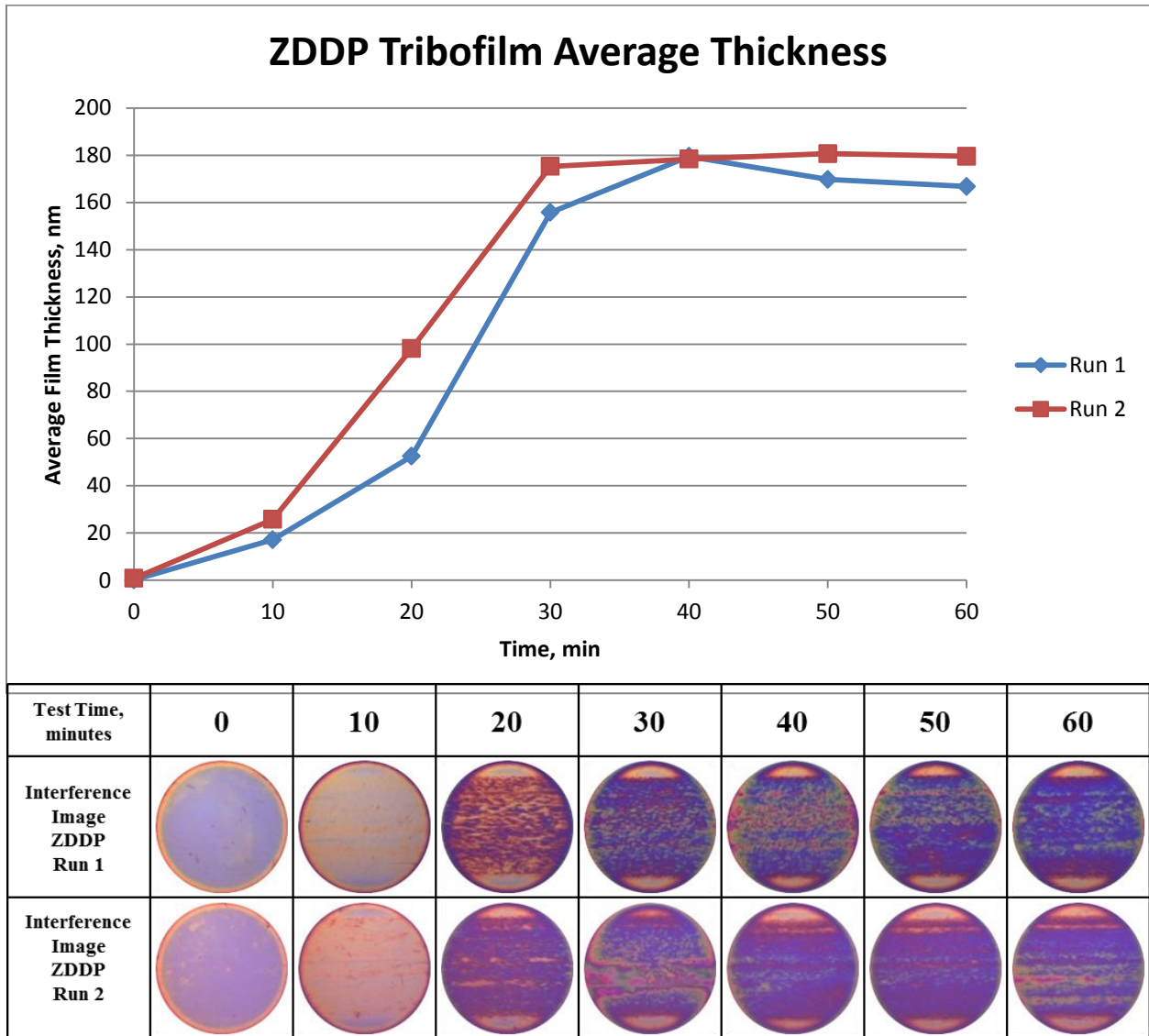


Figure 3 - 3 MTM-SLIM analysis of ZDDP tribofilm growth over a one hour period with interference images that were used to convert to thickness.

The MTM-SLIM also measures the surface roughness throughout tribofilm growth. The tribofilm roughness throughout film growth for ZDDP is shown in Figure 3 - 4. In the case of ZDDP, tribofilm roughness follows the thickness plot, with a rapid increase of roughness during the initial formation of the film, at the 20 to 30 minute mark. This roughness is also apparent in

the interference images. There is some variability during the initial tribofilm growth peak, but this is largely due to the nature of the patchy film growth of the ZDDP. In both cases, the end-of-test result is similar.

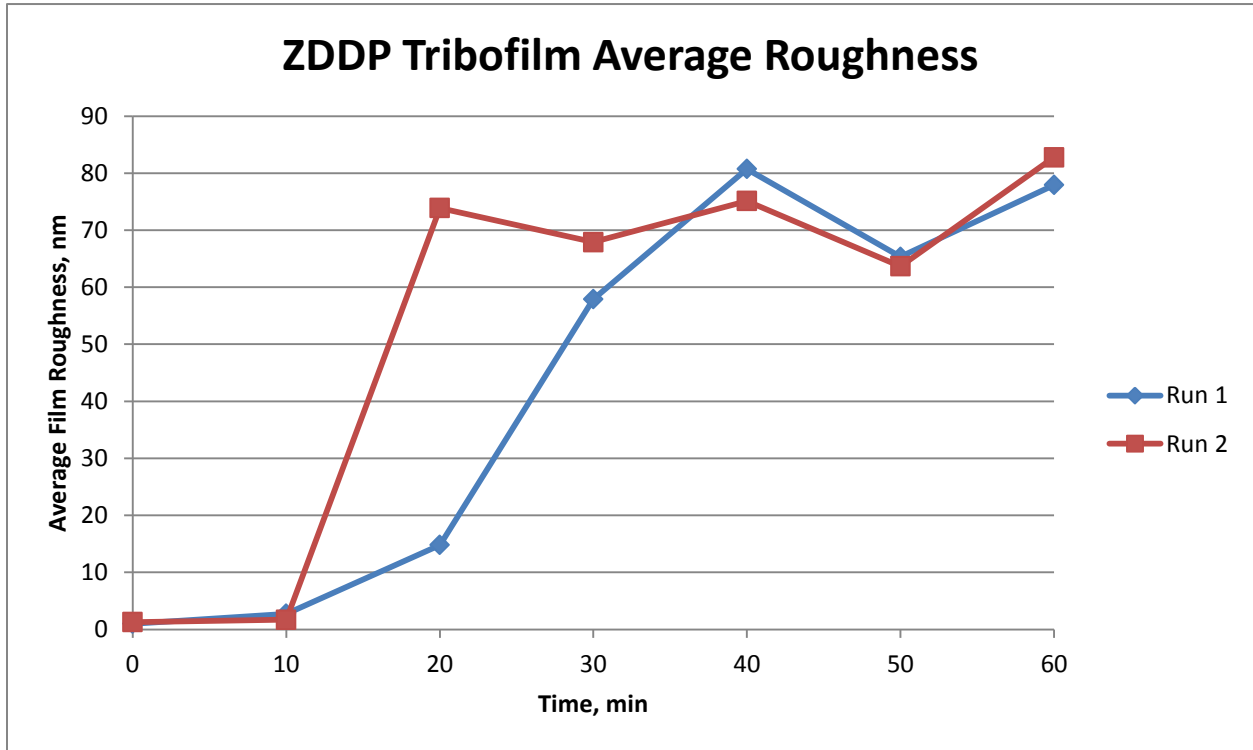


Figure 3 - 4 Average roughness of ZDDP tribofilm throughout film formation process over one hour.

The MTM-SLIM is equipped with a force transducer that can track friction throughout the tribofilm growth process. The coefficient of friction is measured continuously. The friction for the two ZDDP runs are shown in Figure 3 - 5. It is not unusual to observe a higher coefficient of friction during the peak of tribofilm growth then lowering over time. This effect can visually be observed in the interference images, with the highest friction point around 20 minutes resulting in the patchiest film. The thick patches of ZDDP film appear in the image, surrounded by valleys of no film formation. As the tribofilm begins to cover these valleys

throughout the remainder of the test, friction is reduced and leveled off. As the deep valleys begin to cover with tribofilm covering the steel surface, the patchy areas that were already covered with tribofilm are also growing. This effect is observed in the roughness plot, where roughness does not appear to decrease over time unlike friction.

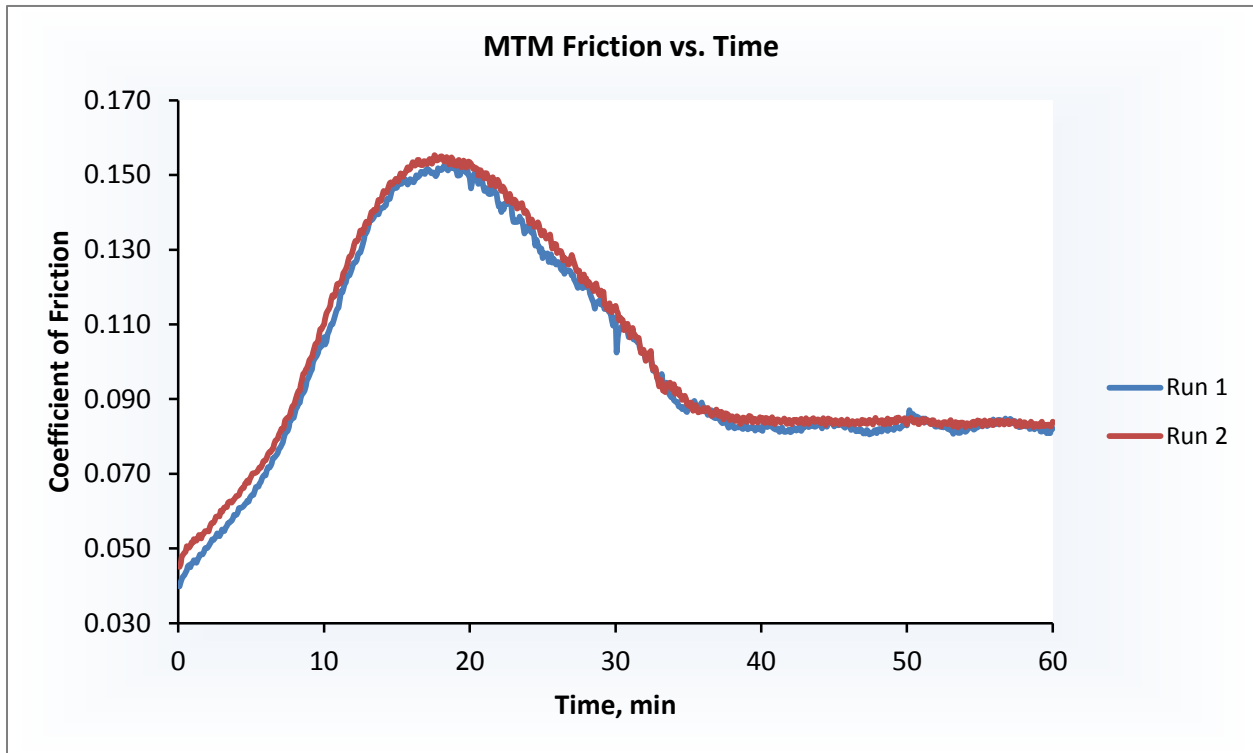


Figure 3 - 5 The coefficient of friction of ZDDP tribofilms forming over one hour.

3.1.2 ZDDP Tribofilm Analysis

After the tribofilm formation is complete, the steel ball is cleaned and evaluated for elemental composition using the SEM-EDX. The SEM-EDX measures the elemental composition over an area of the tribofilm selected for measurement. The SEM-EDX image and spectra of the selected areas of the ZDDP tribofilm are shown in Figure 3 - 6. The SEM-EDX spectra and image for each of the two ZDDP runs and is nearly identical. In both cases we

observe a large peak for iron derived from the steel ball. This peak is present in all the SEM-EDX spectra with the intensity varying with the film thickness.

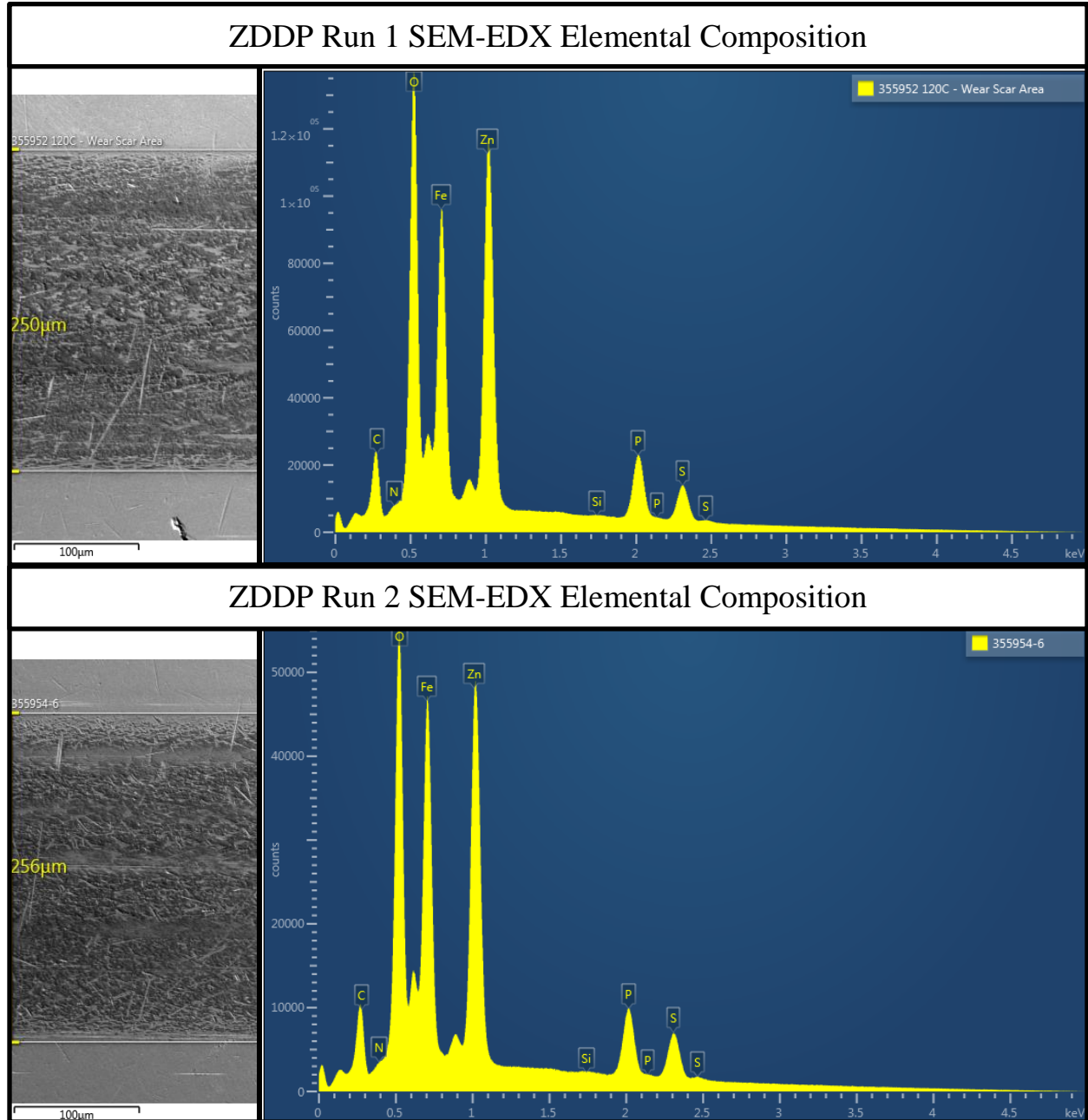


Figure 3 - 6 SEM-EDX images and spectra for two ZDDP tribofilm runs.

The distribution of each element is extracted from the SEM-EDX spectra resulting in a percent composition of each element, with a sum of 100 wt.%, Table 3 - 1. Since the penetration depth of the electron beam is deeper than the thickness of the tribofilm on the surface the amount of iron between tribofilms can vary, with higher iron contents observed in thinner films. A normalization factor is calculated from the iron content using the equation below.

$$\textit{Normalization Factor} = \frac{100}{(100 - Fe)}$$

Each of the elements of interest are multiplied by the normalization factor, eliminating the Fe signal from the underlying steel. This allows for the comparison of tribofilm compositions independent of their thickness.

Table 3 - 1 Elemental composition of ZDDP tribofilms from SEM-EDX spectra including normalized values.

Elemental Composition	ZDDP Run 1	ZDDP Run 2
C (at wt.%)	9.32	9.30
N (at wt.%)	0.82	0.66
O (at wt.%)	29.40	26.65
Si (at wt.%)	0.10	0.13
P (at wt.%)	7.96	7.62
S (at wt.%)	5.84	6.76
Fe (at wt.%)	29.36	32.46
Zn (at wt.%)	17.19	16.43
Total	100.0	100.0
Normalization Factor	1.42	1.48
Normalized wt.% P	11.27	11.28
Normalized wt.% S	8.27	10.01
Normalized wt.% Zn	24.33	24.33

After normalizing the elements of interest for our study on ZDDP tribofilm composition, we can then evaluate the phosphorus to sulfur and zinc to phosphorus ratios. By looking at the elemental ratios, we can determine if the structure of the ZDDP tribofilm changes in the presence of other additives. The elemental ratios of the two ZDDP runs, Figure 3 - 7, shows the reproducibility in the test. The ratio of phosphorus to sulfur are between 1.0 - 1.5:1.0 with the selected ZDDP. The zinc content is much higher, with a zinc to phosphorus ratio of just about 2.2:1.0.

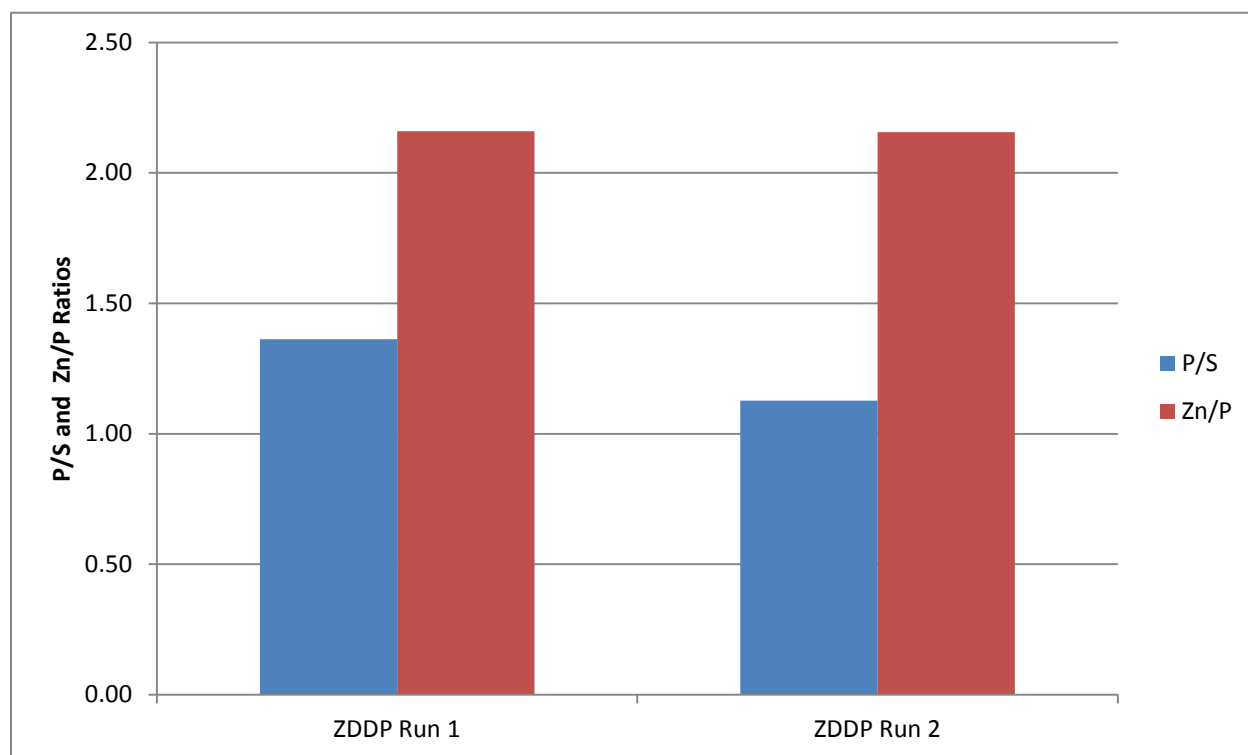


Figure 3 - 7 Elemental analysis of ZDDP tribofilms and reproducibility.

All of the analysis techniques described above were used to evaluate dispersant effects on ZDDP tribofilms. The ZDDP shown above remained consistent throughout all testing with a concentration of 1.00 wt.% in base oil. We varied dispersant chemistries and concentrations and

blended them with 1.00 wt.% ZDDP in base oil and ran them in the MTM-SLIM using the same standard conditions, and analyzed the elemental composition of tribofilms.

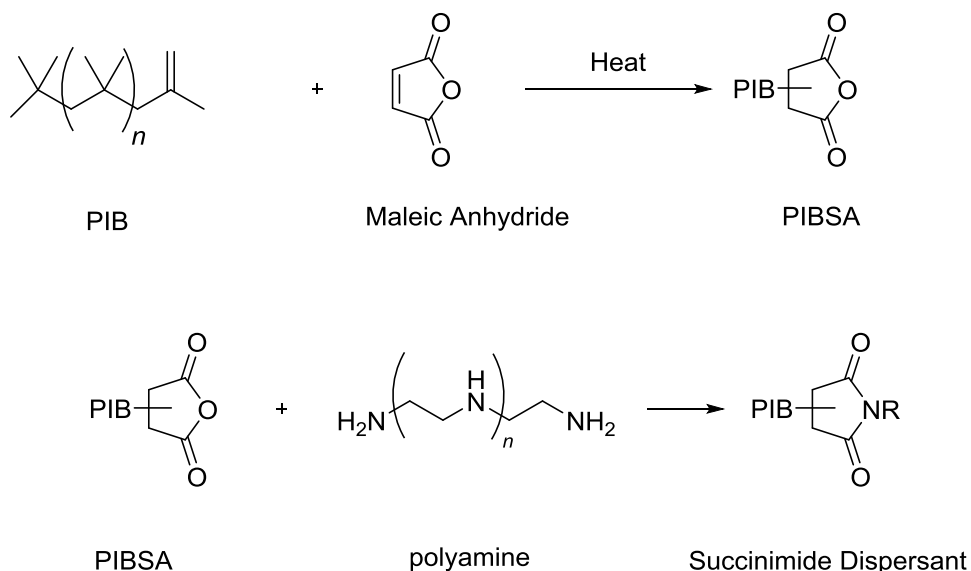
3.2 Dispersant Effects on ZDDP Tribofilms

3.2.1 Dispersant Chemistries

Dispersant chemistries are high molecular weight metal-free polyisobutenyl succinimides (PIBSI). The polar head group consists of an amine or polyamine group, which is linked to a hydrocarbon tail via a succinimide. The hydrocarbon tail, polyisobutylene (PIB), is a low cost hydrocarbon chain commonly used in the petroleum industry. The PIB chain can be polymerized to the desired molecular weight. The PIB chain length is major factor controlling the molecular weight of the dispersant with molecular weights of typical dispersants ranging from 1000 to 3000 g/mol. Different amine chemistries are used to form dispersants based on the desired functionality of the molecule.

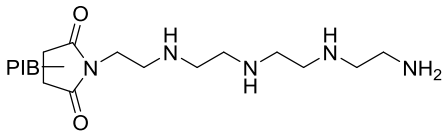
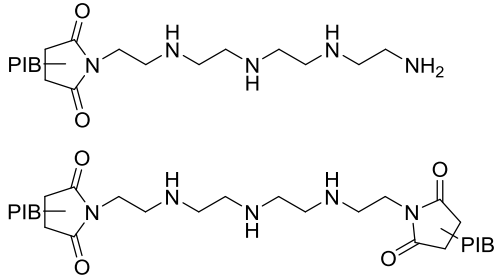
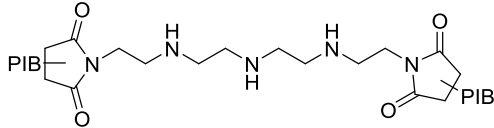
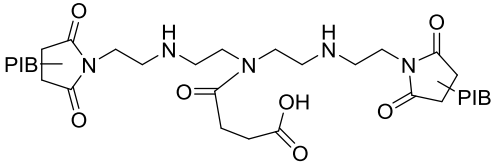
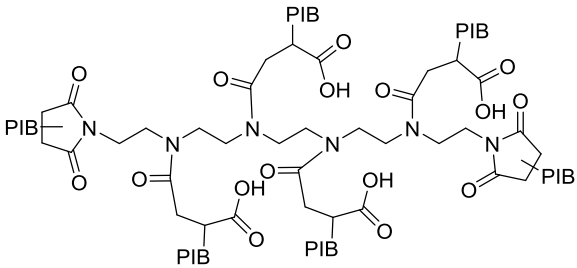
Dispersants are synthesized from a polyisobutylene succinic anhydride (PIBSA) reaction with an amine. The resulting dispersants can vary in molecular weight, amine group, and stoichiometric ratio of PIBSA and amine. The combination can result in varying functionalities. The difference in molecular weight can be achieved by reacting a desired molecular weight PIB molecule with maleic anhydride, resulting in the PIBSA dispersant precursor. The biggest difference in functionality is by changing the stoichiometric ratio of PIBSA to amine, which results in capping free amine groups with PIBSA molecules. Varying the amine group will also result in a different functionality. A generic structure of a PIBSI dispersant synthesis scheme is shown in **Scheme 3 - 1**.

Scheme 3 - 1 Generic PIBSI dispersant synthesis.



We selected dispersants that varied in molecular weight, stoichiometric ratio of PIBSA and amine, and a number of polyamine groups, Table 3 - 2. Four of the five dispersants were synthesized with the same starting amine, tetraethylenepentamine (TEPA). The functionality of these dispersants varies by changing the stoichiometric ratio of PIBSA and amine, resulting in mono-succinimide, bis-succinimide, and, tris-succinimide chemistries. The last dispersant was synthesized with a different amine, and an increase in the stoichiometric ratio of the PIBSA and amine. The dispersants were blended at 1.00 wt.% and 0.50 wt.% into the 1.00 wt.% ZDDP in base oil sample. All the oil samples were run in the MTM-SLIM for one hour, with interference imaging every 10 minutes. After the tribofilms were formed with the dispersants, the films were then analyzed using the SEM-EDX.

Table 3 - 2 Dispersant chemistries selected for evaluation of their effects on ZDDP tribofilms.

Dispersant	PIBSA : Amine	Structure
Dispersant A	1 : 1	
Dispersant B	1.5 : 1	
Dispersant C	2 : 1	
Dispersant D	3 : 1	
Dispersant E	6 : 1	

3.2.2 Dispersant A

The first dispersant selected for testing, Dispersant A, is a mono-succinimide dispersant with a 1:1 PIBSA to amine ratio. Dispersant A was tested at concentrations of 1.00 wt.%, 0.50 wt.%, and 0.25 wt.% with 1.00 wt.% ZDDP in base oil to evaluate concentration effects on tribofilm growth. Dispersant A is the most unstable out of the selected dispersants, with

structural shifts occurring over time. The unique feature of Dispersant A is that it can be present in three different structures depending on the sample age, mostly pure polyamide, mostly pure imide, and a mixture of both amide/imide forms. We will test all three structures. The original structure of Dispersant A is shown in Figure 3 - 8, as a mono-succinimide dispersant. This is a thermodynamic product that forms at elevated temperatures approaching 190°C. The dispersant polymerizes upon aging at ambient temperature resulting in the polyamide form of the molecule.

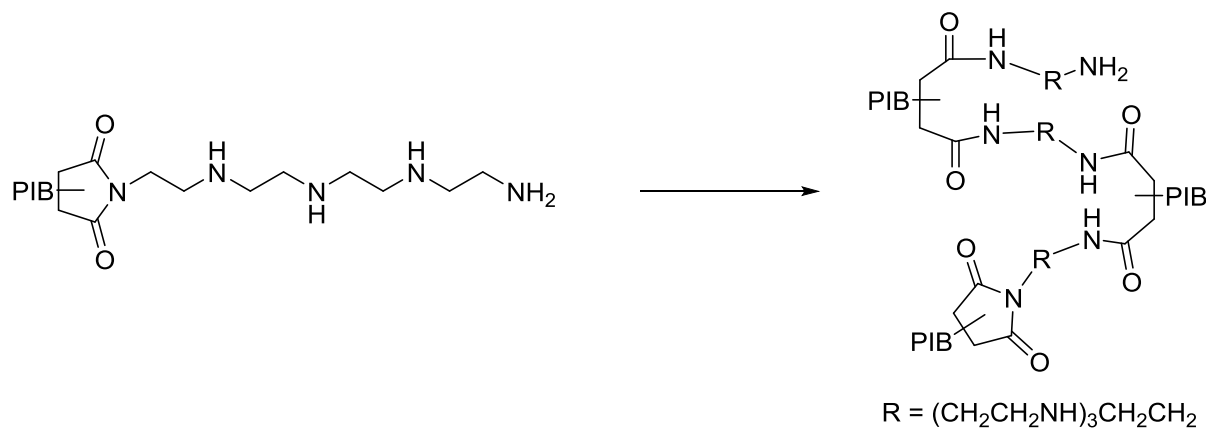


Figure 3 - 8 Dispersant A structure and polymerization upon aging.

We began evaluating the polyamide structure of Dispersant A because it is most likely to appear in this form. The samples with varying concentrations of Dispersant A were run in the MTM-SLIM for one hour under standard operating conditions. We immediately observed a hindrance on tribofilm growth, even at a concentration of 0.25 wt.% Dispersant A, Figure 3 - 9. All concentrations of Dispersant A resulted in the same tribofilm thickness, indicating the hindering effect from the dispersant is not concentration dependent, or it is saturated above 0.25 wt.%. The end-of-test interference images for ZDDP tribofilms formed with Dispersant A are in

Figure 3 - 10. The interference images that were captured for conversion to tribofilm thickness throughout the test can be found in Appendix 1.

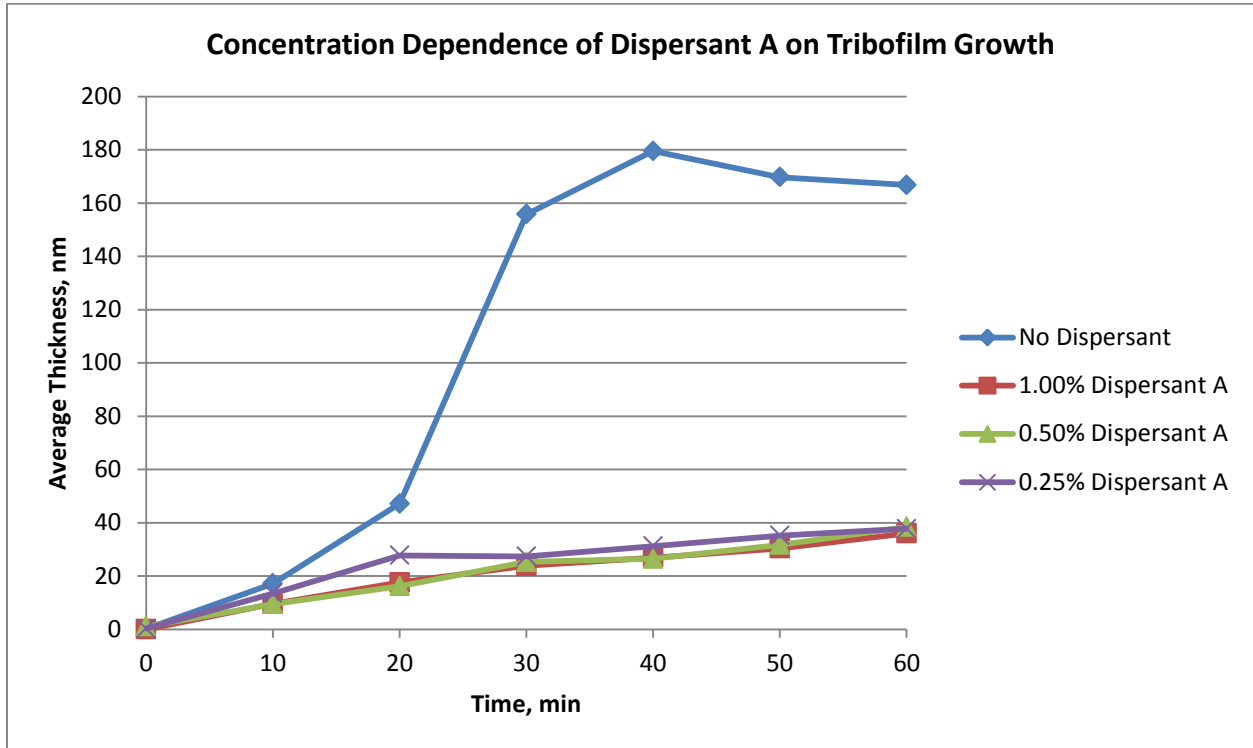


Figure 3 - 9 Concentration dependence of Dispersant A on ZDDP tribofilm growth in the MTM-SLIM over one hour.

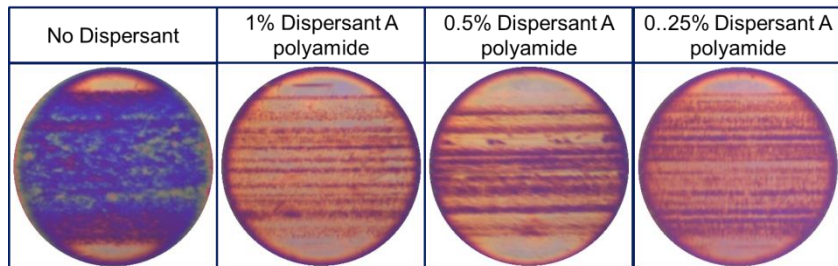


Figure 3 - 10 End-of-test images of ZDDP tribofilms formed in presence of Dispersant A.

The average roughness of the ZDDP tribofilms throughout film growth can be found in Figure 3 - 11. Surface roughness can be analyzed through the interference images and is not always correlated to the average thickness of the film. Dispersant A resulted in the formation of a very thin and smooth film, although interference images show patchy film formation along the rubbing track. In the case of Dispersant A, the film thickness was so low that it resulted in a low average roughness.

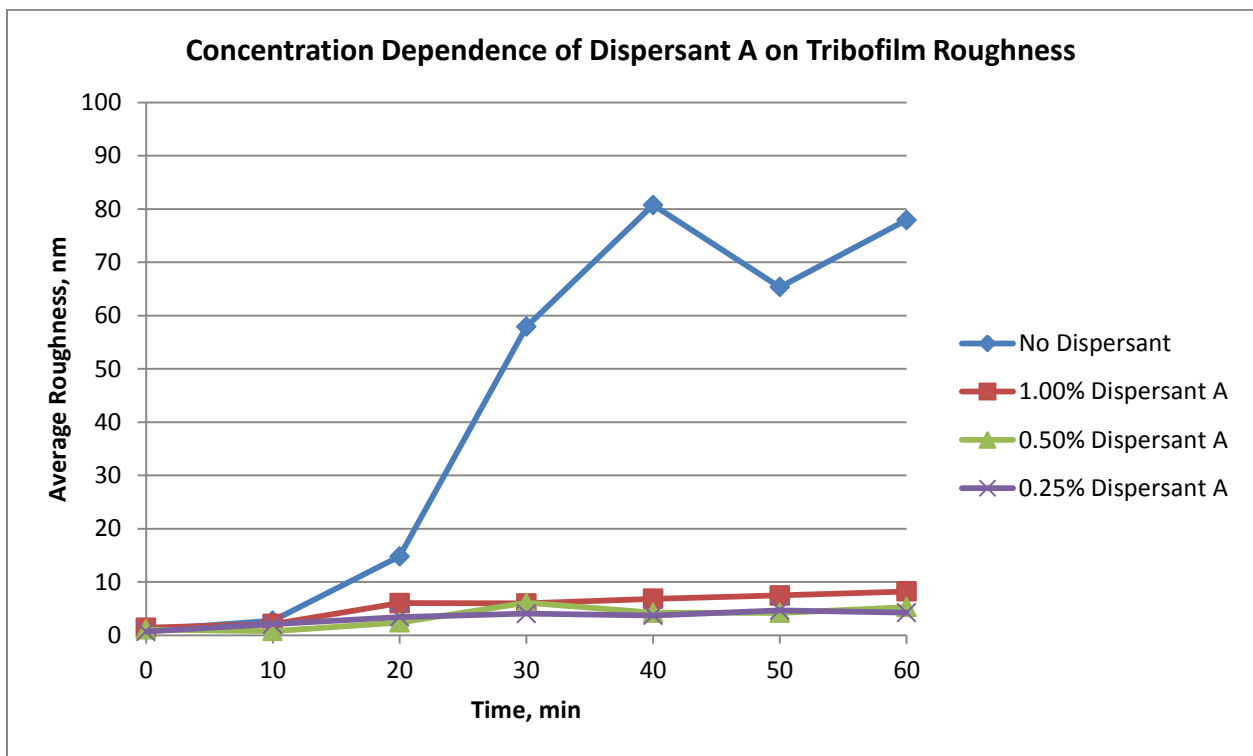


Figure 3 - 11 Concentration dependence of Dispersant A on ZDDP tribofilm roughness.

The MTM-SLIM analysis also includes evaluating friction throughout the tribofilm growth process. The friction throughout the film formation at the varying concentrations of Dispersant A is shown in Figure 3 - 12. The coefficient of friction throughout tribofilm growth at all three concentrations indicates Dispersant A improves friction during tribofilm growth by

eliminating the peak friction during the initial tribofilm formation. The end-of-test friction in all three cases was similar to the film with no dispersant or slightly above. There was no trend between concentration and friction.

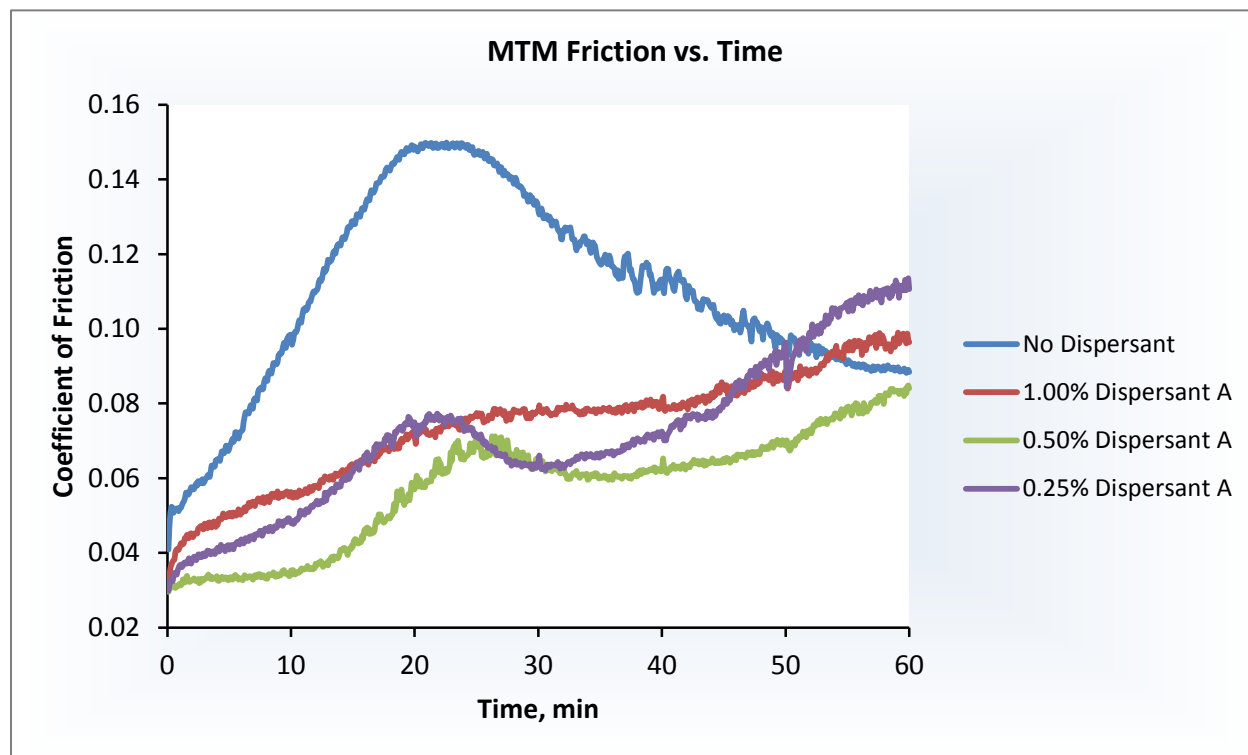


Figure 3 - 12 Concentration dependence of Dispersant A on friction throughout tribofilm growth.

After the tribofilm formation in presence of dispersants was complete, the tribofilms were analyzed using the SEM-EDX. The complete SEM-EDX analysis including images, spectra, and composition can be found in Appendices 2 and 3. We were interested in any changes in tribofilm structure so we only evaluated phosphorus, sulfur, and zinc levels in relation to one another. The phosphorus to sulfur ratios of each of the tribofilms formed with the three concentrations of Dispersant A are shown in Figure 3 - 13. We observed films with higher sulfur than phosphorus at all three concentrations of Dispersant A, as opposed to a higher phosphorus

film that is observed with no dispersant present. The zinc to phosphorus ratios of the tribofilms formed with Dispersant A, Figure 3 - 13, also indicated the tribofilm structure is different when Dispersant A is present. The tribofilms were much richer in zinc and sulfur when compared to the tribofilm with no dispersant. The SEM-EDX analysis confirms the structure of the ZDDP tribofilms is different when Dispersant A is present.

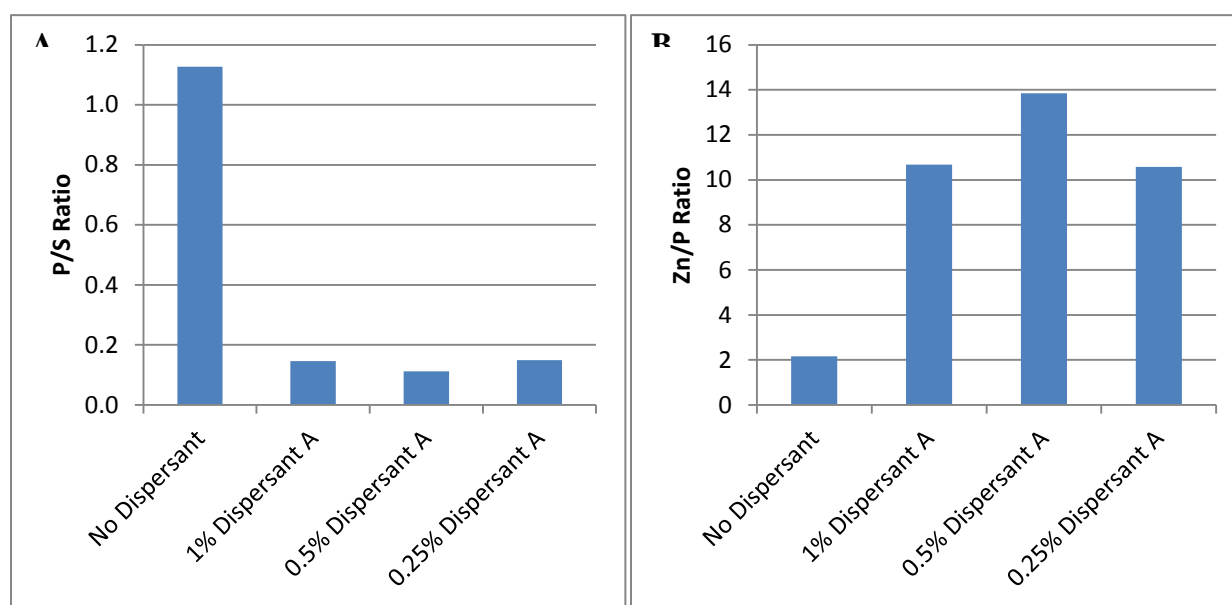


Figure 3 - 13 (A) Phosphorus to sulfur ratios of ZDDP tribofilms formed with varying concentrations of Dispersant A. (B) Zinc to phosphorus ratios of ZDDP tribofilms formed with varying concentrations of Dispersant A.

3.2.3 Effects of Dispersant A Structure

Dispersant A is able to convert back to the original imide structure when heated to 190°C. In order to analyze the effects of the varying structures of Dispersant A, we converted Dispersant A back to the imide form, and sampled at 110°C in order to obtain a mixed polyamide and imide sample. The three samples of mostly polyamide, mostly imide, and mixed

amide/imide were blended at 1.00 wt.% with 1.00 wt.% ZDDP in base oil run in the MTM-SLIM under standard operating conditions. The average thicknesses of films in Figure 3 - 14 show that very thin tribofilms form, again indicating the hindering of full ZDDP tribofilm growth. We did see a slight trend indicating there were differences in the structure of Dispersant A, with the fully imide form resulting in the thinnest films. The interference images of the tests shown below can be found in Appendix 1. We did observe visually different films between the mostly polyamide, mostly imide, and mixed amide/imide structures.

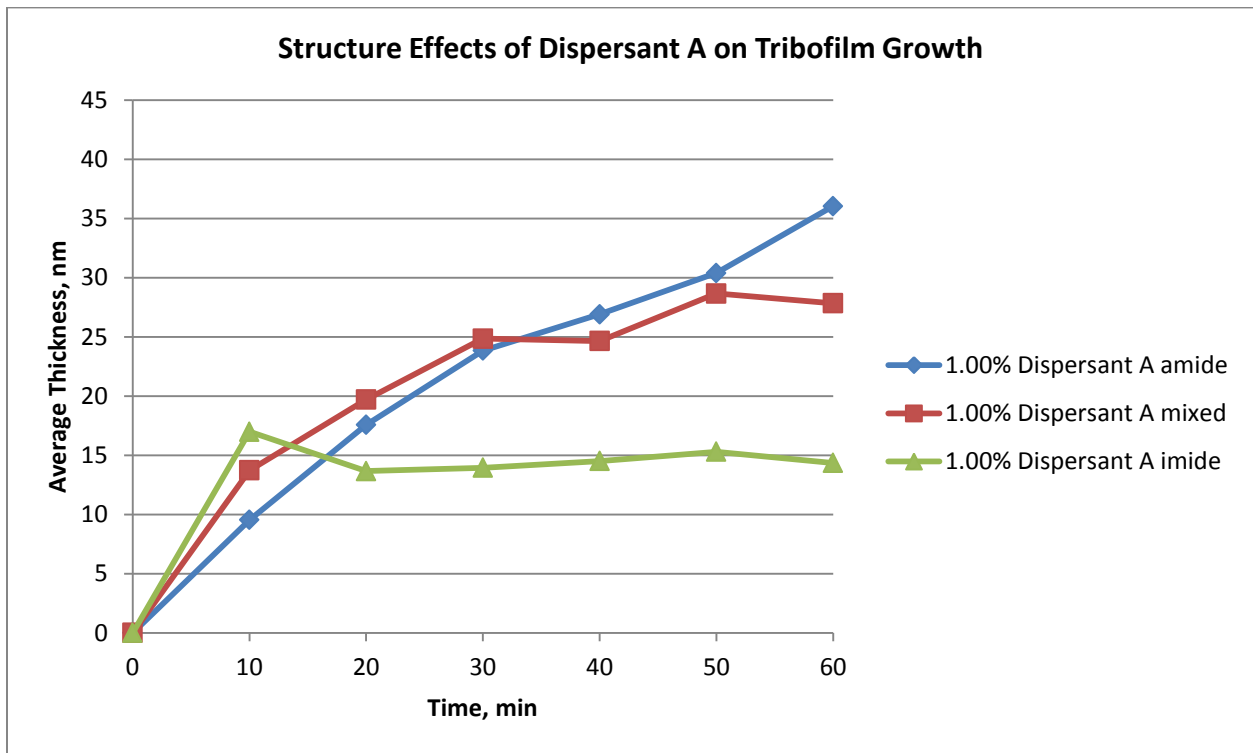


Figure 3 - 14 Dispersant A structure effects on ZDDP tribofilm growth in the MTM-SLIM over one hour.

The average roughness of the tribofilms were much lower than the film with no dispersant. This is primarily due to the much thinner film when Dispersant A is present, and in some cases almost no film forming. The average roughness of the tribofilms formed with the

three Dispersant A structures are shown in Figure 3 - 15. Again, we see the lower roughness with the imide form of Dispersant A, however, this is more likely due to the lack of tribofilm formation.

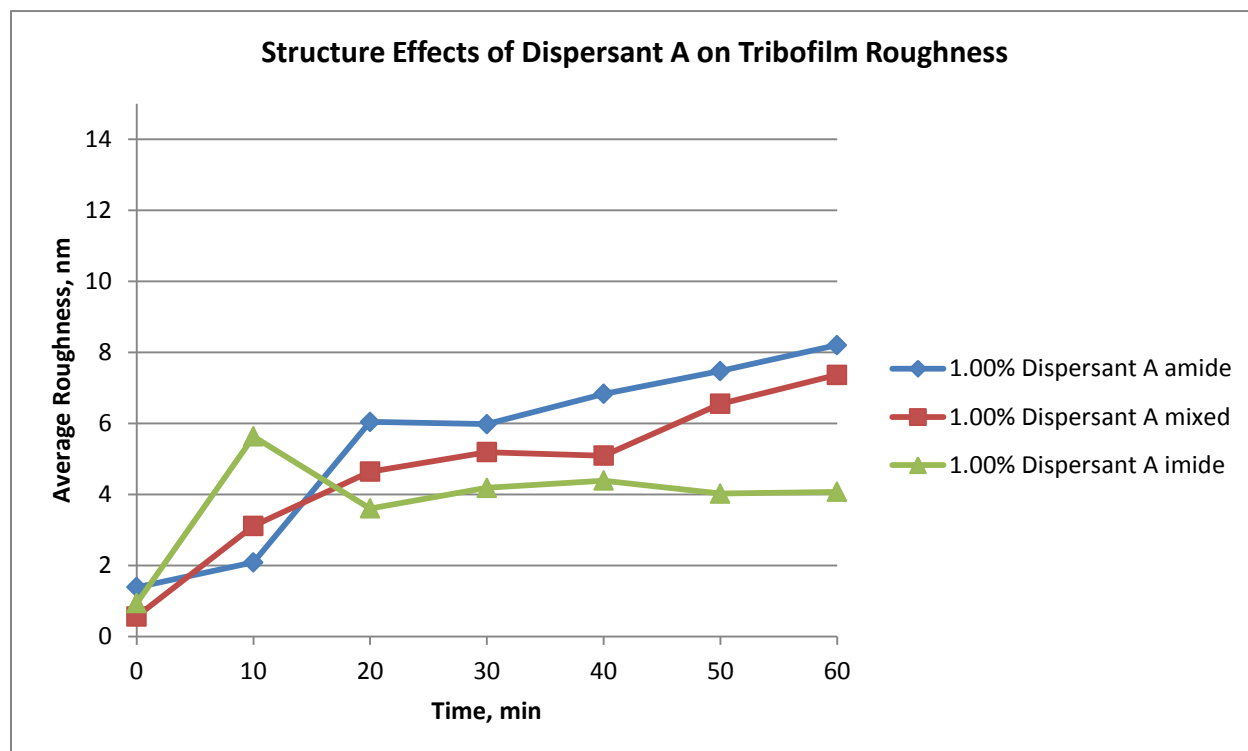


Figure 3 - 15 Dispersant A structure effects on ZDDP tribofilm roughness.

The friction of the tribofilm over time is shown in Figure 3 - 16, with the mixed and imide forms of Dispersant A resulting in lower friction than the polyamide. This is also most likely due to the lack of film formation with the mixed and imide forms of Dispersant A. In all cases of tribofilm thickness, roughness, and friction, we do see a trend in a difference in film growth when converting from the poly-amide form of Dispersant A to the imide form of Dispersant A, which forms nearly no tribofilm.

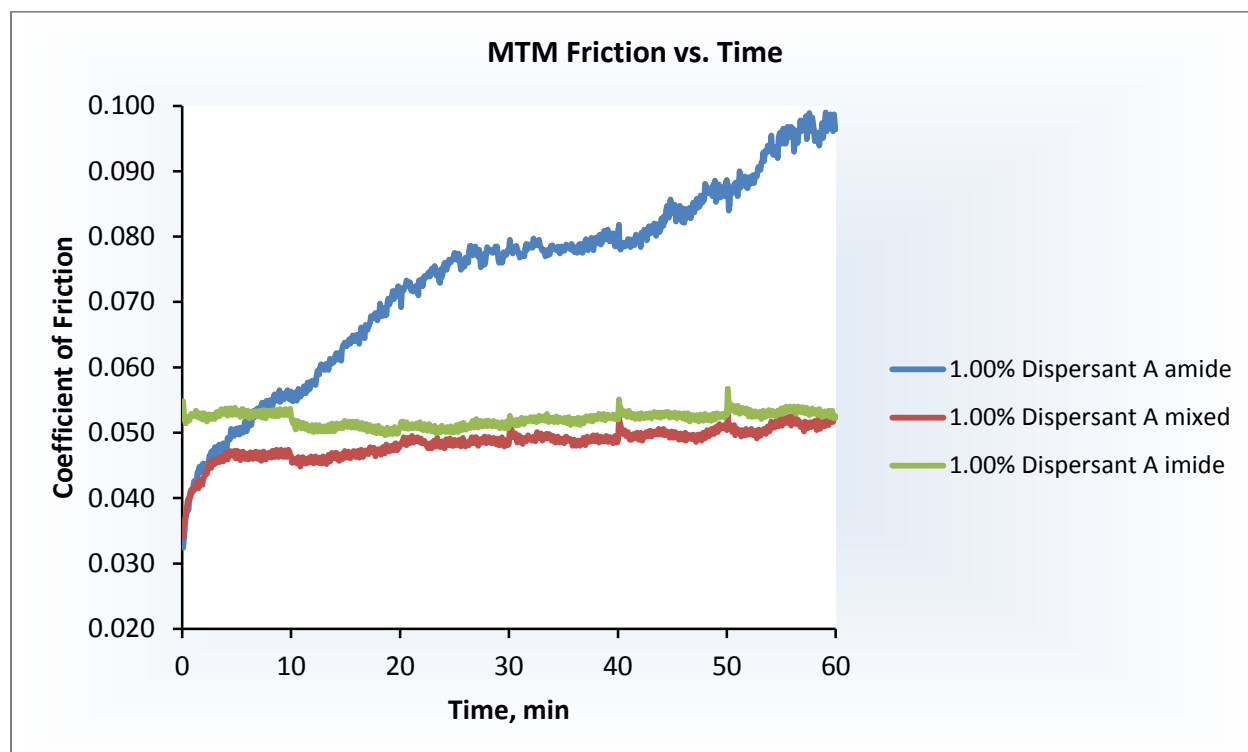


Figure 3 - 16 Dispersant A structure effects on friction during ZDDP tribofilm growth.

The evaluation of Dispersant A on ZDDP tribofilms instantly revealed the antagonistic effect on ZDDP tribofilm growth. We did not see any concentration dependence of Dispersant A on the observed effect, but there was a difference between Dispersant A structures. It appears that the poly-amide structure results in the thickest film, and as the structure converts back to imide, it has a bigger impact on tribofilm growth with nearly no film forming observed. Surface roughness was very low in all cases, but was mostly attributed to the low tribofilm thickness. SEM-EDX analysis of the tribofilms formed with the polyamide structure indicated the tribofilm is structurally different than that when no dispersant is present. We did observe lower friction throughout tribofilm growth with the polyamide structure, but it showed similar end-of-test friction as the tribofilm with no dispersant. The friction of the tribofilms formed with the intermediate and the imide structures was very low due to lack of tribofilm formation.

3.2.4 Dispersant B

The next dispersant selected for evaluation, Dispersant B, has a slightly higher ratio of PIBSA to amine than we saw in Dispersant A, at 1.5:1.0. This change in the stoichiometric ratio results in a mixed mono-succinimide and bis-succinimide dispersant, Figure 3 - 17. Dispersant B is a more stable molecule, which does not result in the structural shift we see with Dispersant A. The concentration dependence of Dispersant B on the ZDDP tribofilm was tested similar to Dispersant A.

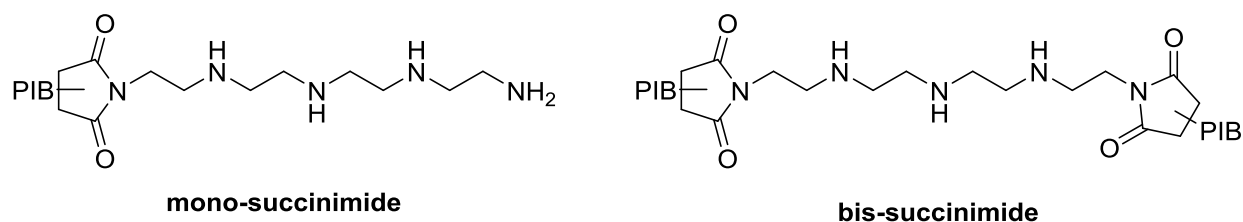


Figure 3 - 17 Dispersant B structures of mixed mono-succinimide and bis-succinimide.

Dispersant B was tested at concentrations of 1.00 wt.% and 0.50 wt.% with 1.00 wt.% ZDDP in base oil and run in the MTM-SLIM under standard operating conditions. The tribofilms formed with Dispersant B resulted in a thicker and more even film than observed with Dispersant A (see Figure 3 - 18). We observed tribofilm growth of up to 60 nm thick which was still much lower than the tribofilm formed with no dispersant. We did not observe a major concentration dependence with Dispersant B, but the lower concentration resulted in a thicker tribofilm that formed faster, whereas the higher concentration resulted in a thicker tribofilm at the end-of-test. The end-of-test- interference images for Dispersant B are shown in Figure 3 - 19. The interference images for both concentrations of Dispersant B that were used to calculate average thickness can be found in Appendix 1.

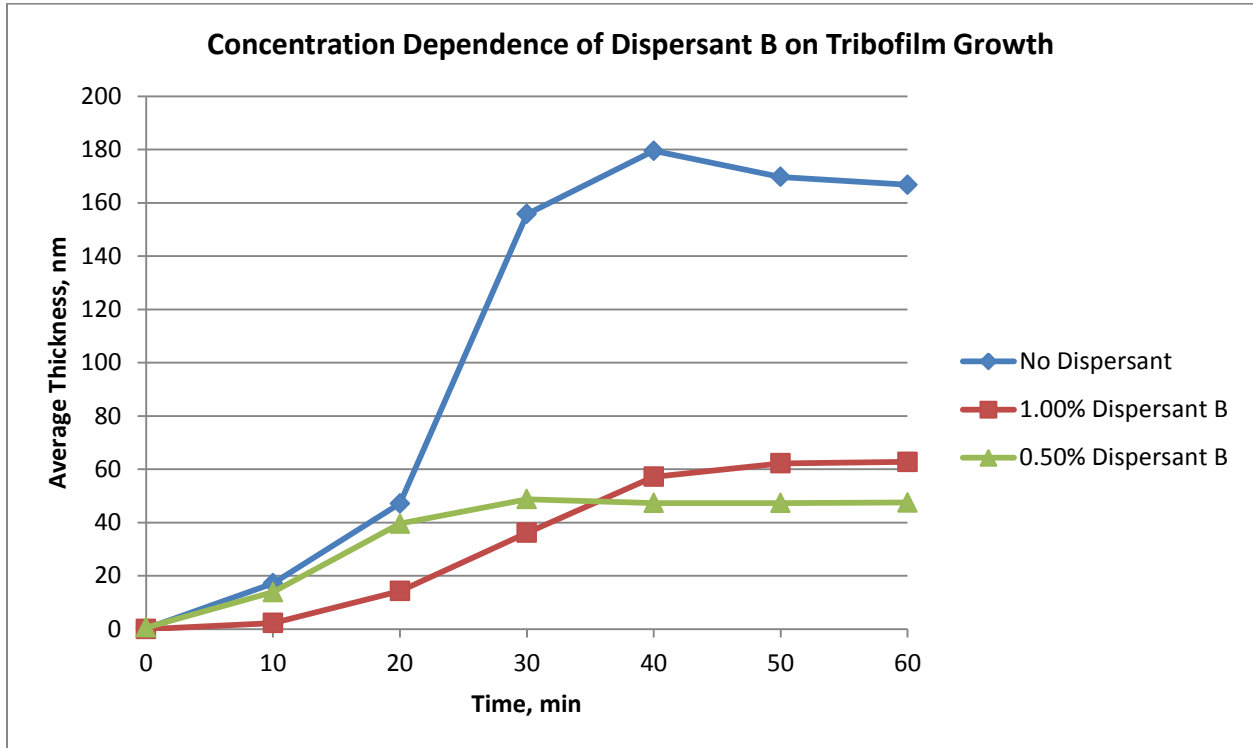


Figure 3 - 18 Concentration dependence of Dispersant B on ZDDP tribofilm growth in the MTM-SLIM over one hour.

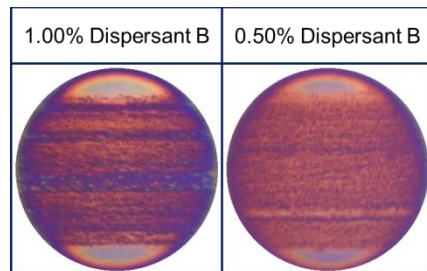


Figure 3 - 19 End-of-test interference image of ZDDP tribofilms formed in presence of Dispersant B.

The average roughness of the ZDDP tribofilms formed with Dispersant B did result in a difference between the two concentrations, shown in Figure 3 - 20. The tribofilm formed with 1.00 wt.% Dispersant B present resulted in a much rougher film than that of 0.50 wt.%

Dispersant B. The interference images show a visually patchier film forming with 1.00 wt.% Dispersant B between 20 and 30 minutes of rubbing time, resulting in a patchier film at the end-of-test. Like Dispersant A, both concentrations of Dispersant B resulted in a reduced average thickness and roughness compared to the tribofilm with no dispersant present.

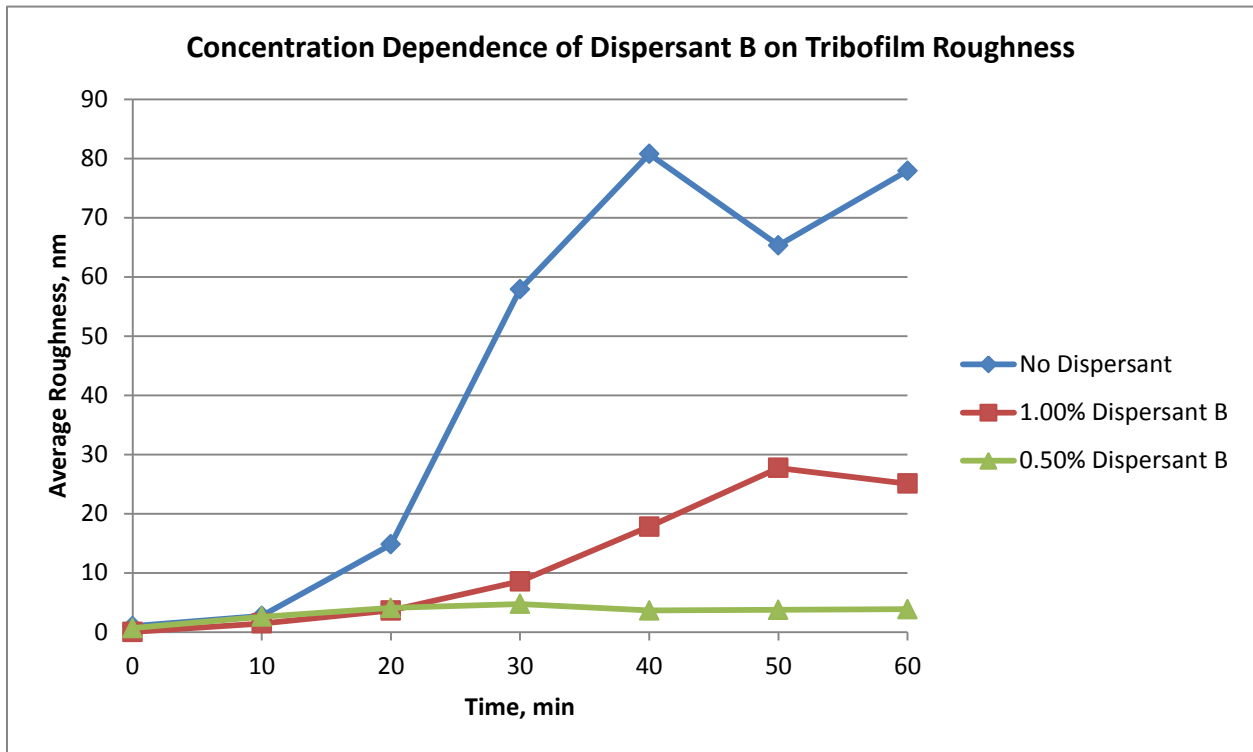


Figure 3 - 20 Concentration dependence of Dispersant B on ZDDP tribofilm roughness.

Both concentrations of Dispersant B resulted in higher friction throughout the tribofilm growth, Figure 3 - 21. In both cases, we observed a peak in friction similar to the friction of the film with no dispersant present. When Dispersant B was present, the friction did not decrease after the peak of the test, resulting in extremely higher friction at the end-of-test. We observed slightly higher friction with the tribofilm formed with the higher concentration, but they were

both similar. Since the lower concentration of Dispersant B resulted in a smooth film, but high friction, we determined tribofilm roughness is not correlated to friction.

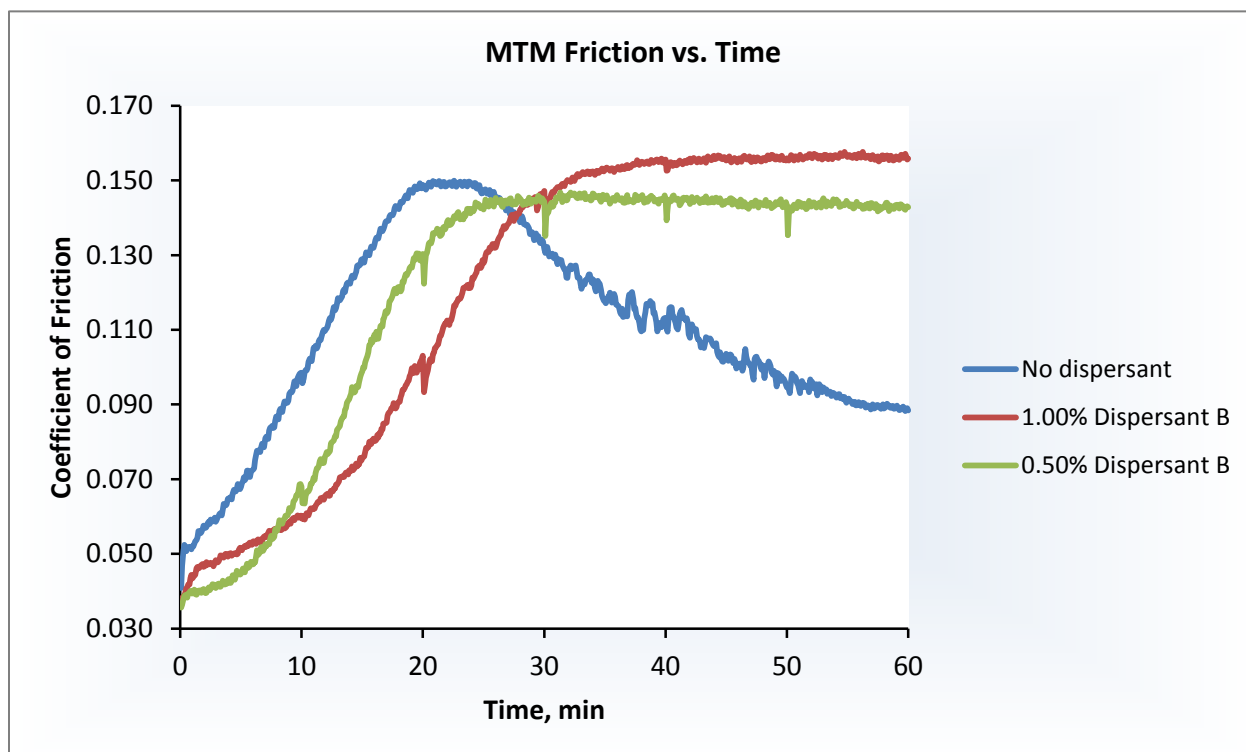


Figure 3 - 21 Concentration dependence of Dispersant B on friction throughout tribofilm growth.

The SEM-EDX images, spectra, and composition of tribofilms formed with Dispersant B can be found in Appendices 2 and 3. Similarly to Dispersant A, the phosphorus to sulfur ratio of the films formed in presence of Dispersant B was lower than the tribofilm with no dispersant present, indicating the tribofilm was higher in sulfur, Figure 3 - 22. The zinc to phosphorus ratio of the tribofilms formed with Dispersant B was also higher than the film with no dispersant present indicating there was a higher zinc content in the tribofilm. We did not observe any major

difference between the two concentrations, but the lower concentration of Dispersant B resulted in higher sulfur and higher zinc than the higher concentration of Dispersant B. In both cases, we do observe a structurally different film than that formed when no dispersants present.

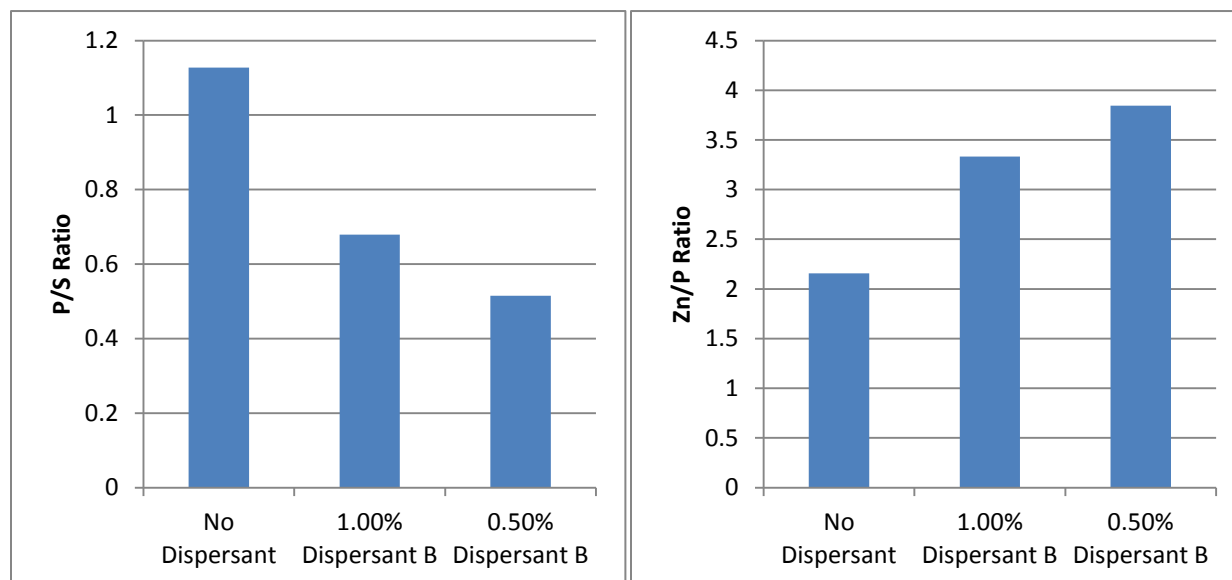


Figure 3 - 22 (A) Phosphorus to sulfur ratios of ZDDP tribofilms formed with varying concentrations of Dispersant B. (B) Zinc to phosphorus ratios of ZDDP tribofilms formed with varying concentrations of Dispersant B.

The tribofilms formed in presence of Dispersant B also resulted in much lower thicknesses when compared to ZDDP tribofilms formed with no dispersant present. We did observe a difference from Dispersant A, with thicker and fuller tribofilms forming. The higher concentration of Dispersant B resulted in a slightly thicker tribofilm and rougher than the lower concentration, but in both cases the thickness and roughness was lower than that of no dispersant. Both concentrations of Dispersant B resulted in an increase in friction throughout the tribofilm growth and at the end-of-test when compared to no dispersant. Similarly to Dispersant A, we observed higher sulfur in the films than phosphorus, which is opposite of the ZDDP

tribofilm with no dispersant. Dispersant B resulted in a higher zinc content than no dispersant, but it was not as high as the zinc content in films formed in the presence of Dispersant A.

3.2.5 Dispersant C

After testing a fully mono-succinimide dispersant, and a mixed mono-succinimide and bis-succinimide dispersant, we moved on to a fully bis-succinimide dispersant, Dispersant C. This dispersant has an increased PIBSA content of 2:1 PIBSA to amine ratio. Dispersant C also varied in molecular weight, with the PIB tail length being double that of the other dispersants. The structure of Dispersant C is below in Figure 3 - 23.

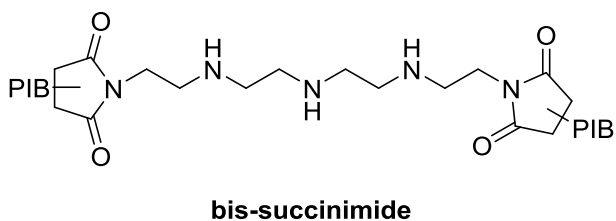


Figure 3 - 23 Dispersant C bis-succinimide structure.

Dispersant C was tested at concentrations of 1.00 wt.% and 0.50 wt.% with 1.00 wt.% ZDDP in base oil and tested in the MTM-SLIM under standard operating conditions. Similar to Dispersants A and B, we observed hindered triofilm growth when Dispersant C was present. Unlike the other two dispersants, we observed more of a difference in concentration dependence on ZDDP triofilm growth (see Figure 3 - 24). The higher concentration of Dispersant C resulted in nearly no triofilm growth as observed in the end-of-test image, Figure 3 - 25, with a

very narrow patch of tribofilm along the middle of the rubbing track. The lower concentration of Dispersant C resulted in a thicker and more even tribofilm which is also visibly very different.

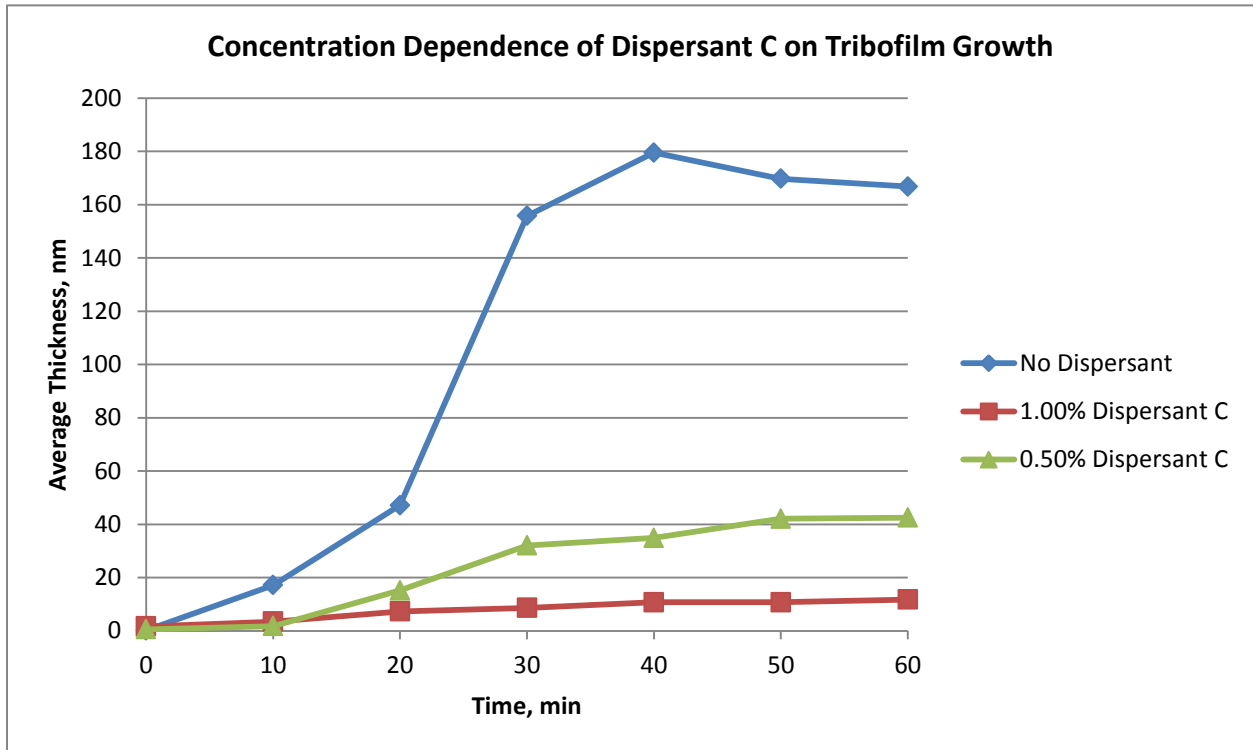


Figure 3 - 24 Concentration dependence of Dispersant C on ZDDP tribofilm growth in the MTM-SLIM over one hour.

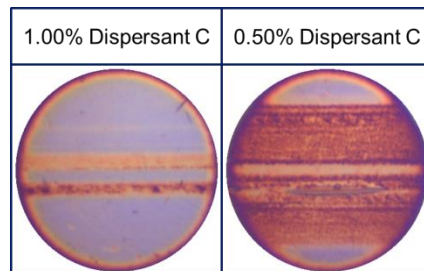


Figure 3 - 25 End-of-test images of ZDDP tribofilms formed with Dispersant C present.

We did not observe a concentration dependence on tribofilm roughness with Dispersant C, Figure 3 - 26. Since the higher concentration of Dispersant C formed almost no film, the roughness is expected to be extremely low. The lower concentration of Dispersant C which resulted in a thicker tribofilm was also very smooth although some patchiness was visually present. Again, in the case where dispersant was present and formed a tribofilm at 0.50 wt.%, the average thickness and roughness was much lower than the tribofilm that formed with no dispersant present.

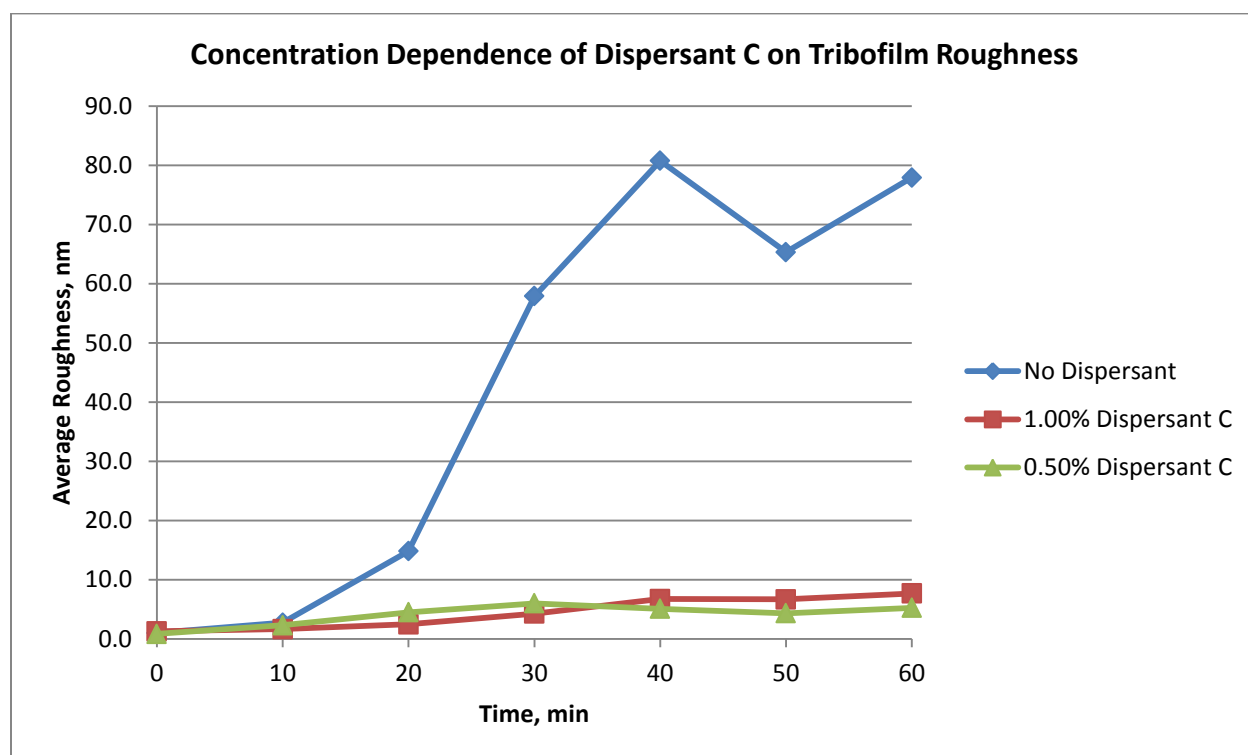


Figure 3 - 26 Concentration dependence of Dispersant C on ZDDP tribofilm roughness.

The friction throughout the tribofilm growth with 0.50 wt.% Dispersant C present resulted in a higher friction throughout and at the end-of-test compared to a film with no dispersant present, Figure 3 - 27. The friction for the higher concentration of Dispersant C was

low due to the lack of tribofilm formation. A slower progression in friction increasing was observed with dispersant present. Again, this case shows that tribofilm thickness is not correlated to tribofilm smoothness.

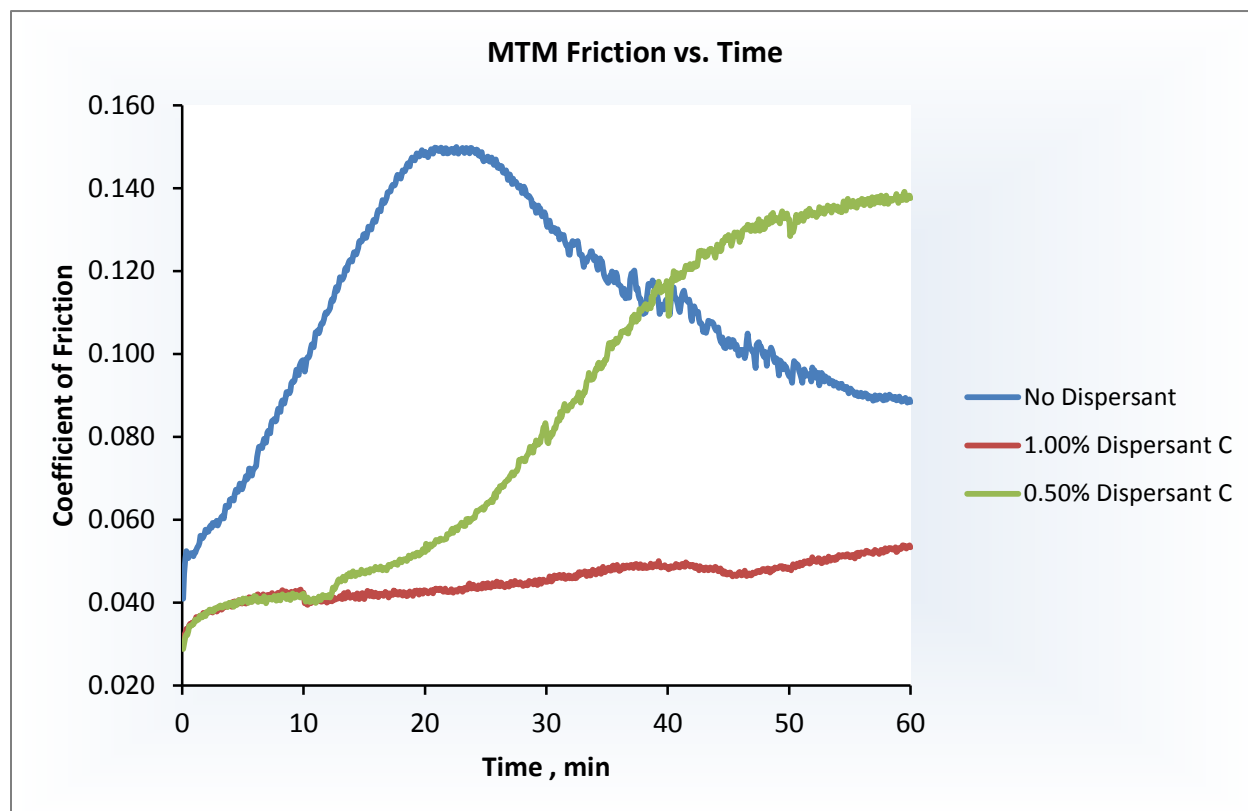


Figure 3 - 27 Concentration dependence of Dispersant C on friction throughout tribofilm growth.

The SEM-EDX images, spectra, and composition of tribofilms formed with Dispersant C can be found in Appendices 2 and 3. The evaluation of phosphorus to sulfur ratio was similar to Dispersants A and B, with a higher sulfur content rather than phosphorus in the tribofilms, Figure 3 - 28. The zinc to phosphorus ratio was closer to the film with no dispersant present, but was still slightly higher in zinc. We observed more sulfur and zinc in the tribofilm with less dispersant present.

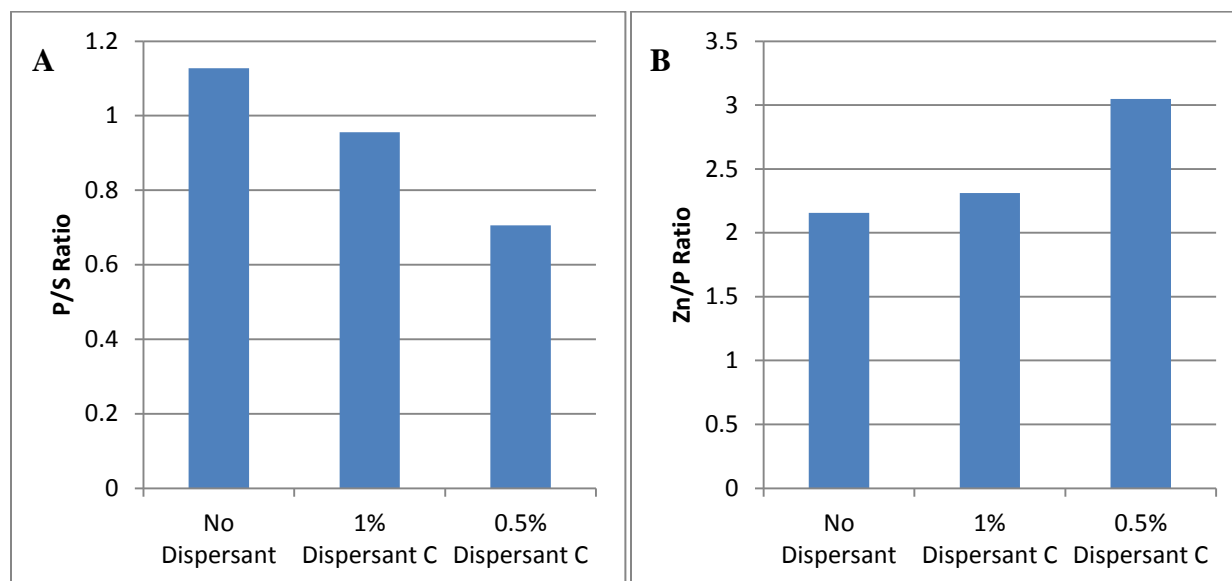


Figure 3 - 28 (A) Phosphorus to sulfur ratios of ZDDP tribofilms formed with varying concentrations of Dispersant C. (B) Zinc to phosphorus ratios of ZDDP tribofilms formed with varying concentrations of Dispersant C.

Dispersant C was the first dispersant that exhibited a major difference in tribofilm growth due to concentration. It was also the first dispersant to result in almost no tribofilm formation at the higher concentration. Although the difference between the concentrations were large in terms of tribofilm growth, it did not appear to result in a major difference in roughness, with the tribofilm formed with a lower concentration of Dispersant C being very smooth. The friction during the tribofilm growth of the film formed with a lower concentration was higher throughout the test and at the end-of-test compared to the tribofilm with no dispersant present. The SEM-EDX analysis indicates the tribofilm structure is different when Dispersant C is present.

3.2.6 Dispersant D

The next dispersant selected for testing, Dispersant D, further increases the PIBSA to amine ratio to 3.0:1.0. The resulting structure is a bis-succinimide with an acid-amide group occupying the central nitrogen, Figure 3 - 29. This structure uses the same amine reacted as the previous dispersants, but the increased PIBSA content resulted in the unique functional acid-amide group. Like the previous dispersants, Dispersant D was evaluated for its concentration dependent effects on ZDDP tribofilms.

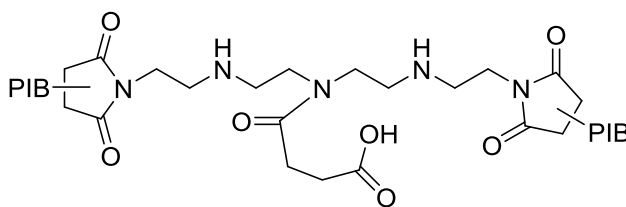


Figure 3 - 29 Dispersant D structure.

Dispersant D was tested at concentrations of 1.00 wt.% and 0.50 wt.% with 1.00 wt.% ZDDP in base oil and run in the MTM-SLIM under standard operating conditions. The same effect was observed with the use of Dispersant D as was with other dispersants compared to the tribofilm with no dispersant present. We observed much lower tribofilm growth with both concentrations of Dispersant D with differences between the two concentrations Figure 3 - 30. The end-of-test thicknesses of the two tribofilms were similar, but we observed less tribofilm growth when the higher concentration of Dispersant D was present. The end-of-test images, Figure 3 - 31, show a distinct difference between the two concentrations, with the higher

concentration of Dispersant D forming a film only in the middle of the rubbing track. The interference images of both concentrations throughout tribofilm formation can be found in Appendix 1.

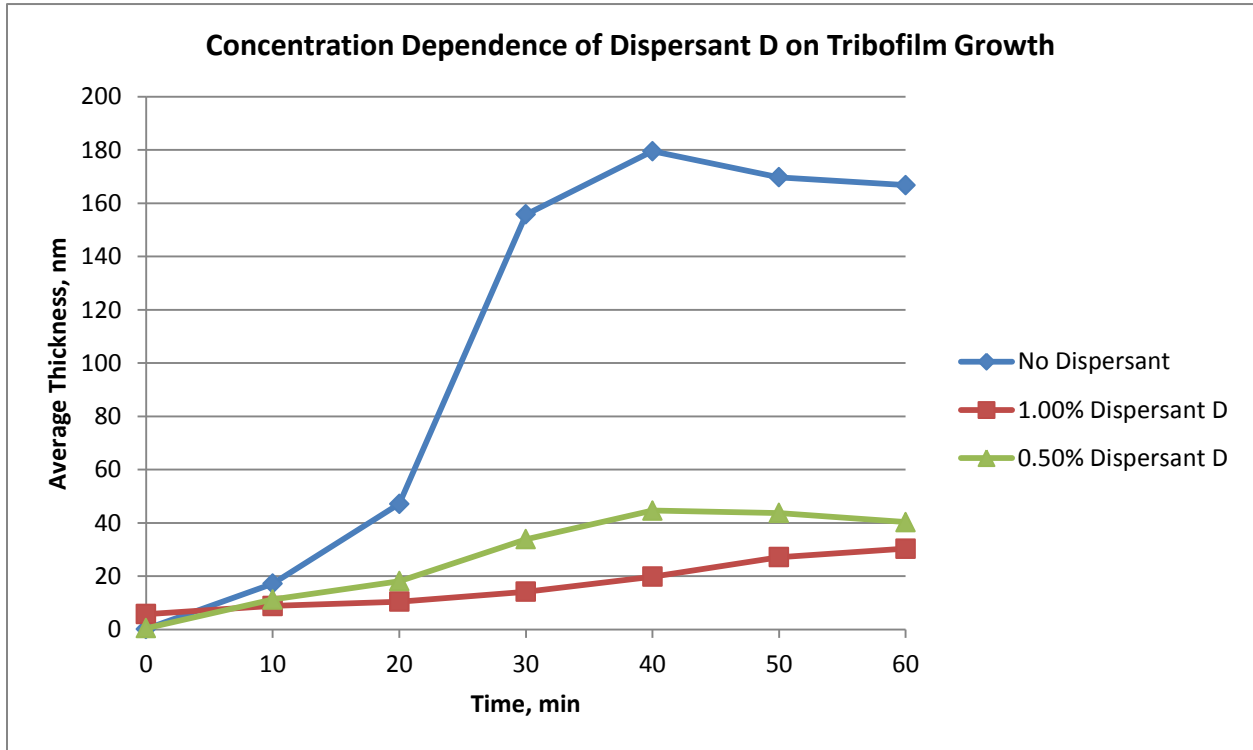


Figure 3 - 30 Concentration dependence of Dispersant D on ZDDP tribofilm growth in the MTM-SLIM over one hour.

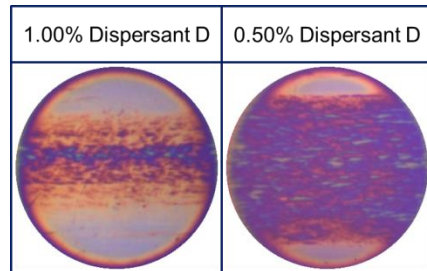


Figure 3 - 31 End-of-test images of ZDDP tribofilms formed in presence of Dispersant D.

Although the end-of-test images appear to form rough and patchy tribofilms, the average roughness at both concentrations of Dispersant D present were low, Figure 3 - 32. The two tribofilms followed nearly the same roughness track, with one minor discrepancy at the 50 minute mark. Again, the tribofilm roughness does not follow the average thickness, with the thicker film resulting in the same roughness as the thinner film, and in both cases the average thickness and roughness was lower than the tribofilm with no dispersant present.

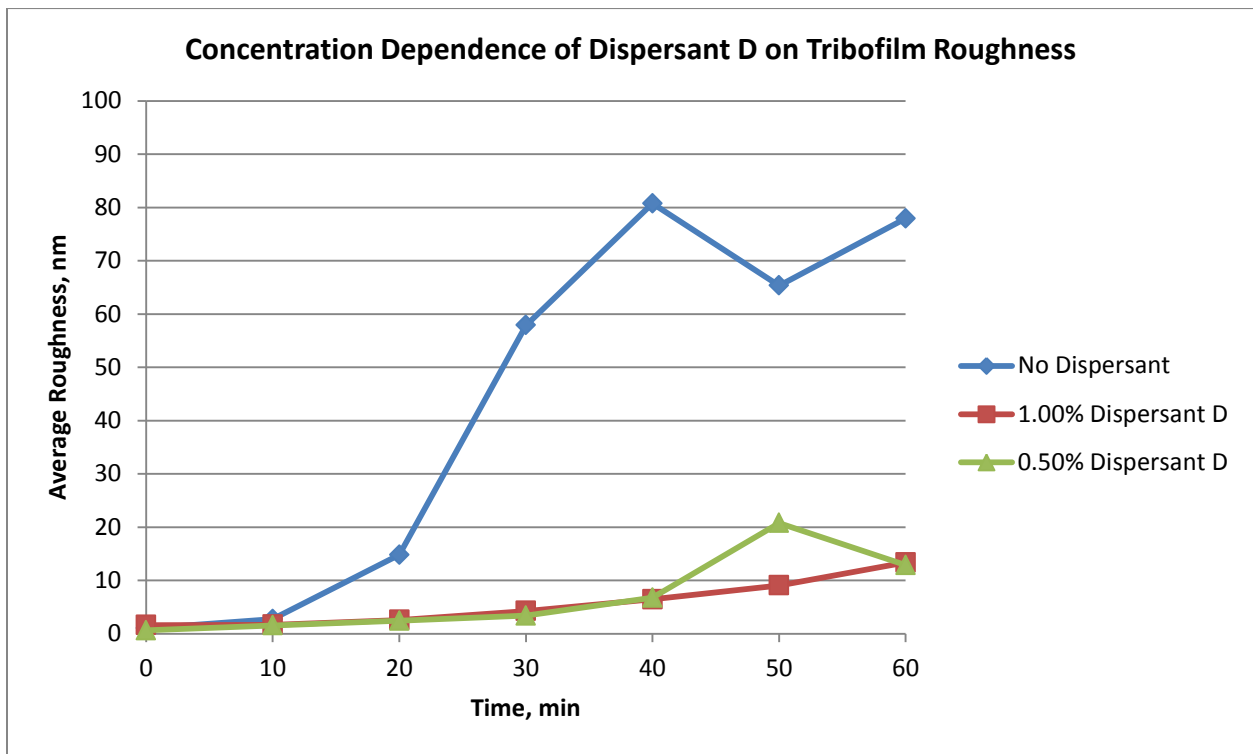


Figure 3 - 32 Concentration dependence of Dispersant D on ZDDP tribofilm roughness.

The tribofilms formed in the presence of Dispersant D both resulted in higher friction at the end-of-test than the tribofilm formed with no dispersant, Figure 3 - 33. The lower concentration of Dispersant D resulted in higher friction throughout the test and remained high at

the end-of-test. The higher concentration of dispersant had lower friction throughout most of the test, and was lower at the end-of-test. The friction of tribofilms formed with Dispersant D present followed closely with the average thickness of the films rather than the roughness.

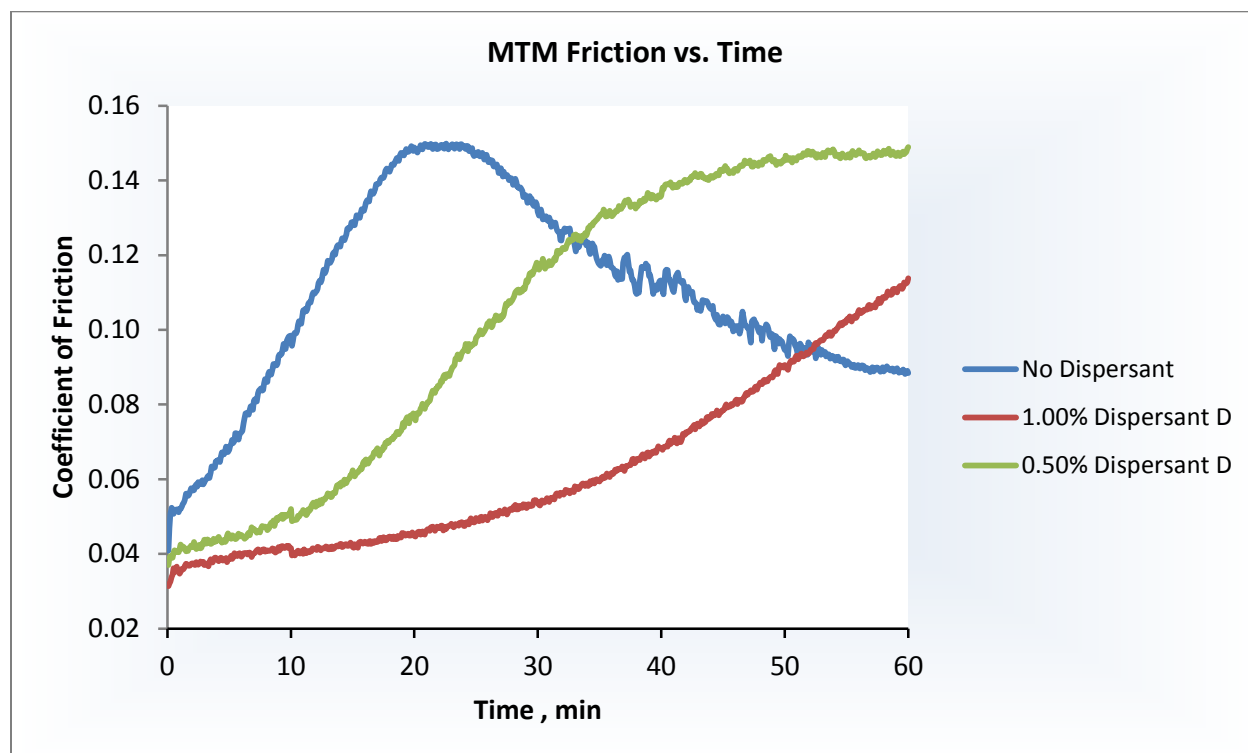


Figure 3 - 33 Concentration dependence of Dispersant D on friction throughout tribofilm growth.

The SEM-EDX image, spectra, and composition of tribofilms formed with Dispersant D can be found in Appendices 2 and 3. Dispersant D was the first dispersant where we observed a noticeable difference in tribofilm composition when compared to the previous dispersants. The phosphorus to sulfur ratio of tribofilms formed with dispersant D, Figure 3 - 34, was higher than the tribofilm with no dispersant present. With the previous dispersants, we observed the opposite

effect of lower phosphorus to sulfur ratios when compared to the tribofilm with no dispersant present. Those films were all higher in sulfur content compared to phosphorus. In the case of Dispersant D, not only is the phosphorus higher than sulfur, but the phosphorus to sulfur ratio is higher than when no dispersant is present. We observed a zinc to phosphorus ratio more similar to the ZDDP film with no dispersant present.

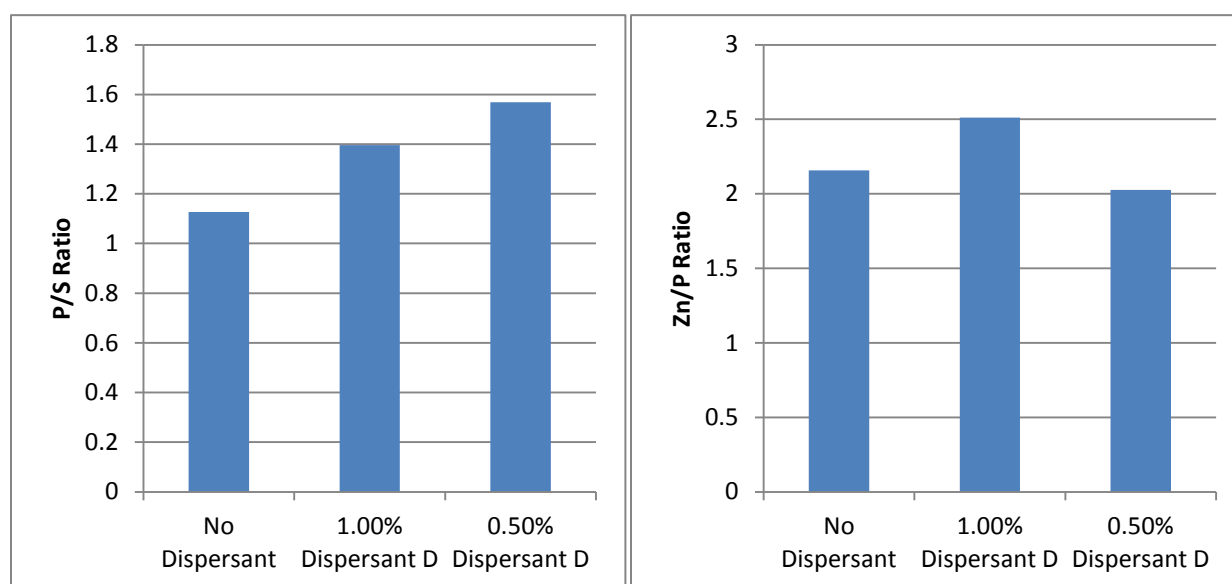


Figure 3 - 34 (A) Phosphorus to sulfur ratios of ZDDP tribofilms formed with varying concentrations of Dispersant D. (B) Zinc to phosphorus ratios of ZDDP tribofilms formed with varying concentrations of Dispersant D.

Dispersant D has a more unique structure than the previous dispersants with the added acid-amide functional group. Similarly to Dispersant C, we observed a concentration effect of this dispersant, with the higher concentration forming a film only in the middle of the rubbing track. The tribofilm roughness was low at both concentrations, but the friction was higher at the lower concentration of Dispersant D present. The elemental analysis indicates we formed a

different tribofilm structure than previously observed in all other dispersants, with Dispersant D being the first case where we observed higher phosphorus than sulfur content in the tribofilm.

3.2.7 Dispersant E

The final dispersant we selected for testing, Dispersant E, was synthesized with a different starting amine from all the previous dispersants. Dispersant E was also synthesized with the highest PIBSA to amine ratio at 6.0:1.0. The starting amine, pentaethylenehexamine, PEHA, has one more nitrogen group than the TEPA amine that was used in the previous dispersants. The resulting structure is a bis-succinimide with four acid-amide groups, Figure 3 - 35, leaving no uncapped nitrogen.

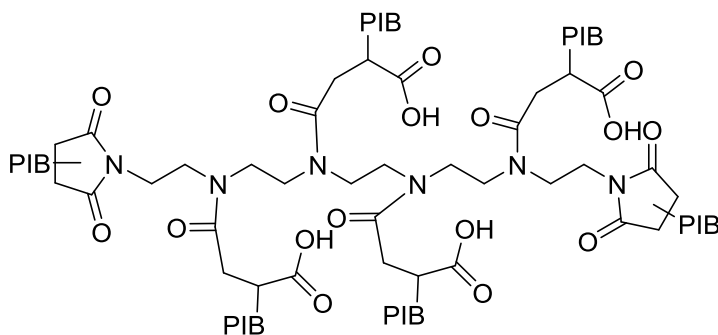


Figure 3 - 35 Dispersant E structure.

Dispersant E was blended at 1.00 wt.% and 0.50 wt.% with 1.00 wt.% ZDDP in base oil and ran in the MTM-SLIM under standard operating conditions. We observed a similar result as the other dispersants, with a much thinner film forming with Dispersant E present, Figure 3 - 38. We did see a difference between the two concentrations, with the higher concentration forming almost no tribofilm, Figure 3 - 39. Even when 0.50 wt.% Dispersant E was present, we observed

a much thinner tribofilm forming mostly in the middle of the rubbing track. The interference images for the entire test can be found in Appendix 1.

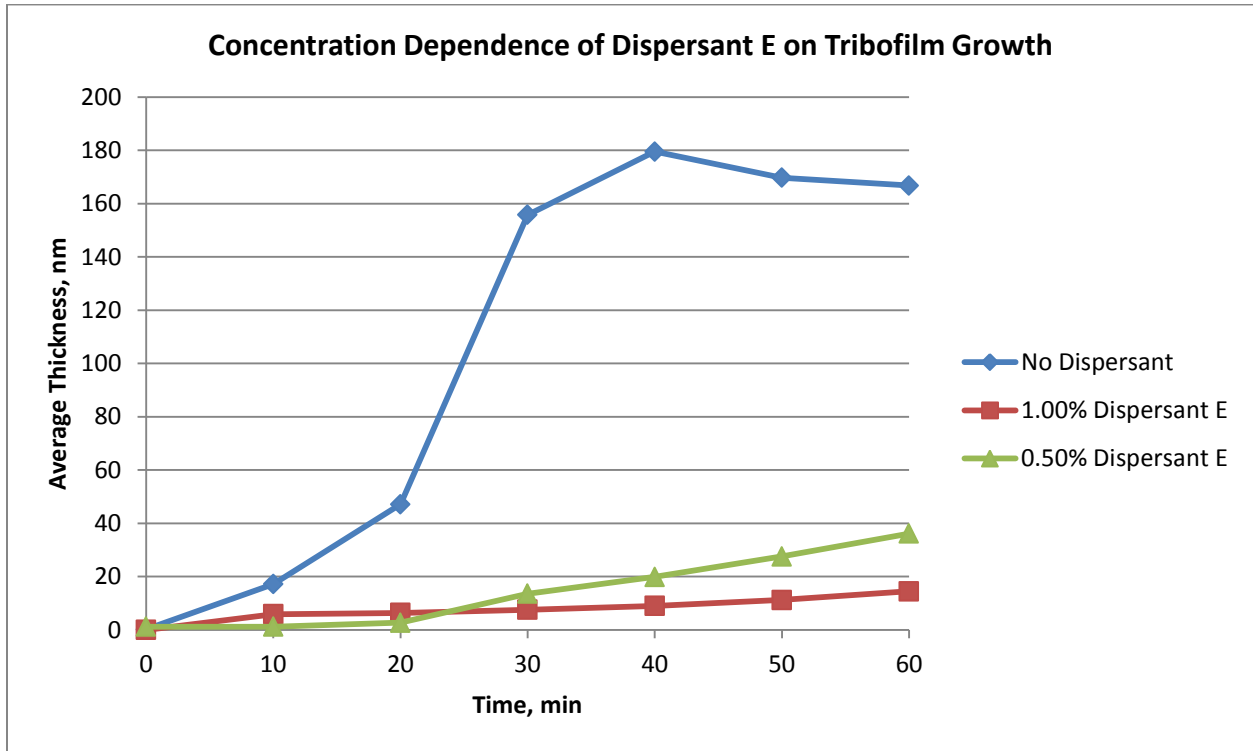


Figure 3 - 36 Concentration dependence of Dispersant E on ZDDP tribofilm growth in the MTM-SLIM over one hour.

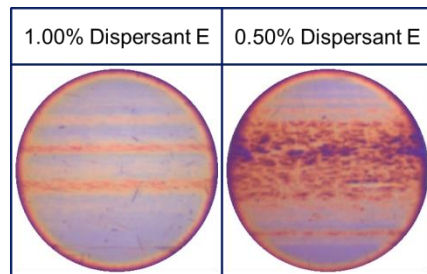


Figure 3 - 37 End-of-test images of ZDDP tribofilms formed in presence of Dispersant E.

We observed very low tribofilm roughness when both concentrations of Dispersant E were present, Figure 3 - 38. The patchy tribofilm that formed with 0.50 wt.% Dispersant E resulted in only a slightly higher roughness than the higher concentration. The roughness at both concentrations was far below the roughness we observed when no dispersant was present, similar to all the previous dispersants tested.

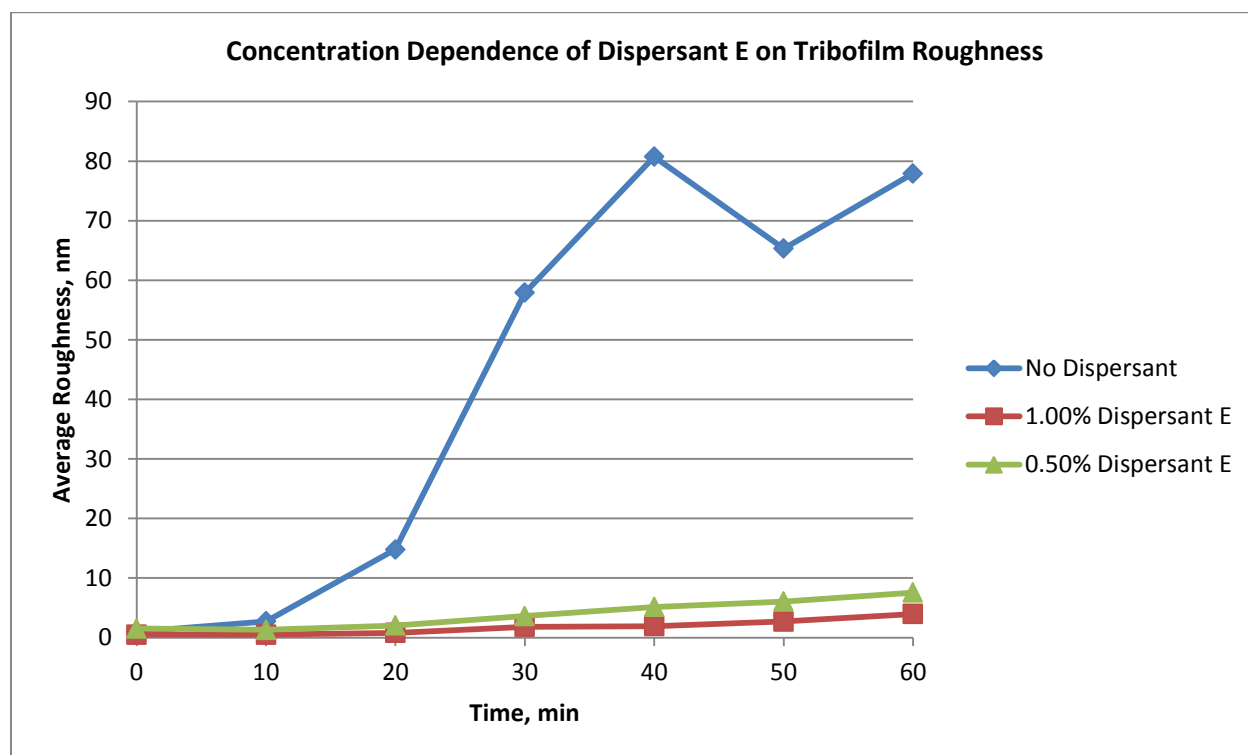


Figure 3 - 38 Concentration dependence of Dispersant E on ZDDP tribofilm roughness.

The friction of the tribofilm formed with the higher concentration of Dispersant E was low, as expected due to the lack of tribofilm formation (see Figure 3 - 39). The lower concentration of Dispersant E resulted in lower friction throughout the tribofilm growth, but ended with a higher friction than the tribofilm with no dispersant present. This observation is

similar to the previous dispersants, but the tribofilm formed with the lower concentration of dispersant resulted in lower friction during tribofilm growth than the previous dispersants.

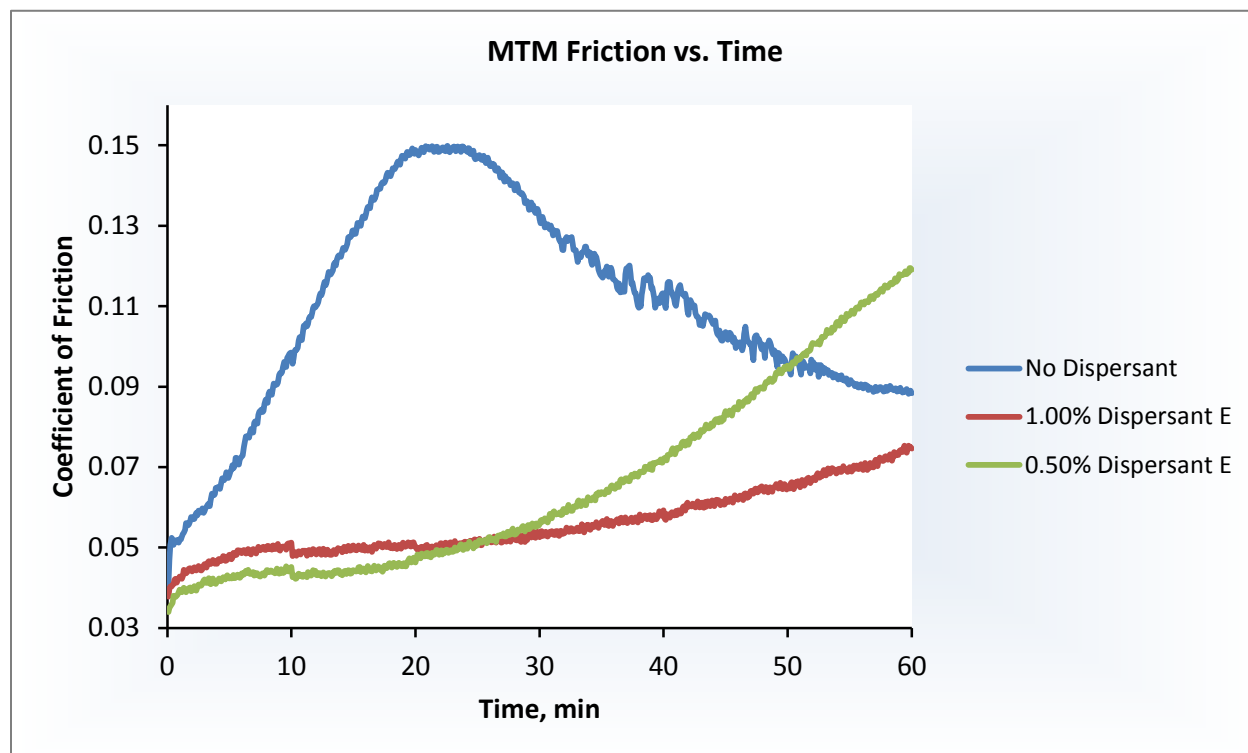


Figure 3 - 39 Concentration dependence of Dispersant E on friction throughout tribofilm growth.

The SEM-EDX images and spectra tribofilms formed with Dispersant E can be found in Appendices 2 and 3. Similarly to Dispersant D, Dispersant E was the only other film to result in a higher phosphorus content than sulfur content in the tribofilm, and with the phosphorus to sulfur ratios being higher than the film with no dispersant Figure 3 - 40. The zinc to phosphorus ratio remained close to the film with no dispersant. This observation indicates some similarity between Dispersant D and E tribofilm composition that varied from the tribofilms formed with all other dispersants present.

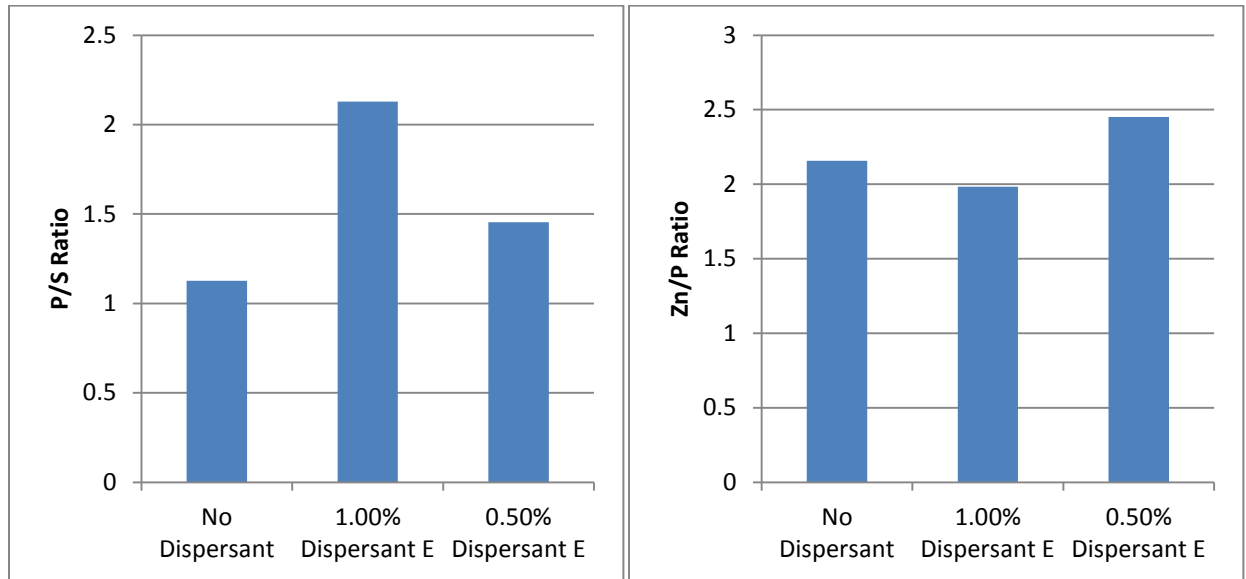


Figure 3 - 40 (A) Phosphorus to sulfur ratios of ZDDP tribofilms formed with varying concentrations of Dispersant E. (B) Zinc to phosphorus ratios of ZDDP tribofilms formed with varying concentrations of Dispersant E.

Dispersant E showed a similar trend as all the other dispersants by significantly reducing the amount of tribofilm present. It did vary from other dispersants due to almost no tribofilm formation when 1.00 wt.% dispersant was present. We did not observe any correlation between tribofilm thickness and roughness, but saw a slight correlation with tribofilm thickness and friction. The thicker film resulted in the higher friction, but the friction throughout tribofilm growth was not as high as previously observed with other dispersants. Dispersant E tribofilm composition was closely related to that of Dispersant D, and both dispersants varied from all the previous dispersants.

3.2.8 Summary of Dispersant Effects on ZDDP Tribofilms

All the dispersants we tested hindered ZDDP tribofilm growth at concentrations as low as 0.25 wt.%. The tribofilms that were formed in presence of the different dispersants were visibly different films and in the case of higher concentrations of Dispersant C and Dispersant E, no tribofilm formed. We also observed no tribofilm growth with the higher concentration of the imide form of Dispersant A. The tribofilm growth of all the dispersants in comparison with tribofilm growth of a ZDDP film with no dispersant present are combined in Figure 3 - 41 and Figure 3 - 42. Due to the overwhelming effect of the dispersants hindering ZDDP tribofilm growth, we did not observe any major correlations with dispersant structure and tribofilm thickness or roughness.

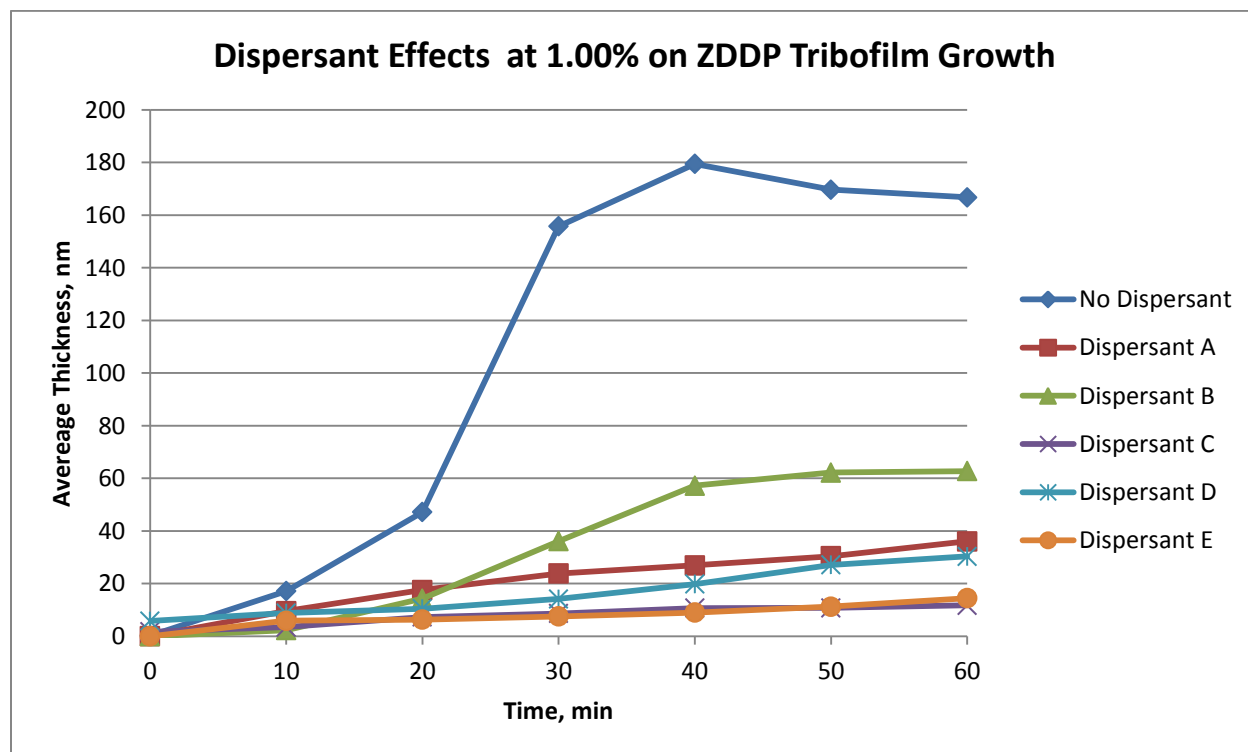


Figure 3 - 41 Dispersant effect on ZDDP tribofilm growth at a 1:1 ratio of ZDDP and dispersant.

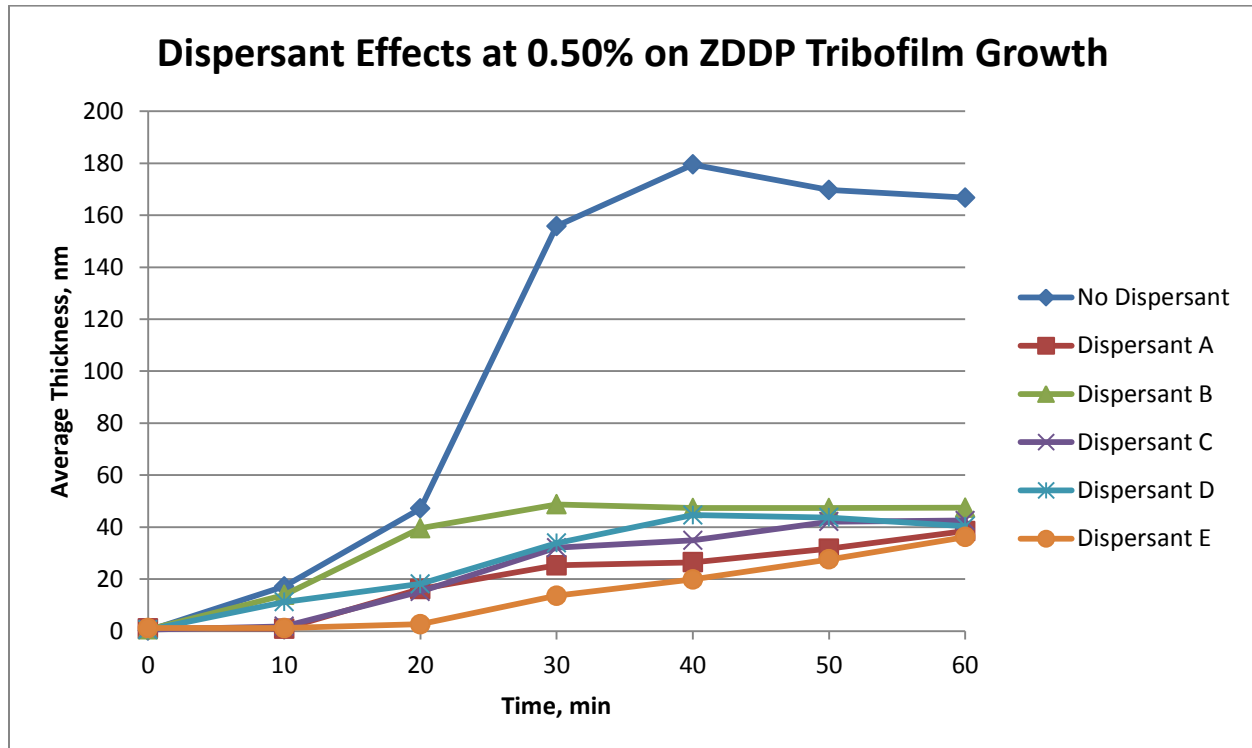


Figure 3 - 42 Dispersant effect on ZDDP tribofilm growth at a 1:0.5 ratio of ZDDP and dispersant.

The friction throughout tribofilm growth of the dispersants at the lower concentration of 0.50 wt.% are combined in Figure 3 - 43. The friction of Dispersants B, C, and D were the highest out of all the dispersants. Dispersants A and E resulted in a more gradual increase in friction rather than the rapid increase. The only dispersant resulting in similar friction as the tribofilm with no dispersant was the poly-amide form of Dispersant A. We focused on the lower concentration due to the lack of tribofilm formation at the higher concentration of some of the dispersants resulting in low friction numbers. The tribofilm friction did not appear to correlate with roughness. We did observe a correlation between the tribofilm thicknesses and friction. Dispersants B, C, and D, all resulted in the thickest tribofilms as well as the highest friction during tribofilm growth. Interestingly, all three of these films were significantly thinner than the

ZDDP film formed with no dispersant present, but they all resulted in nearly double the friction at the end-of-test.

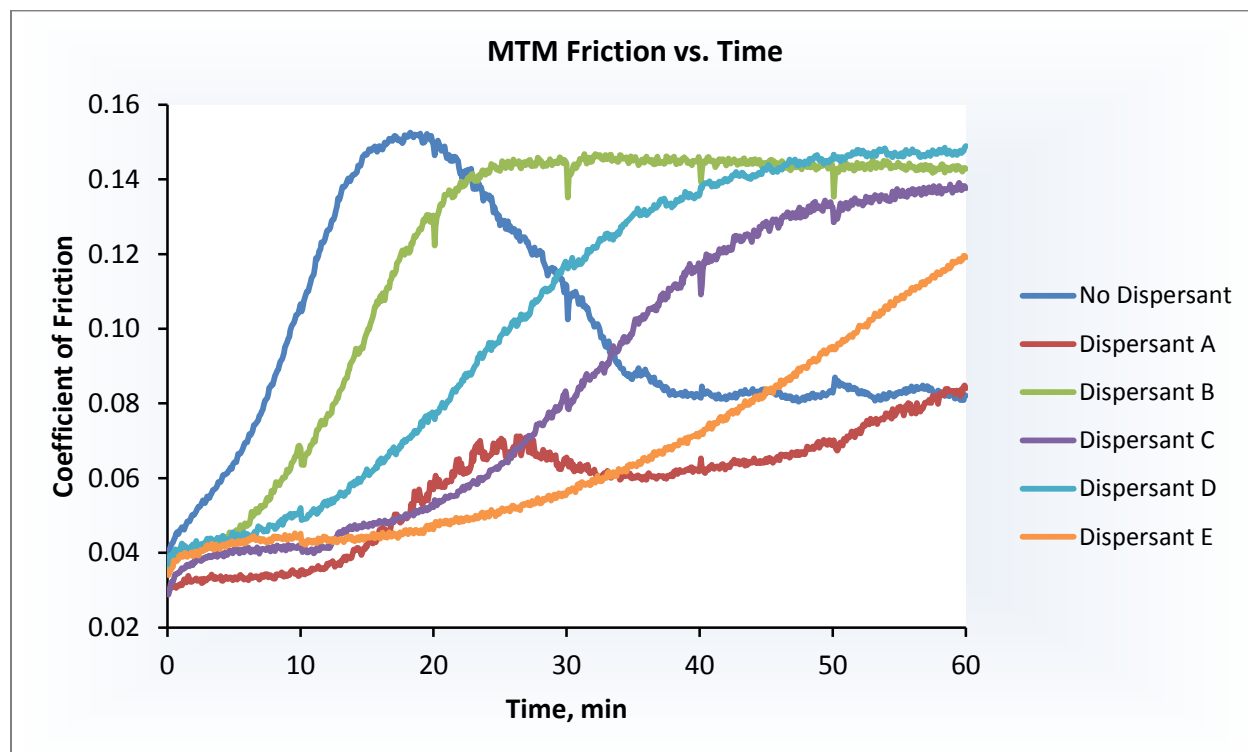


Figure 3 - 43 Dispersant effect on friction during ZDDP tribofilm growth at a 1:0.5 ratio of ZDDP and dispersant.

The most noteworthy trend we observed in ZDDP tribofilms formed with the various dispersants was after analyzing the elemental composition of all the dispersants combined. The combined phosphorus to sulfur ratios of the dispersants at both concentrations are in Figure 3 - 44. We immediately observed a distinct trend moving from Dispersant A to Dispersant E with increasing phosphorus to sulfur ratios. Dispersant D and Dispersant E were the only dispersants with more phosphorus in the tribofilm than sulfur, which is closer to the tribofilm with no dispersant. The combined zinc to phosphorus ratios of all the dispersants at both concentrations are shown in Figure 3 - 45. The Zn/P ratio remained similar between all the dispersants with the

exception of Dispersant A. Dispersant A resulted in a zinc rich film, and also had the most visually different tribofilm. The SEM-EDX analysis is indicative of different film structures in presence of the various dispersants as well as a trend moving from Dispersant A to Dispersant E. We observed a distinct difference in tribofilm composition with Dispersant D and Dispersant E that varied from all other dispersants, and was more similar to the tribofilm concentration of just a ZDDP film.

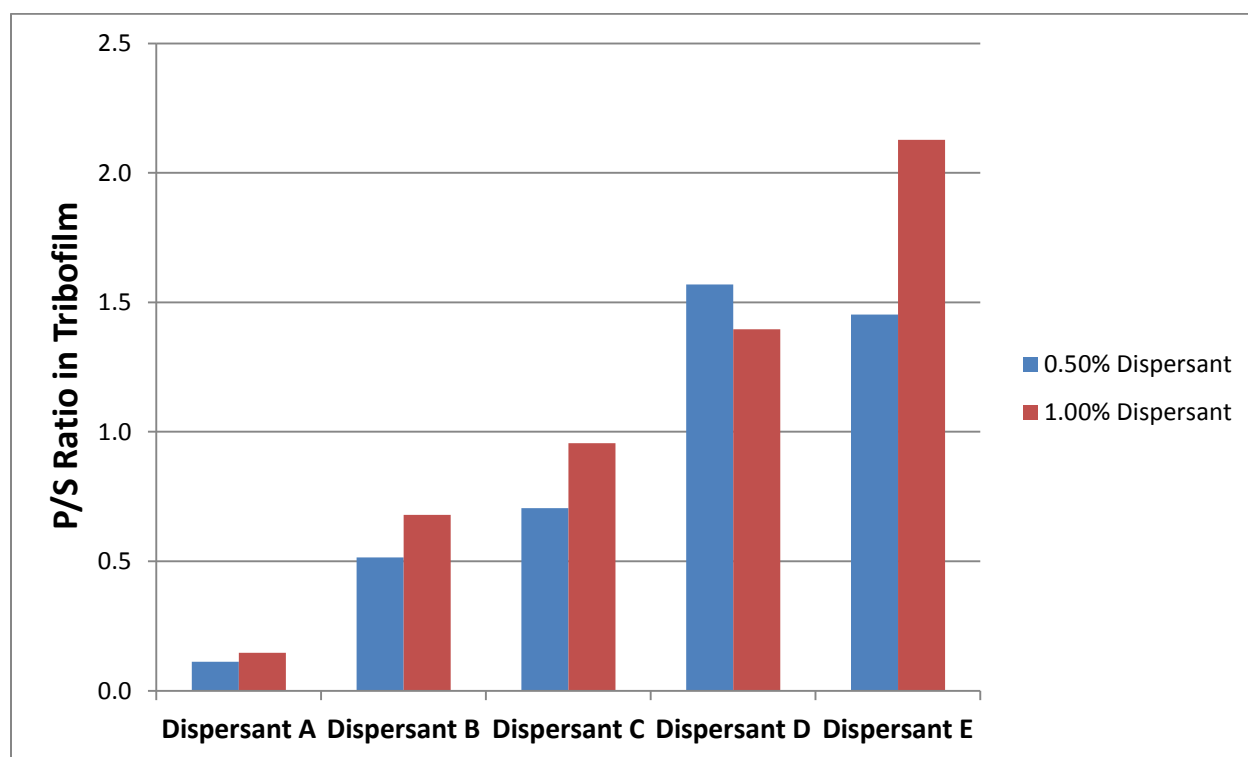


Figure 3 - 44 SEM-EDX phosphorus and sulfur analysis of ZDDP tribofilms formed in presence of dispersants.

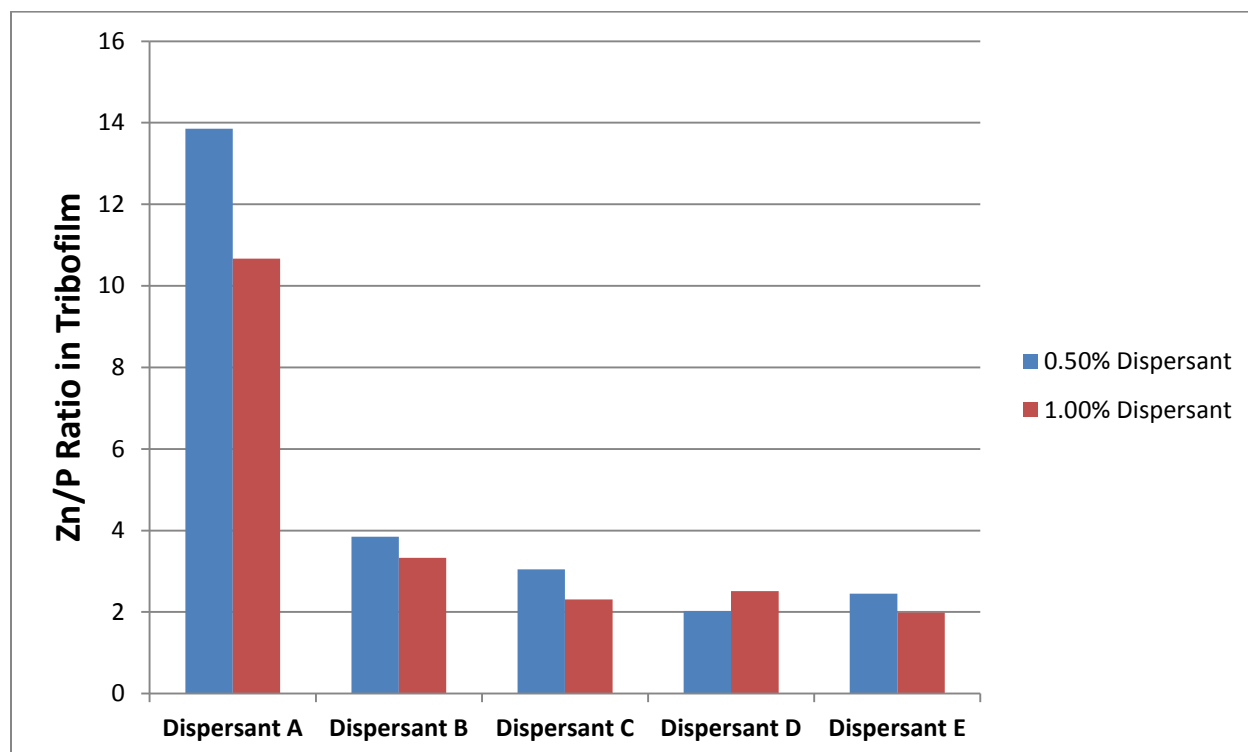


Figure 3 - 45 SEM-EDX zinc and phosphorus analysis of ZDDP tribofilms formed in presence of dispersant

Due to the noticeable trend in the phosphorus to sulfur ratio when moving from Dispersant A to Dispersant E, we decided to take a further look at differences between these dispersants. We increased the PIBSA to amine ratio when we moved from Dispersant A to Dispersant E, so we plotted the PIBSA to amine ratio against the phosphorus to sulfur ratio, Figure 3 - 46. The results indicated that we increase the phosphorus to sulfur ratio, or phosphorus content, in the tribofilm composition as we increased the number of PIBSA molecules on the amine. The two dispersants with acid-amide groups present were also the only two groups with more phosphorus than sulfur in the tribofilm.

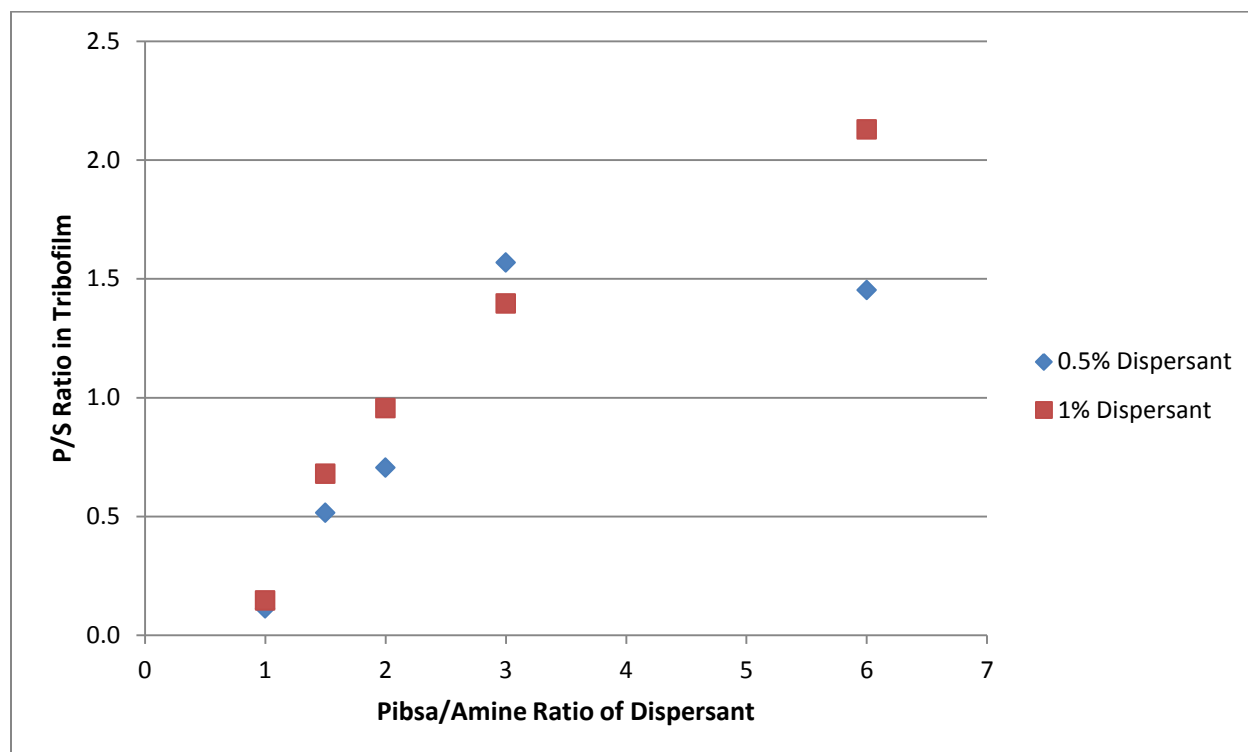


Figure 3 - 46 Phosphorus to sulfur ratio in relation to PIBSA to amine ratio in dispersant.

After combining all the results, we concluded that all the dispersants we evaluated significantly reduce ZDDP tribofilm growth at concentrations as low as 0.25 wt.%. Some dispersants even resulted in no tribofilm growth at higher concentrations. Tribofilm roughness was low in the case of all the tribofilms that were formed with dispersants present, most likely due to the films being so thin. We did not observe a correlation between tribofilm thickness and roughness. Friction was more relatable to tribofilm thickness. All tribofilms formed in presence of dispersants resulted in a higher end-of-test friction than the tribofilm formed with no dispersant present. The most significant correlation we made was after analyzing the tribofilm composition. The tribofilm composition of Dispersant D and Dispersant E varied from all the others, with higher phosphorus than sulfur in the tribofilm. These two dispersants were the only

dispersants with acid-amide groups present due to the higher PIBSA to amine ratio. The finding encouraged us to investigate the dispersant's precursors, including PIBSA.

3.3 Dispersant Precursor Effects on ZDDP Tribofilms

3.3.1 PIB

The evaluation of different dispersant's effects on ZDDP tribofilms led to a main difference in ZDDP tribofilm composition resulting from a higher ratio of the starting material. We decided to test ZDDP tribofilms formed in presence of the PIB hydrocarbon tail and the PIBSA for reference. A 1000MW PIB was blended at 1.00 wt.% and 0.50 wt.% with 1.00 wt.% ZDDP in base oil and run in the MTM-SLIM under standard operating conditions. ZDDP tribofilm growth in presence of PIB followed the growth of ZDDP tribofilms formed with no PIB present, Figure 3 - 47, confirming that there is no interaction between PIB and ZDDP. Interference images of both concentrations of PIB throughout the test are in Appendix 1.

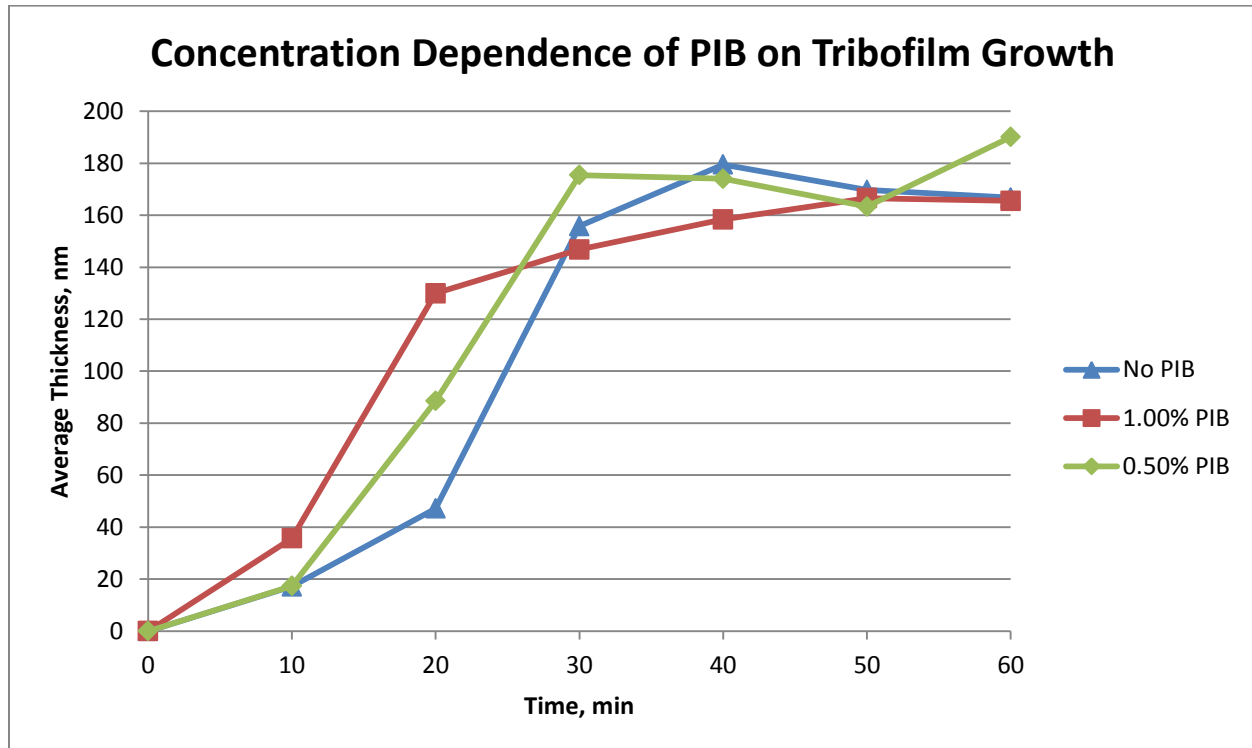


Figure 3 - 47 Concentration dependence of PIB on ZDDP tribofilm growth in the MTM-SLIM over one hour.

The friction throughout the tribofilm growth in presence of PIB resembled that of ZDDP forming with no dispersant present, regardless of PIB concentration, Figure 3 - 48. This confirmed that there is no interaction between PIB and ZDDP, and PIB does not interfere with tribofilm growth, unlike what was observed with the dispersants. We concluded that PIB has no effect on ZDDP tribofilm formation.

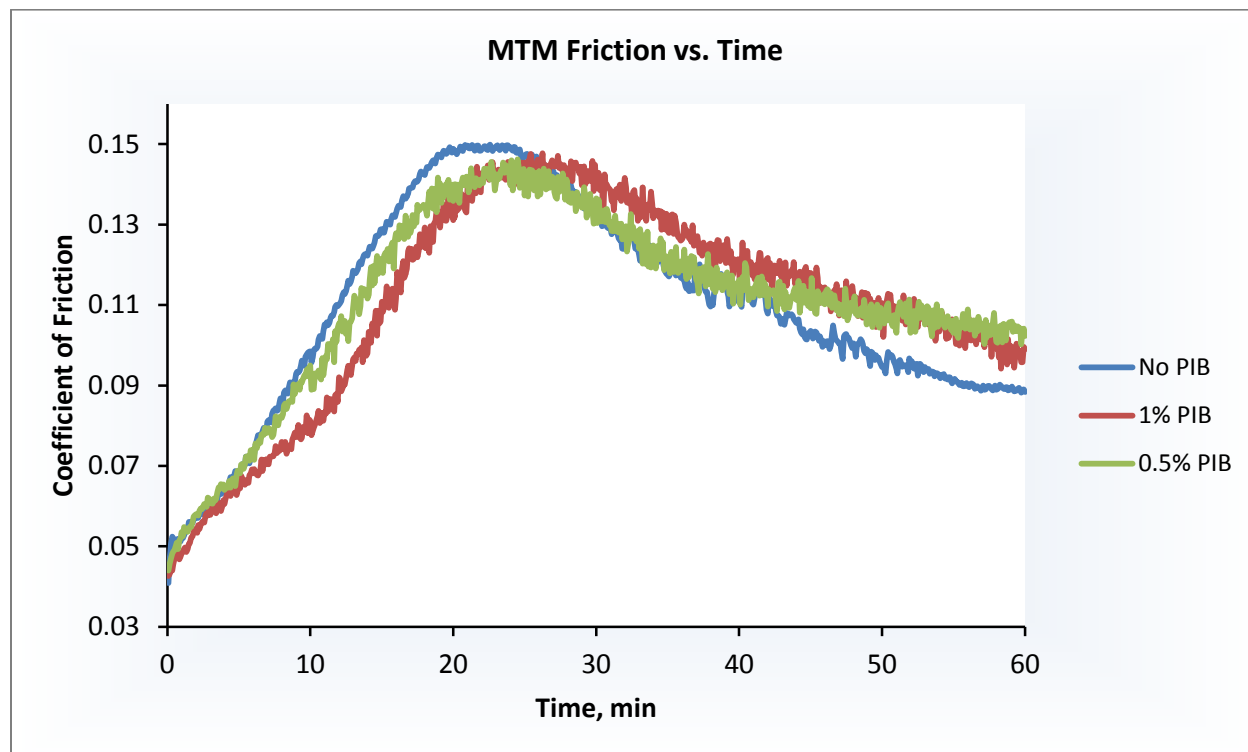


Figure 3 - 48 Concentration dependence of PIB on friction throughout tribofilm growth.

3.3.2 PIBSA

We moved forward with evaluating the dispersant's precursor, PIBSA. A 1000 MW PIBSA that was identical to the precursors of all of the dispersants was selected for testing. Due to the observed effect in tribofilm composition of dispersants correlating to PIBSA, it was evaluated more thoroughly at concentrations ranging from 0.25 wt.% to 1.00 wt.% with 1.00 wt.% ZDDP in base oil. All samples were run in the MTM-SLIM under standard operating conditions. To our surprise, the ZDDP tribofilms formed with PIBSA present had similarities to the tribofilms formed in presence of dispersants, Figure 3 - 49. The higher concentrations of PIBSA, 0.75 wt.% and 1.00 wt.%, resulted in no tribofilm growth. The tribofilm growth was minimal at 0.50 wt.%, and did not begin forming until after 40 minutes of rubbing. The lowest

concentration of PIBSA resulted in the thickest film, but even that film was lower than the film without PIBSA and the growth was more gradual. The end-of-test images of the tribofilms, Figure 3 - 50, show the film visually disappearing as the PIBSA concentration increases. The interference images of the tribofilms formed in presence of PIBSA can be found in Appendix 1.

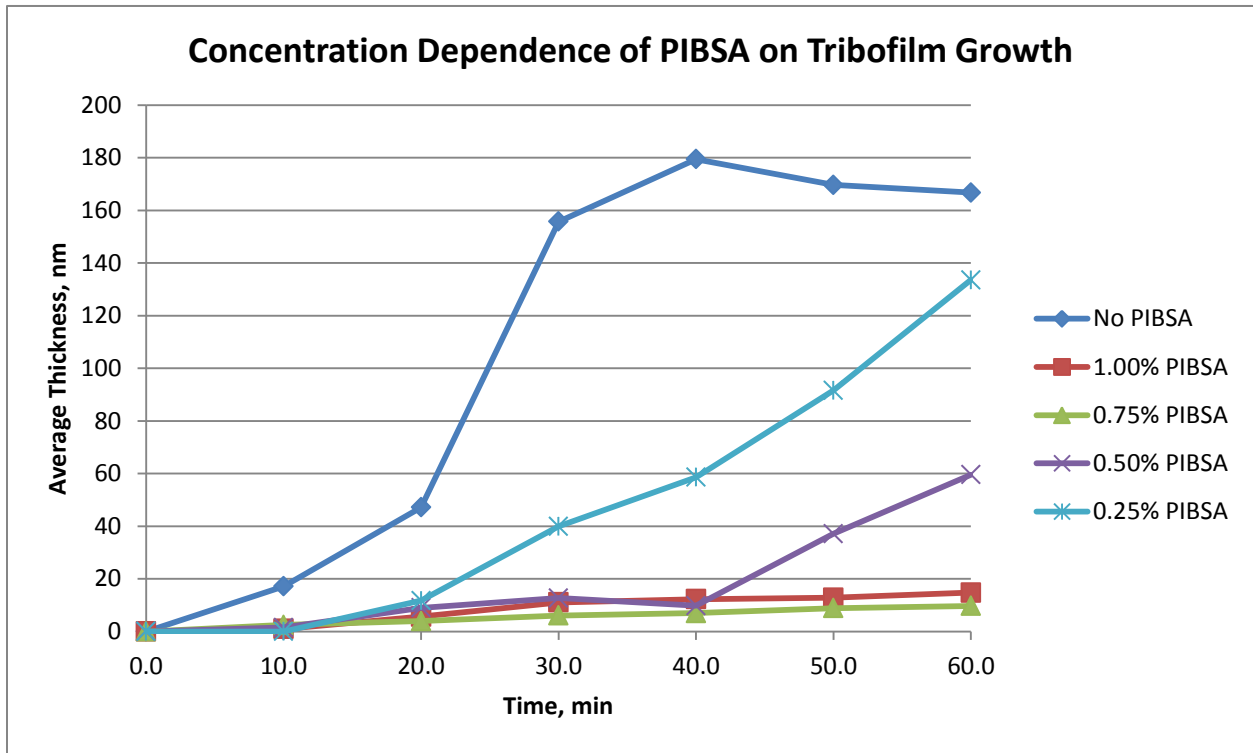


Figure 3 - 49 Concentration dependence of PIBSA on ZDDP tribofilm growth in the MTM-SLIM over one hour.

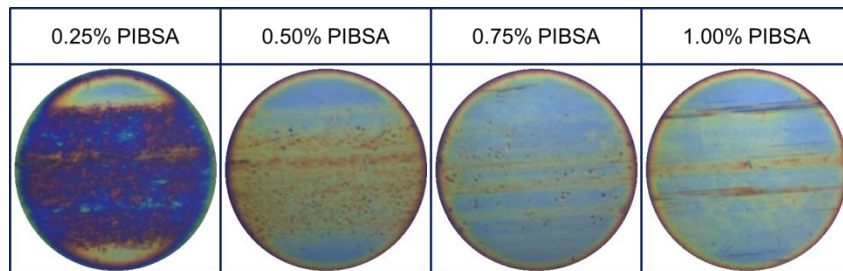


Figure 3 - 50 End-of-test images of ZDDP tribofilms formed in presence of varying concentrations of PIBSA.

The friction throughout ZDDP tribofilm growth in presence of varying concentrations of PIBSA followed closely with the friction of the dispersants that were previously used, Figure 3 - 51. The friction curves of tribofilms formed with PIBSA were concentration dependent, with the lowest concentration of PIBSA resulting in the highest friction. Similar to the tribofilm thickness, we observed a more gradual increase of friction with 0.50 wt.% PIBSA present. The end-of-test friction was still higher than the ZDDP film formed with no PIBSA present. The ZDDP tribofilms formed using higher concentrations of PIBSA resulted in nearly no tribofilm formation and low friction. The friction curves did appear to correlate well with tribofilm thickness.

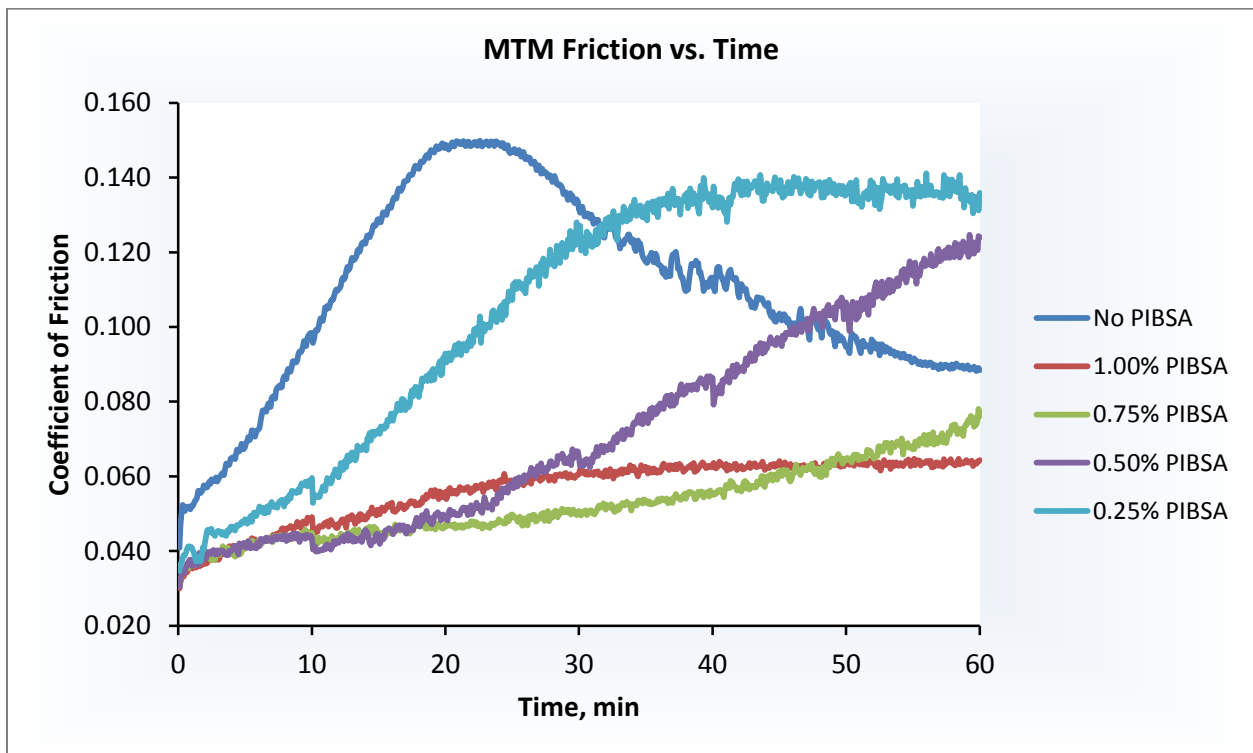


Figure 3 - 51 Concentration dependence of PIBSA on friction throughout tribofilm growth.

The SEM-EDX images and spectra of tribofilms formed in presence of PIBSA can be found in Appendices 2 and 3. The analysis of elemental composition resulted in similar tribofilm composition regardless of the PIBSA concentration, Figure 3 - 52. The phosphorus to sulfur ratios of all the tribofilms formed in presence of PIBSA were higher than the tribofilm formed with ZDDP only. This result was similar to the phosphorus to sulfur ratio of tribofilms formed in presence of Dispersant D and Dispersant E. The zinc to phosphorus ratio was similar to the tribofilm formed with no PIBSA regardless of PIBSA concentration. The composition of the tribofilms formed in presence of PIBSA closely resembled those of the dispersants with high PIBSA charges.

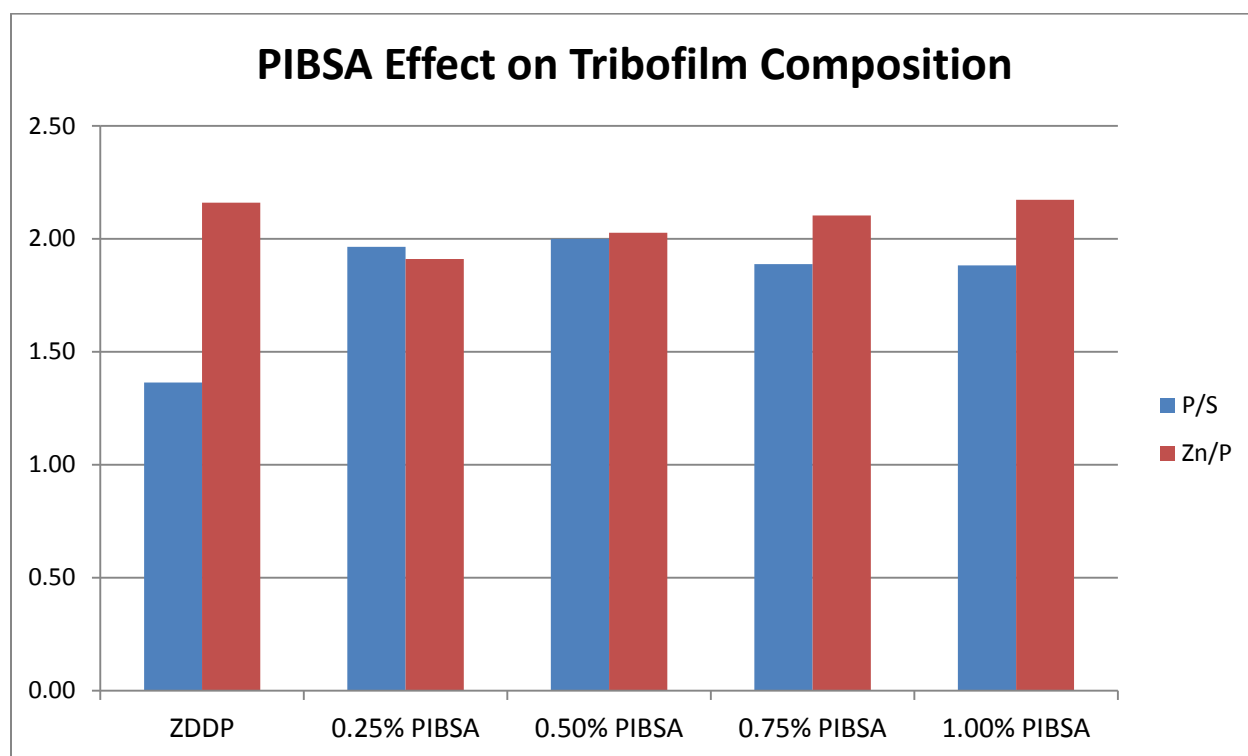


Figure 3 - 52 SEM-EDX phosphorus to sulfur and zinc to phosphorus ratios for ZDDP films formed with varying concentrations of PIBSA.

3.3.3 PIB Di-acid

The correlations between tribofilms formed in presence of PIBSA and the dispersants that used excess PIBSA led us to force open the anhydride ring in order to test the di-acid form of the molecule. The same PIBSA that we used for testing above was hydrolyzed and tested, Figure 3 - 53.

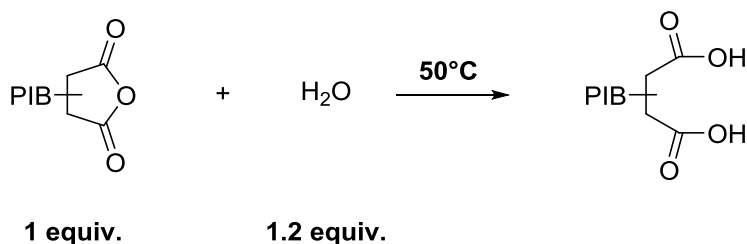


Figure 3 - 53 Conversion of PIBSA to di-acid form.

The di-acid form of PIBSA was blended at lower concentrations of 0.25 wt.% and 0.10 wt.% with 1.00 wt.% ZDDP in base oil and run in the MTM-SLIM under standard operating conditions. The di-acid had a significant effect by hindering ZDDP tribofilm growth at concentrations as low as 0.10 wt.%, Figure 3 - 54. We observed no tribofilm growth with addition of the PIB di-acid at both of the concentrations tested.

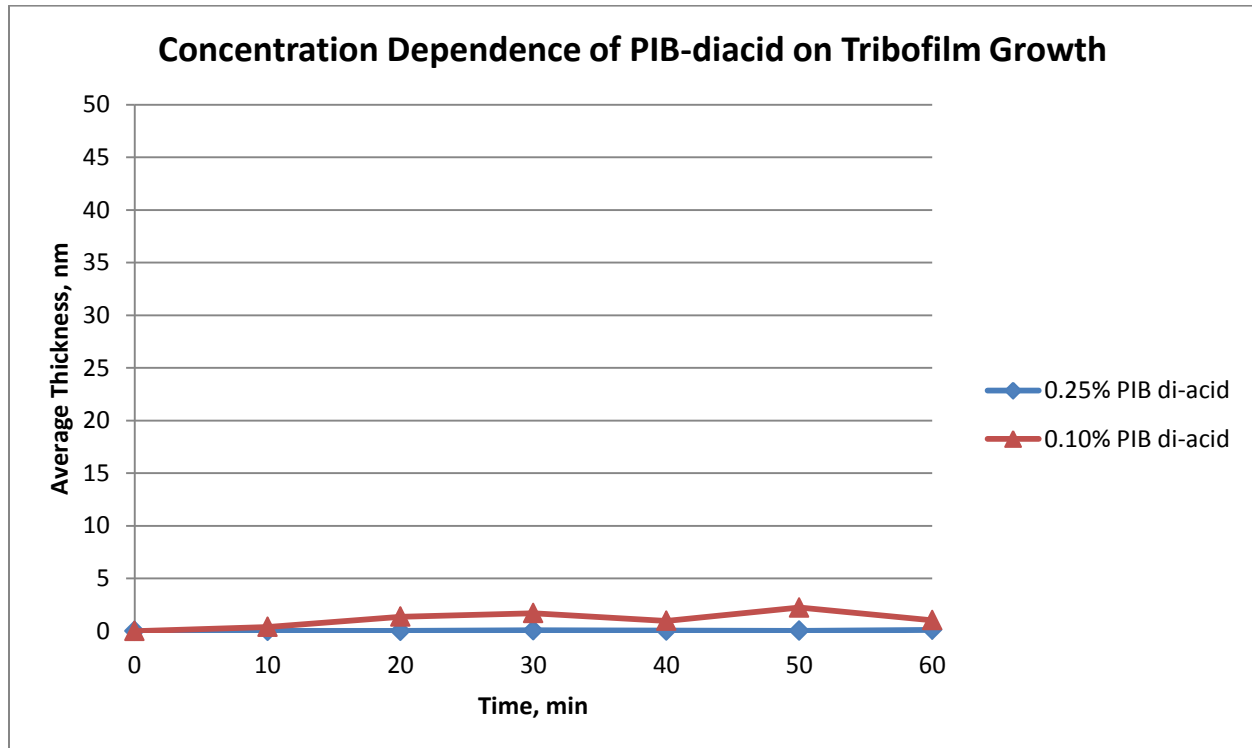


Figure 3 - 54 Concentration dependence of PIB di-acid on ZDDP tribofilm growth in the MTM-SLIM over one hour.

3.4 Dispersant Effects on Tribofilm Removal

After our observations on the dispersant's effect on ZDDP tribofilm formation, we were interested in evaluating the dispersant's ability to remove existing ZDDP tribofilms. ZDDP tribofilms were formed in the MTM-SLIM over the course of one hour with 1.00 wt.% ZDDP in base oil solutions. At the end of the test, we removed the oil with ZDDP and cleaned the ball, disc, and sump from residual oil. Without moving the placement of the ball or disc, we filled the sump with a fresh oil containing a dispersant and ran the test for one hour measuring the tribofilm thickness at the end of the test. With no ZDDP present in the second run, we were able to evaluate if dispersants alone modified the existing tribofilm.

We referenced this test method with just base oil to show that rubbing alone without dispersant does not remove the existing ZDDP tribofilm, the red bar in Figure 3 - 55. A few of the dispersants tested previously were selected and tested at a 0.50 wt.% concentration in base oil. PIBSA was also evaluated at the higher concentration of 1.00 wt.% in order to gain its full effect if there was one. The results indicated that dispersants and PIBSA remove previously existing ZDDP tribofilms, regardless of dispersant structure. The average tribofilm thickness of the existing ZDDP film was reduced by about one half in all cases of dispersant and PIBSA.

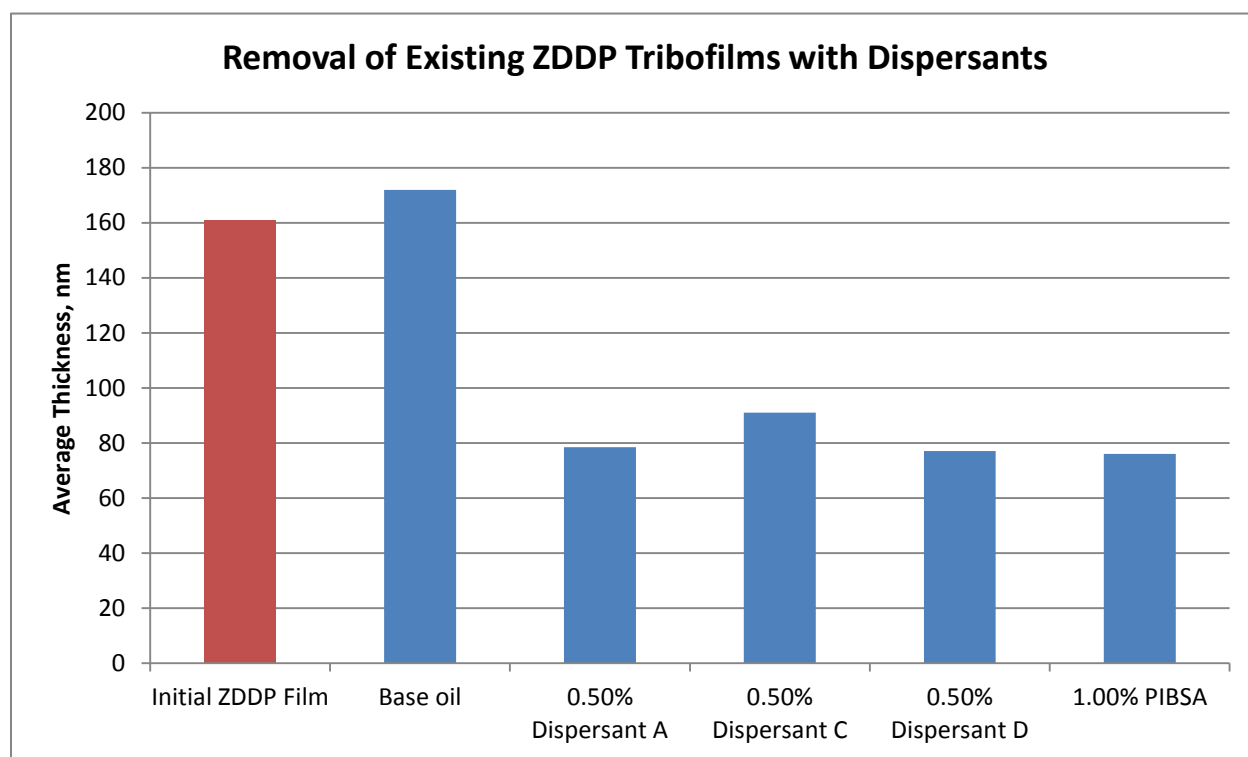


Figure 3 - 55 ZDDP tribofilm removal by dispersants after one hour of rubbing time.

The SEM-EDX images, spectra, and composition of ZDDP tribofilms removed with dispersants can be found in Appendices 2 and 3. The tribofilm composition of ZDDP tribofilms removed by dispersants resembled the composition of the original ZDDP tribofilm indicating

there was no modification to the composition (see Figure 3 - 56). The ZDDP tribofilm removed by PIBSA had slightly lower zinc to phosphorus ratio. We did not observe differences in tribofilm composition as we did with ZDDP tribofilms formed in presence of dispersants and PIBSA. This indicates that the tribofilm growth process in presence of dispersant varies from the tribofilm removal, but in both cases dispersants and PIBSA interact with the ZDDP.

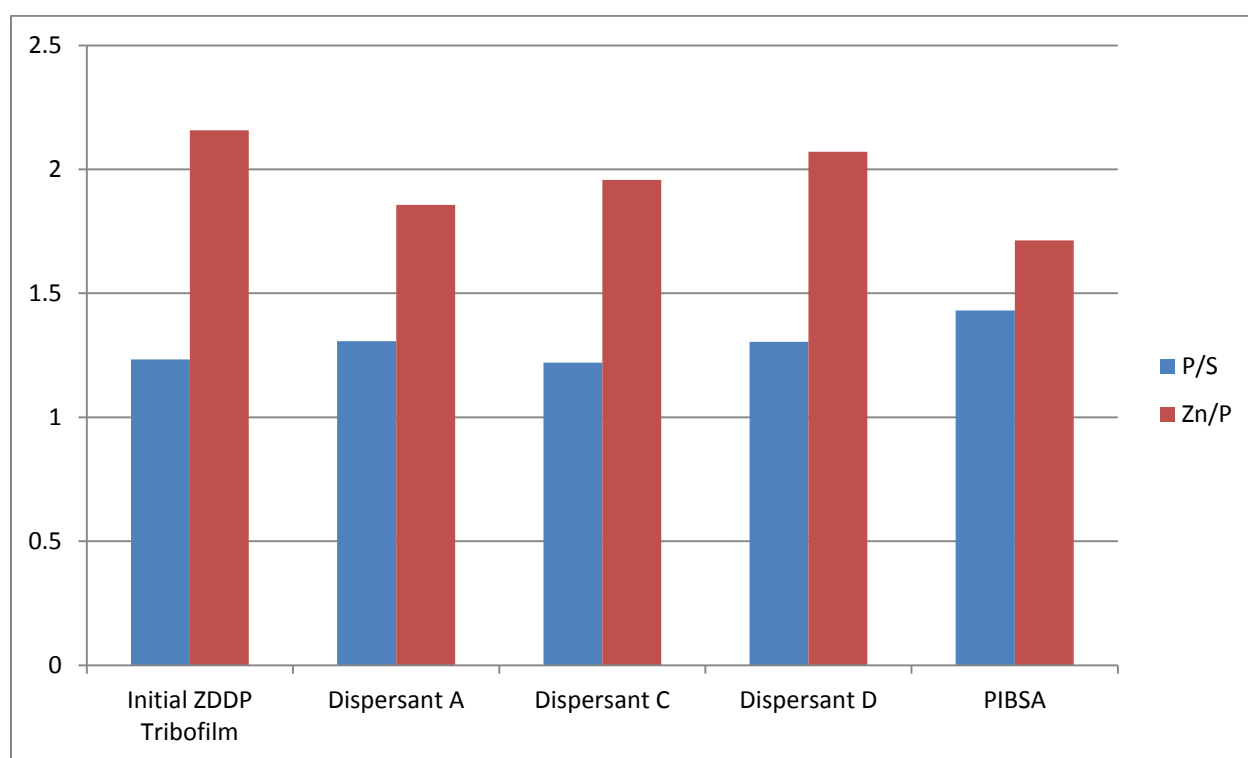


Figure 3 - 56 SEM-EDX analysis of ZDDP tribofilms after removal by dispersants.

3.5 Discussion of Results

All five of the dispersants selected for testing resulted in significant hindrance of ZDDP tribofilm growth with some dispersants resulting in no tribofilm growth at higher concentrations.

There were no major correlations between surface roughness and tribofilm thickness, but the friction throughout tribofilm growth closely correlated with tribofilm thickness. In all cases, the end-of-test friction was higher than the ZDDP tribofilm formed with no dispersant. The major finding from the dispersant work was in the differences in tribofilm compositions. The dispersants with higher PIBSA loading, resulting in acid-amide groups present in the molecule, were the only dispersants with higher phosphorus than sulfur in the composition. This closely resembled the tribofilm that was formed with ZDDP only. The dispersants with only imide functional groups in the molecule all had higher sulfur than phosphorus content.

The higher phosphorus trend with increasing PIBSA led us to test the dispersant precursors. An evaluation of PIB resulted in no interaction with ZDDP, with tribofilms closely resembling that of no PIB present. Surprisingly, we observed a concentration dependence of PIBSA affecting ZDDP tribofilm formation, similar to dispersants. Elemental composition of tribofilms formed in presence of PIBSA also resembled the analysis of the two dispersants with excess PIBSA. We forced open the ring on the PIBSA molecule, forming the PIB di-acid and tested it at very low concentrations. We observed no tribofilm growth even in presence of very low concentrations of PIB di-acid. The evaluation of dispersant precursors validated their correlation with the dispersant effect. The noticeable difference in tribofilm composition of Dispersant D and Dispersant E may be a result of the acid-amide group.

After evaluating the effects of dispersants and their precursors on tribofilm growth, we tested the dispersant's ability to remove existing ZDDP tribofilms. A few of the dispersants and PIBSA were selected for their tribofilm removal properties. In all cases, we observed a removal of nearly half of the ZDDP film. This removal does not occur with just base oil alone, indicating there is some reaction between the dispersants, PIBSA, and ZDDP. The tribofilm composition

of the ZDDP tribofilm that was reduced by dispersants resembled the original ZDDP tribofilm. This indicated there is a difference in tribofilm composition between ZDDP tribofilm growth in presence of dispersants, and removal by dispersants.

After completing the MTM-SLIM work, we can conclude that dispersants hinder ZDDP tribofilm growth and increase friction. Dispersants with acid-amide groups present resulted in higher phosphorus in the tribofilm composition, whereas dispersants without the acid-amid group present were higher in sulfur. We correlated the dispersants with higher PIBSA loading to the PIBSA molecule, and further correlated it to the more extreme case of PIB di-acid. We can also conclude that dispersants and PIBSA not only impact tribofilm growth, but can also remove existing ZDDP tribofilms. After defining the dispersant's effect on ZDDP tribofilms, we moved on in evaluating if this effect was a surface phenomenon or interaction in the bulk fluid.

3.5.1 Surface and Bulk Fluid Interactions

The evaluation of dispersant's effect on ZDDP films using the MTM-SLIM, and analysis of the tribofilms in the SEM-EDX clearly defined the dispersant's role in modifying ZDDP tribofilm growth, removal, and elemental composition. After we observed significant changes in ZDDP tribofilms in presence of dispersants we decided to explore how dispersants may interact with ZDDP tribofilms. We predicted the observations in the MTM-SLIM and SEM-EDX may be due to a surface phenomenon, such as surface competition, or a reaction occurring in the bulk fluid between the dispersant and ZDDP.

A Quartz Crystal Microbalance with Dissipation (QCM-D) was used to measure adsorption of molecules on a stainless steel coated quartz crystal. The QCM-D uses an

oscillating quartz crystal to measure mass adsorbed to the surface by measuring changes in the crystal's initial known frequency. When a sample fluid passes through the cell containing the oscillating quartz crystal, the frequency decreases as mass adsorbs to the surface. The change in frequency is measured, indicating how much mass is adsorbed to the surface. The dissipation feature measures the film elasticity or rigidity by measuring the energy lost as an applied voltage is turned on and off. Dissipation allows us to monitor if films are rigid mono-layers or viscoelastic. As viscoelasticity of films increases, we observe an increase in dissipation, whereas rigid films result in dissipation values around zero.

We began with evaluating ZDDP at 1.00 wt.% in isooctane. Isooctane was the standard solvent used for our QCM-D testing due to base oil being too viscous. Prior to each test a base line frequency was measured using just isooctane. Once a stable base line is achieved, the test sample was flushed into the cell. It is important to note the QCM-D only measures adsorption at temperatures up to 50°C, therefore ZDDP adsorption would be of the molecule prior to its decomposition. The QCM-D analysis of ZDDP over 30 minutes is shown in Figure 3 - 57. The base line measured just isooctane for nearly 10 minutes, and then switched to the test sample. At the end of the 30 minute test sample period, we ran isooctane through the cell to measure desorption. The point at which the sample containing ZDDP entered the cell is apparent in the immediate decrease in frequency. ZDDP was run twice to measure test variability. The dissipation indicates a slightly viscoelastic film, with nearly identical dissipation from Run 1 to Run 2. The steady decrease in frequency indicates that ZDDP was continuously adsorbing to the surface even at the end of the 30 minute period. We did not observe desorption when we ran isooctane after the test sample was completed.

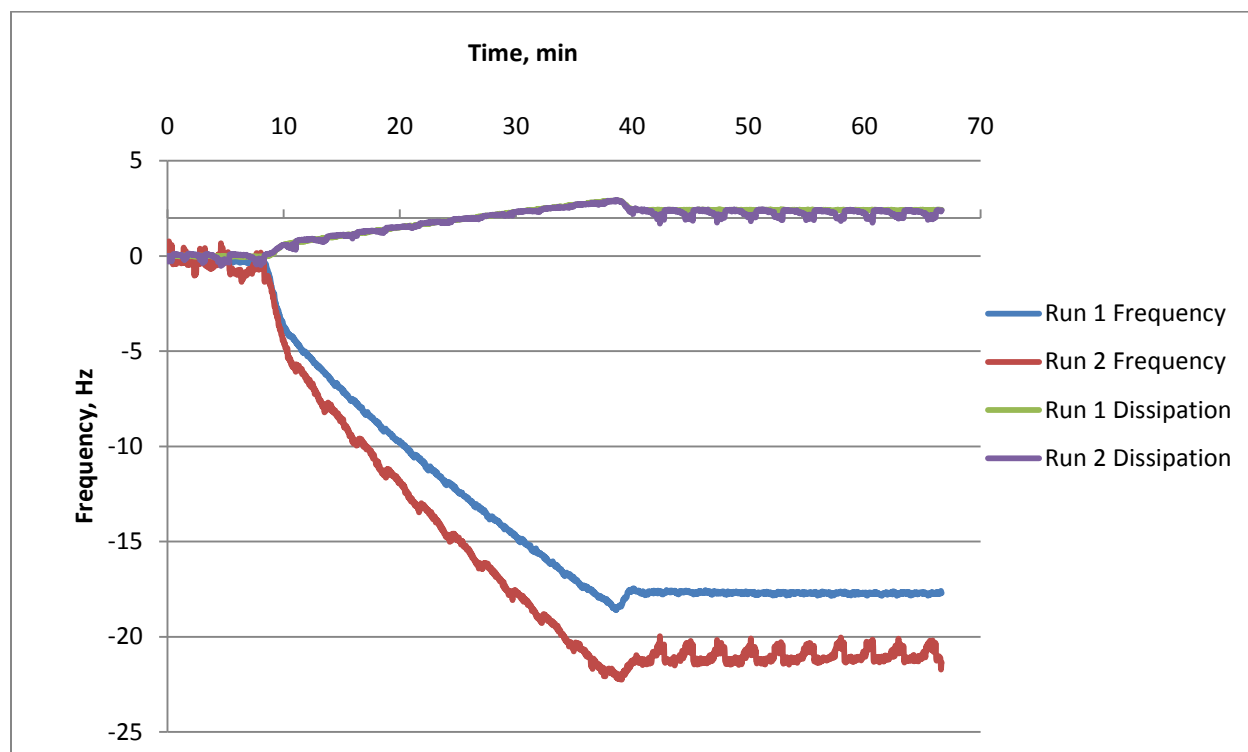


Figure 3 - 57 QCM-D evaluation of 1.00 wt.% ZDDP in isooctane.

After discovering the most notable effect from the dispersants being due to PIBSA content, PIBSA was selected for evaluation in the QCM-D. PIBSA was tested under the same conditions as ZDDP, at 50°C for 30 minutes, followed by isooctane. The adsorption of PIBSA was very different from that of ZDDP, seen in Figure 3 - 58. PIBSA was much more surface active, immediately adsorbing to the surface upon arrival of test sample to the cell. The leveling off of frequency and lack of increase in dissipation indicates a rapid adsorption with no further layering. The isooctane rinse at the end of the 30 minute sample period resulted in a slight desorption of material. The two test runs resulted in good reproducibility.

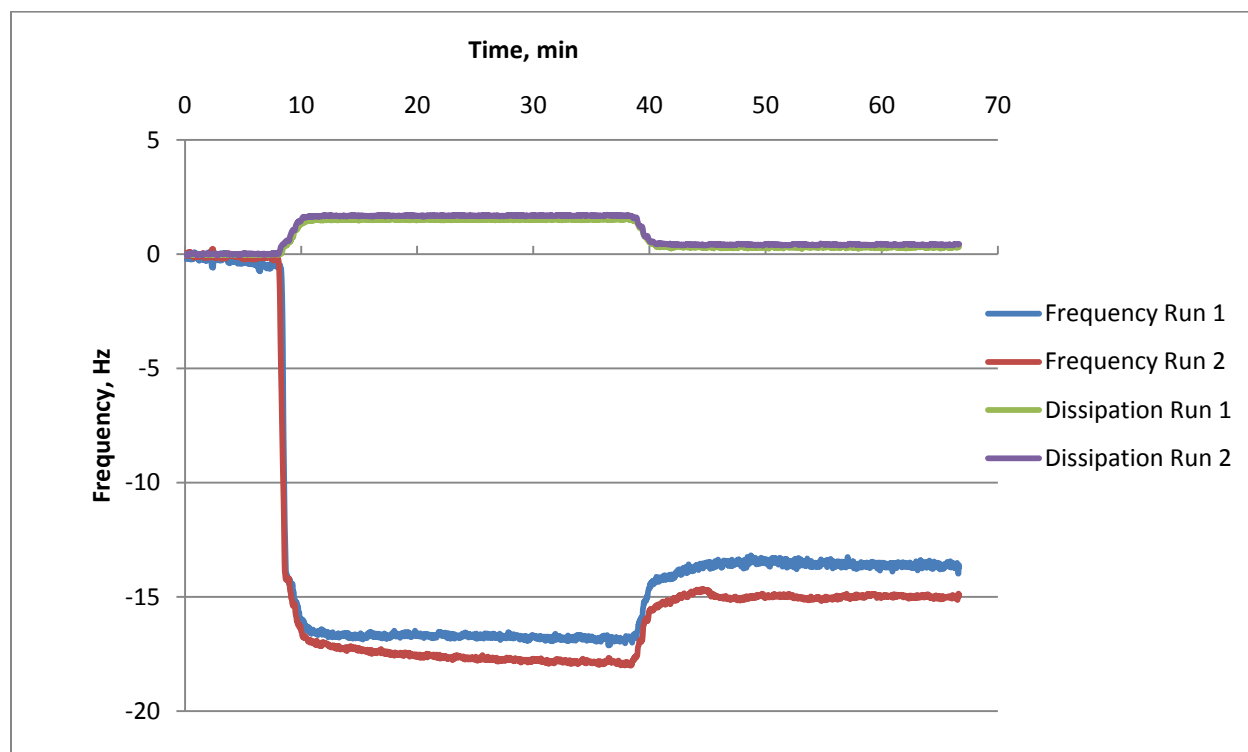


Figure 3 - 58 QCM-D evaluation of 1.00 wt.% PIBSA in isooctane.

ZDDP with varying concentrations of PIBSA was tested next in isooctane. Four samples with varying PIBSA concentrations shown in Table 3 - 3 were blended with 1.00 wt.% ZDDP in isooctane. Samples were run in the QCM-D for one hour at 50°C. The changes in frequency and dissipation of the four samples are shown in Figure 3 - 59. A sharp reduction in frequency similar to that of just PIBSA was observed, indicating that the PIBSA may beat the ZDDP to the surface. Unlike the PIBSA only test run a flat line after the initial adsorption was not observed, but instead a gradual addition throughout the course of one hour was observed. The gradual change in dissipation indicated a slightly viscoelastic film. There was a slight PIBSA concentration dependence, with more frequency and dissipation change at higher concentrations of PIBSA. The difference in frequency change is more apparent at the initial adsorption and will be discussed, but the change in dissipation over time is larger when more PIBSA is present.

Table 3 - 3 Samples of ZDDP with varying PIBSA concentrations in isooctane for QCM-D evaluation.

Sample	ZDDP Concentration, wt.%	PIBSA Concentration, wt.%
A	1.00	0.25
B	1.00	0.50
C	1.00	0.75
D	1.00	1.00

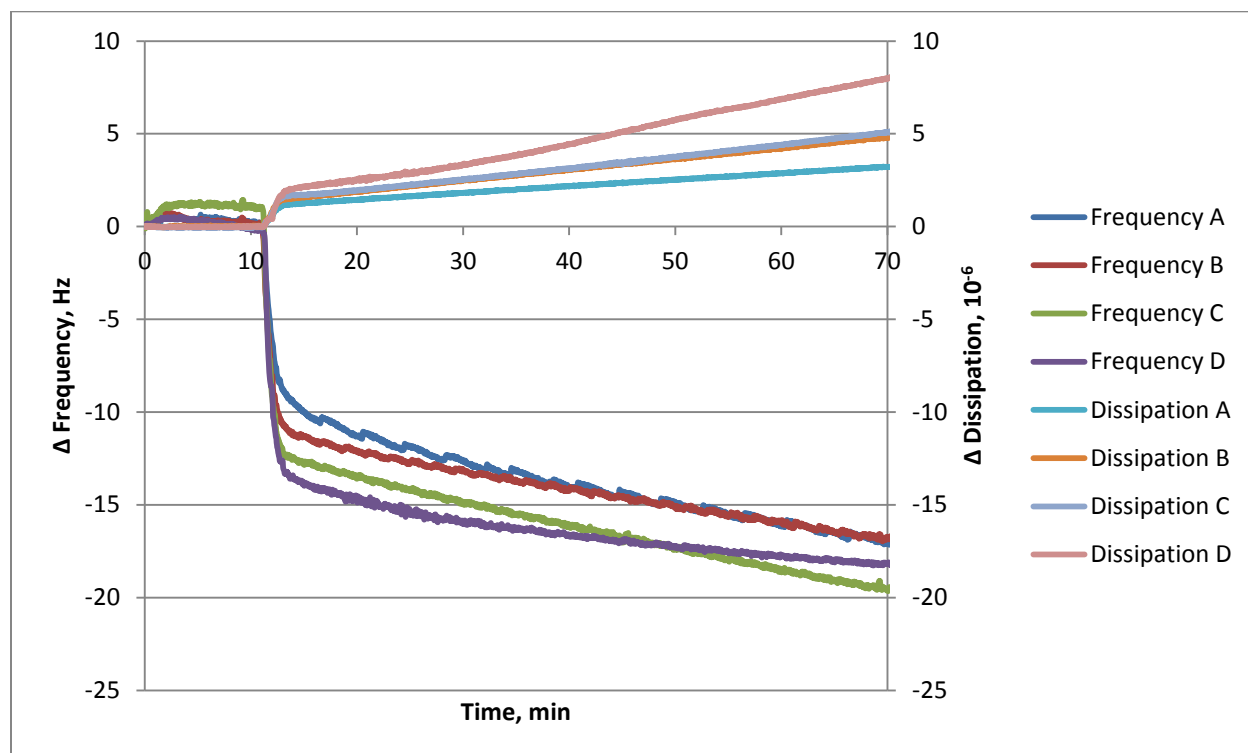


Figure 3 - 59 QCM-D evaluation of samples with ZDDP and varying concentrations of PIBSA.

In order to evaluate the difference in concentration after the initial adsorption, one point in time was selected and evaluated the four different changes in frequency. Due to differences after the initial absorption, the 15 minute mark was selected to plot the change in frequency of all for test samples. The 15 minute mark in the plot above equates to 3.5 minutes of test sample flowing through the cell due to almost 10 minutes of test time being a base line. The change in

frequency of the four samples at this point are shown in Figure 3 - 60, where we clearly observe a PIBSA concentration effect.

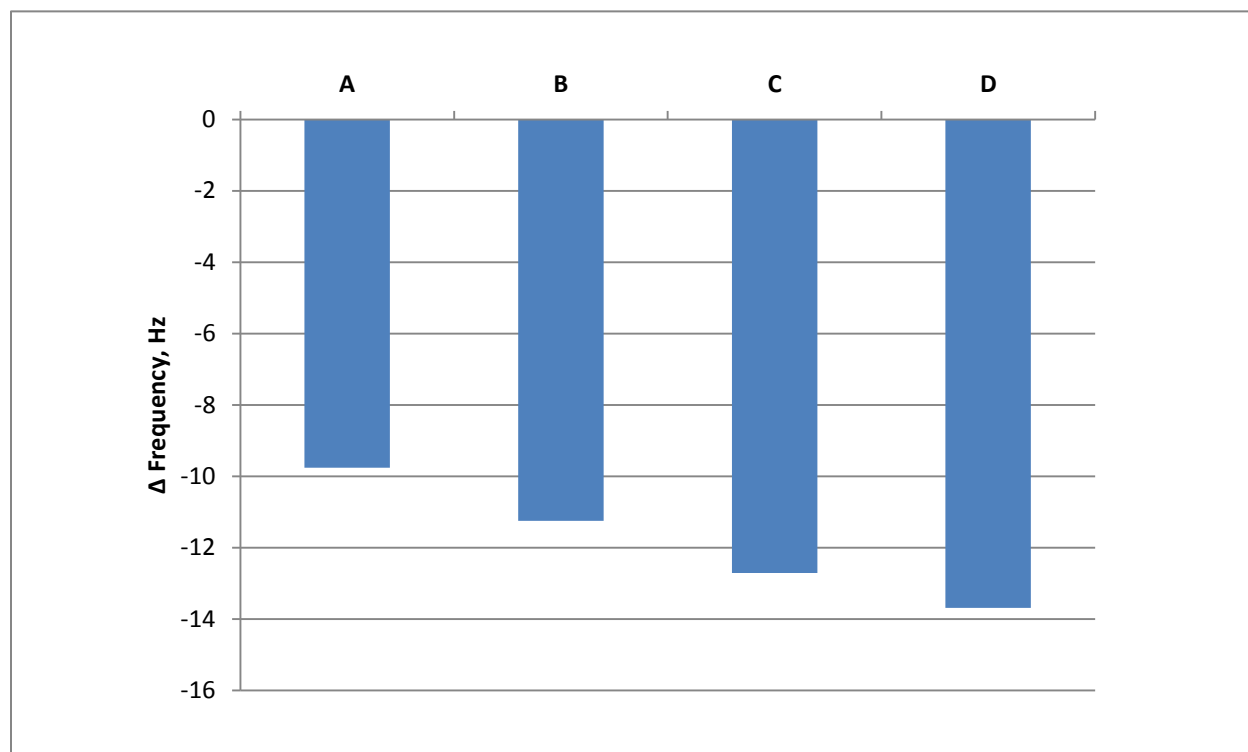


Figure 3 - 60 QCM-D frequency change of varying concentrations of PIBSA and ZDDP after initial adsorption.

The initial change in frequency of the samples with PIBSA and ZDDP were consistent with the adsorption of the PIBSA only sample. A rapid initial adsorption similar to the adsorption of PIBSA was observed, unlike ZDDP which took almost 20 minutes of sample flow time to reach a frequency change of -15 Hz. These results indicate that PIBSA overpowers ZDDP adsorption when present. It appears that ZDDP still slowly adsorbs over time, but when it comes to the race of surface competition, PIBSA clearly wins. With PIBSA being the bigger molecule and reaching the surface quicker than ZDDP, it may explain why we see a lack of

tribofilm growth over a 60 minute period in the MTM-SLIM with PIBSA and other dispersants present.

Phosphorus-31 nuclear magnetic resonance (^{31}P -NMR) spectroscopy was used to evaluate any bulk fluid interactions between dispersants and ZDDP. Of interest was to understand any differences in the ZDDP due to an interaction in the bulk fluid after blending. The same test oils used for MTM-SLIM testing were used for analysis. The spectrum used for reference was ZDDP with no other components present, Figure 3 - 61. All other ^{31}P -NMR spectra are shown in Appendix 5. Any changes in the ZDDP spectrum would indicate there is some reaction in the bulk fluid and the ZDDP has been modified. Out of all the dispersants and dispersant precursors, the only spectrum that was identical to that of ZDDP was the fluid with ZDDP and PIB. The MTM-SLIM testing previously indicated there was no effect from the PIB on ZDDP tribofilms, which was confirmed in the ^{31}P -NMR.

Changes in the ^{31}P -NMR spectra when all other components were present were observed, indicating there is a change in ZDDP chemistry prior to tribofilm growth resulting in the differences we observed in growth and composition. The spectra of ZDDP blended with Dispersant A and Dispersant B only resulted in a slight shift, but there was a difference. Interestingly, the spectra for ZDDP blended with dispersants that had PIBSA to amine ratios greater than 2 resulted in spectra that resembled that of ZDDP blended with PIBSA. The spectrum for ZDDP blended with the diacid form of PIBSA also looked the same as the ZDDP blended with PIBSA. These results confirm the dispersant effect on tribofilm growth, removal, and composition is indeed tied to the PIBSA present in dispersant molecules.

R14004596
1%H1656 in Yubase6
RAN1410452

Sample Wt: 1.5239g
Solvent Wt: 1.5232g

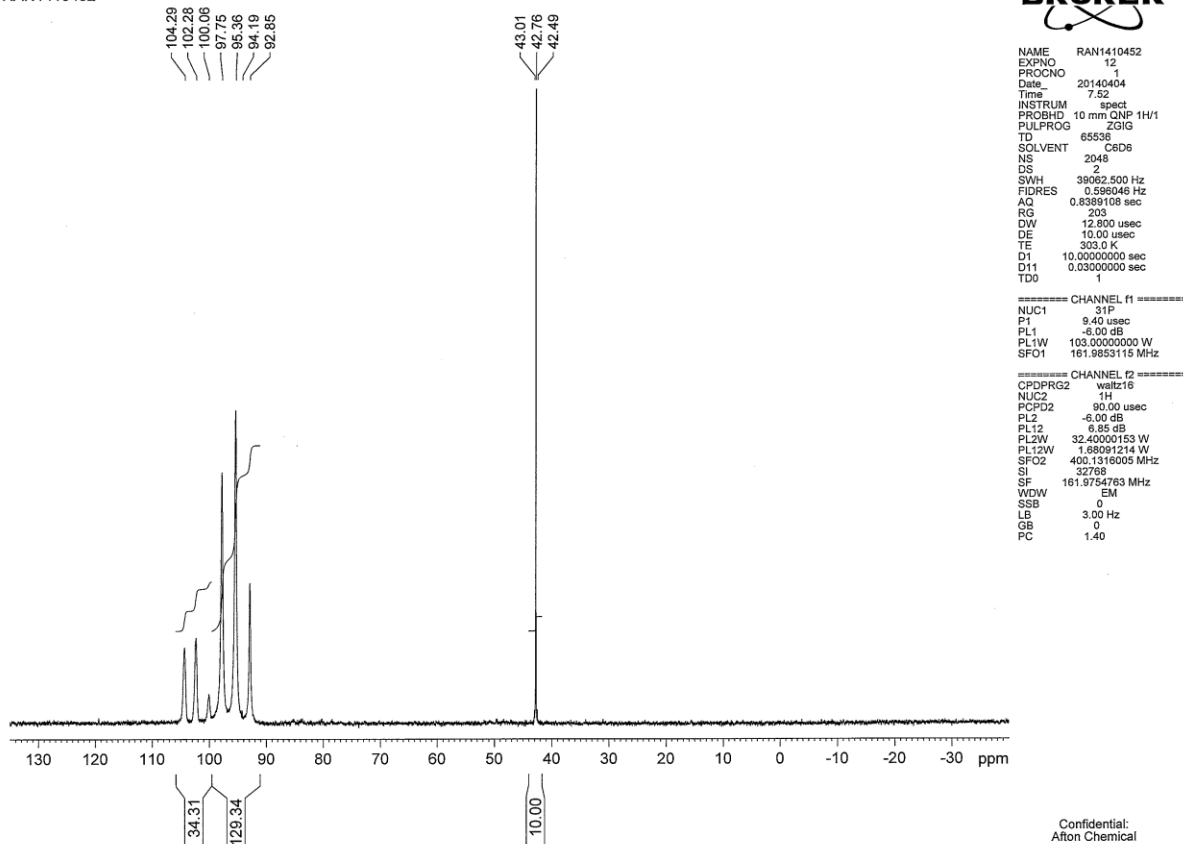


Figure 3 - ^{31}P -NMR spectrum of ZDDP.

The surface interaction and bulk fluid analysis indicated both concepts may result in a difference in ZDDP tribofilms when dispersants are present. The QCM-D analysis confirmed that PIBSA has a higher affinity for the surface when compared to ZDDP. When they are both competing for the surface, it appears that PIBSA gets there first, although ZDDP adsorb over time. The ^{31}P -NMR results show that we also observe an interaction in the bulk fluid between ZDDP and dispersants. This interaction is correlated to the same interaction that ZDDP has with PIBSA, indicating that PIBSA drives the dispersant effect observed in tribofilm growth, removal, and composition. Any modification to the ZDDP prior to decomposition led by an interaction

with PIBSA can result in decomposition species that vary from ZDDP alone. This may result in the different tribofilm structures and composition that we have observed when dispersants or PIBSA are present.

Chapter 4 - Conclusion

Prior to our evaluation, minimal research on dispersant effects on ZDDP tribofilms had been completed. With increasing dispersant levels in lubricant additive packs, and limits on phosphorus and sulfur driving the reduction of ZDDP, the interaction between the two components have been more on the radar. The interaction between the two components had been labeled as an antagonism, with the only research scratching the surface. A structure-activity relationship describing the interaction between the two components remained unknown. We were interested in evaluating various dispersant chemistries' effects on ZDDP tribofilm growth, removal, and composition. It was in our interest to understand this interaction and note any structure-activity relationships between dispersants and ZDDP. We also monitored friction in order to determine if we could skillfully formulate a friction benefit from the interactions between ZDDP and dispersants.

Five dispersants were selected for evaluation with one of the dispersants occurring in 3 forms, resulting in a total of 7 dispersant structures. The structures varied from changes in the starting amine, molecular weight, and functional groups. The major trend between all the dispersants was increasing the stoichiometric ratio of the PIBSA, ranging between 1 and 6 PIBSA's for every 1 basic nitrogen. The dispersants with 3:1 and 6:1 ratios also had acid-amide groups present on the molecule, whereas the other dispersants were mostly imide based. We evaluated the dispersants for any structure-activity interaction with ZDDP.

The ZDDP tribofilms that formed in presence of all dispersants regardless of concentration resulted in a significant reduction in tribofilm growth. In some cases no tribofilm growth was observed when the dispersants were present. There was no strong correlation between dispersant structure and tribofilm thickness or roughness. In the case of almost all the

dispersants a higher coefficient of friction was observed at the end-of-test. There was a correlation between tribofilm thickness and friction.

A structure-activity relationship between dispersants and ZDDP was discovered related to the number of PIBSA's on the molecule. Dispersants with higher PIBSA contents resulted in increased phosphorus to sulfur ratios in the tribofilm. Specifically, the dispersants with acid-amide groups present resulted in higher phosphorus than sulfur in the tribofilm. The dispersants with all imide functionality resulted in more sulfur in the tribofilm. The dispersants with more PIBSA closely resembled the tribofilms formed with ZDDP only.

The differences in tribofilm composition led to the study some of the dispersant precursor's effects on ZDDP tribofilms. An evaluation of PIB resulted in no difference when compared to the ZDDP tribofilm with no PIB present. Surprisingly, when PIBSA was evaluated a similar effects on the ZDDP tribofilm that we saw with films formed in presence of the dispersants was observed. Higher concentrations of PIBSA resulted in no tribofilm formation. The elemental composition of tribofilms formed in presence of PIBSA resembled those with higher PIBSA ratios and acid-amide groups present. We decided to study this concept further and force open the PIBSA ring and form the PIB-diacid. When the diacid form was present, we observed no tribofilm formation even at concentrations as low as 1/10 of the concentration of ZDDP.

After the dispersant and dispersant precursor effects on ZDDP tribofilm growth was observed, the removal of existing ZDDP tribofilms was evaluated by running the MTM-SLIM with oils containing the selected dispersants. The experiment was referenced with base oil, which resulted in no change in tribofilm thickness. Three dispersants and PIBSA were tested for their ability to remove the existing ZDDP tribofilm and in all cases we observed almost half the

film removed after one hour. Elemental composition resulted in similar composition as the ZDDP tribofilm, indicating they may not change the tribofilm composition like they did when present during formation, however, they did have the ability to reduce the existing film.

Surface interactions between ZDDP and PIBSA were evaluated due to the overwhelming effect of PIBSA on ZDDP tribofilms. QCM-D evaluation showed some form of surface competition between ZDDP and PIBSA, with PIBSA adsorbing to the surface much faster than ZDDP. PIBSA adsorbed to the surface very quickly in a rigid mono-layered fashion with no adsorption after the initial adsorption. The ZDDP film took much longer to achieve the same level of adsorption, and a change in dissipation indicated a more viscoelastic film. Samples with both ZDDP and PIBSA present behaved much more like the PIBSA only adsorption, where a quick initial adsorption of the PIBSA was observed. These samples did not level out indicating the ZDDP tribofilm may adsorb over top of the PIBSA. This indicated PIBSA acts at the surface first, taking ZDDP longer to adsorb.

Bulk fluid interactions that occurred prior to tribofilm testing were observed using ^{31}P -NMR. A shift in spectra from ZDDP with all the dispersants present was observed. The spectra's of ZDDP blended with dispersants with higher PIBSA ratios resulted in a clean shift that resembled the shift of ZDDP blended with PIBSA, indicating the dispersant effect is in fact related to the amount of PIBSA in the dispersant. The spectra of the ZDDP blended with PIB diacid also appears like that of ZDDP blended with PIBSA. The ^{31}P -NMR spectra indicate there is a bulk fluid interaction between ZDDP and the dispersants that is correlated to the PIBSA content in the dispersants. The interaction with ZDDP in the blending phase may result in the major reduction in tribofilm formation.

We successfully defined the dispersant effect on ZDDP tribofilm growth and removal. Changing the starting amine, molecular weight, or concentration of dispersant resulted in minimal effects on ZDDP tribofilms. A new structure-activity relationship between dispersants and ZDDP that was previously unknown was also discovered. While minimal differentiation between dispersants and tribofilm thickness was observed, there was a change in tribofilm composition when varying the dispersant structure. The effects we observed from the dispersants was correlated to the dispersant's precursor, PIBSA. Surface analysis indicated the dispersants may compete with ZDDP to the surface, preventing the ZDDP to readily form a tribofilm. Further analysis of the bulk fluid indicated there was an interaction between dispersants and ZDDP after blending, possibly changing the structure of ZDDP prior to tribofilm growth.

The strongest correlation in our work was between the number of PIBSA molecules on the dispersant and the tribofilm composition. This trend was directly correlated to the effects of the starting material, PIBSA, on ZDDP. The significant difference in tribofilm composition when acid-amide groups were present in the dispersant led us to speculate if the anhydride was regenerated under the contact zone. In the case of the 6:1 succinimide dispersant, it is likely to have anhydride present in the dispersant due to the overcrowding of the molecule. In all cases, the anhydride and acid form of the molecule resulted in some interaction with ZDDP. Future work would include evaluation of the dispersant's ability to regenerate PIBSA at higher temperatures and pressures.

Other future work includes evaluation of ZDDP structures. A few MTM-SLIM tests were run to evaluate the effect of the PIBSA on different ZDDP's. This resulted in differences

between mixed, primary and secondary ZDDP's (see Appendix 6). One of the next steps in this project would be further defining the effect of PIBSA on the ZDDP structure.

Further QCM-D analysis of ZDDP, PIBSA, and dispersants would be beneficial in determining if surface competition plays a role in preventing tribofilm growth. There was a rapid adsorption of PIBSA compared to ZDDP which indicated surface competition. PIBSA is a much heavier molecule than ZDDP, so an evaluation of the number of PIBSAs that may be at the surface compared to ZDDP would be of interest. We expect the dispersants to behave similar to the PIBSA, but would further evaluate them for any unknown interactions. SEM-EDX analysis indicated changes in the tribofilm composition. Further analysis of the tribofilms would include X-ray Photoelectron (XPS) spectroscopy in order to obtain more information on composition. Defining the dispersant's effects on ZDDP and the future work will allow Afton Chemical Corporation to gain the ability to formulate lubricant additive packages in favor of this known effect. Once the extent of the interaction is understood, we can formulate specific ZDDP structures with dispersants that we know will modify the tribofilm and lower friction.

Chapter 5 – Experimental

5.1 Sample Preparation

All blends were completed in the same batch of SK Lubricants Yubase 6 base stock oil. The ZDDP and dispersants were blended in the base oil at their respective concentrations. All samples were stirred at 50°C for one hour, or until completely blended. Blended samples were used for MTM-SLIM experiments and ³¹P-NMR. Samples for QCM-D testing were blended in isooctane and stirred at room temperature until fully dissolved.

Dispersant additives were produced from the reaction of polyisobutenyl succinic anhydride (PIBSA, from Afton Chemical) with polyethylenamine in a molar ratio of PIBSA/amine= XX:XX. PIBSA was diluted in base oil under a nitrogen atmosphere. The mixture was heated to 115C. Amine was then added through an addition funnel. The addition funnel was rinsed with additional base oil. The mixture was heated to 180° C for about 2hr under a slow nitrogen sweep. Water was collected in a Dean-Stark trap. Product was obtained as a viscous dark amber oil.

5.2 Instrumentation

5.2.1 Mini Traction Machine with Spacer Layer Image Mapping (MTM-SLIM)

Tribofilm thickness, roughness, and coefficient of friction data was measured using the MTM-SLIM. In the MTM-SLIM, a rolling-sliding contact is generated between a 19.05mm ANSI 52100 steel ball and an ANSI 52100 steel disc that is 46mm in diameter. The mean rolling speed was 100 mm/s with a slide-to-roll ratio of 50%. All tests were performed at 120°C with an applied load of 31N (~1.00 GPa) between the ball and disc. Most tests were run for 1 hour and

stopped periodically so the SLIM technique could be applied to measure the tribofilm thickness and roughness.

Tribofilm removal was measured using the MTM-SLIM by replacing the ZDDP oil with an oil containing no ZDDP and the desired dispersant. ZDDP tribofilms were formed for one hour, then the oil containing ZDDP was drained and cleaned out of the sump. The sump, ball, and disc were cleaned thoroughly with heptane to remove any ZDDP containing oil. A new oil containing the desired dispersant was placed into the sump and the test was run under normal conditions.

5.2.2 Scanning Electron Microscopy – Energy Dispersive X-ray – SEM-EDX

After selected MTM-SLIM tests, the MTM balls were cleaned with heptane followed by isopropyl alcohol to remove any excess oil. The area of the ball that made contact with the disc was examined with a FEI Quanta 650 Scanning Electron Microscope (SEM). The SEM was equipped with an Oxford Instruments X-MAX^N 150 Silicon Drift Detector for performing Energy Dispersive X-ray Spectroscopy (EDX) to allow elemental analysis of the tribofilm. SEM images and EDX spectra were recorded at 5 keV incident beam energy.

5.2.3 Quartz Crystal Microbalance with Dissipation (QCM-D)

Surface adsorption of ZDDP and PIBSA on a steel surface was measured using the QCM-D. The QCM-D has primarily been used in biological and aqueous applications, but has not widely been adopted for use in lubricant applications. Isooctane was chosen as the solvent due to its low viscosity and solubility of additives. The quartz crystals were coated with steel in

placed in flow cells that allowed the measurement of adsorption of additives as the sample flowed through the cell.

The QCM-D measures adsorption through a change in frequency of the oscillating quartz crystal. A voltage is applied to the quartz crystal causing it to oscillate at a known initial frequency. As a sample flows through the cell and adsorption occurs, changes in mass on the quartz surface are related to the changes in frequency of the oscillating crystal. The change in frequency is directly correlated to the mass of a rigid film on the surface. Soft and viscoelastic films that do not fully couple to the oscillating crystal are measured using the dissipation technique. Dissipation occurs when the driving voltage to the crystal is shut off and the energy from the oscillating crystal dissipates from the system. Softer and less rigid adsorbed films will result in higher dissipation times.

5.2.4 ³¹P Phosphorus Nuclear Magnetic Resonance Spectroscopy (³¹P-NMR)

Phosphorus NMR spectroscopy was used to measure bulk fluid interactions of ZDDP and dispersants using a Bruker AV3-400 MHz instrument. 1.5 grams of the sample was weighed out and diluted with 1.5 grams of solvent, benzene-d₆ containing triphenylphosphine sulfide (TPPS) as a reference.

5.2.5 Fourier Transform Infrared (FTIR) Spectroscopy (FTIR)

Changes in Dispersant A structures were observed using Fourier Transform Infrared (FTIR) spectroscopy with a Horizontal Attenuated Total Reflectance (HATR). The spectrophotometer was a Perkin Elmer Model GX Series FTIR with a 45° ZnSe HATR crystal.

The scan range was set to 650 cm^{-1} due to ZnSe transmission cut off. Four background scans and four sample scans were measured.

References

¹ *FY 2014 Vehicles FOA 991 Selection Table*. Office of Energy Efficiency & Renewable Energy, Department of Energy, Washington, DC, 2014.

² Tung, S.; McMillan, M. Automotive tribology overview of current advances and challenges for the future. *Tribol. Int.* 2004, *37*, 517-536.

³ Torbacke, M.; Rudolphi, A.; Kassfeldt, E. Introduction to Tribology. *Lubricants – Introduction to Properties and Performance*, 1; Wiley: New Jersey, 2014; pp 3-17.

⁴ Anderson, S.; Parry, I.; Sallee, J.; Fischer, C. *Review of Environmental Economics and Policy*. 2011, *5*, 89-108.

⁵ *Summary of Fuel Economy Performance*; U.S. Department of Transportation, NHTSA, NVS-220: Washington, DC, 2014.

⁶ Environmental Protection Agency; U.S. Department of Transportation. Light-Duty Vehicle Greenhouse Gas Emission Standards and Corporate Average Fuel Economy Standards; Final Rule. *Fed Regist.* 2010, *75*, 25324-25728.

⁷ Environmental Protection Agency; U.S. Department of Transportation. 2017 and Later Model Year Light-Duty Vehicle Greenhouse Gas Emissions and Corporate Average Fuel Economy Standards. *Fed Regist.* 2012, *77*, 62624-63200.

⁸ Department of Transportation. *Summary of CAFE Fines Collected*; National Highway Traffic Safety Administration: Washington, DC, 2014.

⁹ Yang, Z. Some upcoming changes in the ICCT global passenger vehicle GHG standard comparison charts. Publication for The International Council on Clean Transportation: Washington, DC, 2014.

¹⁰ Holmberg, K.; Andersson, P.; Erdemir, A. Global energy consumption due to friction in passenger cars. *Tribol. Int.* 2012, *47*, 221-234.

¹¹ Priest, M.; Taylor, C. Automobile engine tribology – approaching the surface. *Wear.* 2000, *241*, 193-203.

- ¹² Ma, Y.; Shenghua, L.; Jin, Y. Impacts of friction-modified fully formulated engine oils on tribological performance of nitride piston rings sliding against cast iron cylinder bores. *Tribol. Trans.* 2004, *47*, 421-429.
- ¹³ Challen, J.; Oxley, P. An explanation of the different regimes of friction and wear using asperity deformation models. *Wear.* 1979, *53*, 229-243.
- ¹⁴ Caines, A.; Haycock, R. Introduction and Fundamentals. In *Automotive Lubricants Reference Book*, 2nd edition; Haycock, R.; Hillier, J., Eds.; SAE International: Pennsylvania, 2004; 1-44.
- ¹⁵ Caines, A.; Haycock, R. Constituents of Modern Lubricants. In *Automotive Lubricants Reference Book*, 2nd edition; Haycock, R.; Hillier, J., Eds.; SAE International: Pennsylvania, 2004; 45-88.
- ¹⁶ Spikes, H. The history and mechanisms of ZDDP. *Tribol. Lett.* 2004, *17*, 469-489.
- ¹⁷ Fujita, H.; Spikes, H. Study of zinc dialkyldithiophosphate antiwear film formation and removal processes, part II: Kinetic Model. *Tribol. Trans.* 2005, *48*, 567-575.
- ¹⁸ Onodera, T.; Kuriaki, T.; Morita, Y.; Suzuki, A.; Koyama, M.; Tsuboi, H.; Hatakeyama, N. Endou, A.; Takaba, H.; Del Carpio, C.; Kubo, M.; Minfray, C.; Martin, J.; Miyamoto, A. Influence of nanometer scale film structure of ZDDP tribofilm on its mechanical properties: a computational chemistry study. *Appl. Surf. Sci.* 2009, *256*, 976-979.
- ¹⁹ Willermet, P.; Dailey, D.; Carter, R.; Schmitz, P.; Zhu, W. Mechanism of formation of antiwear films from zinc dialkyldithiophosphates. *Tribol. Int.* 1995, *28*, 177-187.
- ²⁰ Fuller, M.; Kasrai, M.; Bancroft, G.; Fyfe, K.; Tan, K. Solution decomposition of zinc dialkyl dithiophosphate and its effect on antiwear and thermal film formation studied by X-ray absorption spectroscopy. *Tribol. Int.* 1998, *31*, 627-644.
- ²¹ Topolovec-Miklozica, K.; Forbus, T.; Spikes, H. Film thickness and roughness of ZDDP antiwear films. *Tribol. Lett.* 2007, *26*, 161-171.
- ²² Graham, J.; McCague, C.; Norton, P. Topography and nanomechanical properties of tribochemical films derived from zinc dialkyl and diaryl dithiophosphates. *Tribol. Lett.* 1999, *6*, 149-157.
- ²³ Spikes, H. Origins of the friction and wear properties of antiwear additives. *Lubr. Sci.* 2006, *18*, 223-230.

- ²⁴ Kapadia, R.; Glyde, R.; Wu, Y. In situ observation of phosphorus and non-phosphorus antiwear films using a mini traction machine with spacer layer image mapping. *Tribol. Int.* 2007, *40*, 1667-1679.
- ²⁵ Fujita, H.; Spikes, H. Study of Zinc Dialkyldithiophosphate Antiwear Film Formation and Removal Processes, Part I: Experimental. *Tribol. Trans.* 2005, *48*, 558-566.
- ²⁶ Canning, G.; Fuller, M.; Bancroft, G.; Kasrai, M.; Cutler, J. Stasio, G.; Gilbert, B. Spectromicroscopy of tribological films from engine oil additives. Part I. Films from ZDDP's. *Tribol. Lett.* 1999, *6*, 159-169.
- ²⁷ Aktary, M.; McDermott, M.; McAlpine, G. Morphology and nanomechanical properties of ZDDP antiwear films as a function of tribological contact time. *Tribol. Lett.* 2002, *12*, 155-162.
- ²⁸ Devlin, M.; Guevremont, J.; Garelick, K.; Hux, K.; Smith, A. *Boundary film formation properties of lubricant additives*. Quarterly Technical Report for Afton Chemical Corporation: Richmond, VA, October 2008.
- ²⁹ Devlin, M.; Guevremont, J.; Garelick, K.; Hux, K.; Warren, S.; Schwab, Z. *Effects of tribofilms on friction, wear, and fatigue*. Quarterly Technical Report for Afton Chemical Corporation: Richmond, VA, October 2011.
- ³⁰ Rizvi, S. Dispersants. In *Lubricant Additives: Chemistry and Applications*. Rudnick, L.; Marcel Dekker, Inc.: New York, 2003; 137-170.
- ³¹ Taylor, L.; Spikes, H. Friction-enhancing properties of ZDDP antiwear additive: Part I – Friction and morphology of ZDDP reaction films. *Tribol. Trans.* 2003, *46*, 303-309.
- ³² Guevremont, J.; Guinther, G.; Szemenyei, D.; Devlin, M.; Jao, T. Enhancement of engine oil wear and friction control performance through titanium additive chemistry. *Tribol. Trans.* 2008, *51*, 324-331.
- ³³ Mansuy, H.; Beccat, P.; Huiban, Y.; Palermo, T. Investigation of interactions between antiwear and dispersant additives and their effect on surface activity of ZDDP. *Lubr. Lubr.* 1995, *30*, 423-432.
- ³⁴ Rounds, F. Additive interactions and their effect on the performance of a zinc dialkyl dithiophosphate. *Tribol. Trans.* 1978, *21*, 91-101.
- ³⁵ Mosey, N.; Muser, M.; Woo, T. Molecular Mechanisms for the Functionality of Lubricant Additives. *Science*, 2005, *307*, 1612-1615.

³⁶ Gosvami, N.; Bares, J.; Mangolini, F.; Konicek, A.; Yablon, D.; Carpick, R. Mechanisms of antiwear tribofilm growth revealed in situ by single-asperity sliding contacts. *Science*, 2015, 348, 102-106.

³⁷ Zhang, J.; Yamaguchi, E.; Spikes, H. The antagonism between succinimide dispersants and a secondary zinc dialkyl dithiophosphate. *Tribol. Trans.* 2014, 57, 57-65.

³⁸ MTM2 Mini-Traction-Machine Technical Sheet. PCS Instruments: London, UK, 2015; 1-12.

Appendices

Appendix 1

MTM-SLIM interference images used to obtain average thickness and roughness graphs of ZDDP tribofilms. Differences in interference image shades are from two MTM-SLIM instruments.

Table A1-1 MTM-SLIM interference images for ZDDP tribofilms formed in presence of Dispersant A.

Test Time, minutes	0	10	20	30	40	50	60
Dispersant A Polyamide 1.00%							
Dispersant A Polyamide 0.50%							
Dispersant A Polyamide 0.25%							
Dispersant A Intermediate 1.00%							
Dispersant A Imide 1.00%							

Table A1-2 MTM-SLIM interference images for ZDDP tribofilms formed in presence of Dispersant B.

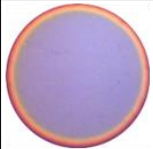
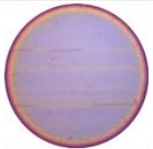
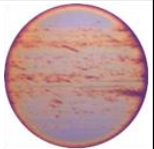
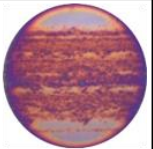
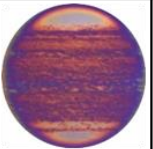
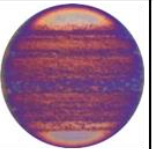
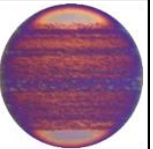



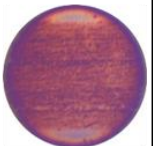
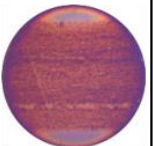
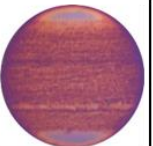
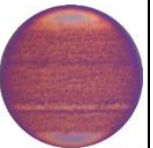
Test Time, minutes	0	10	20	30	40	50	60
Dispersant B 1.00%							
Dispersant B 0.50%							

Table A1-3 MTM-SLIM interference images for ZDDP tribofilms formed in presence of Dispersant C.


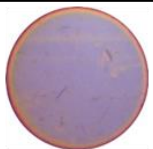

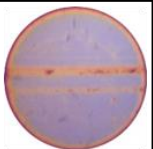
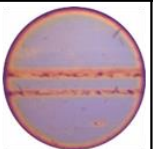
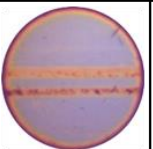
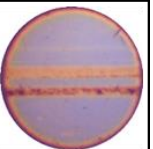
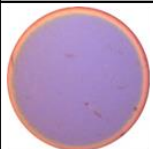
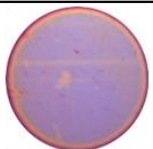
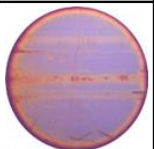
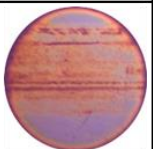
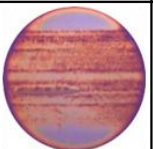
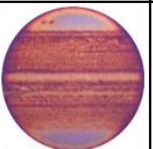
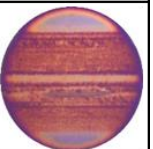
Test Time, minutes	0	10	20	30	40	50	60
Dispersant C 1.00%							
Dispersant C 0.50%							

Table A1-4 MTM-SLIM interference images for ZDDP tribofilms formed in presence of Dispersant D.

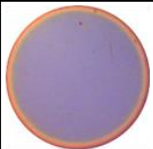
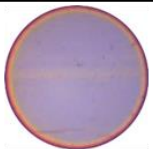
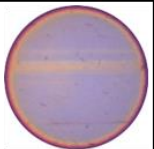
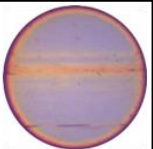
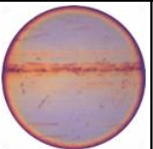
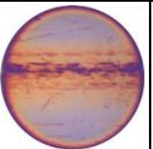
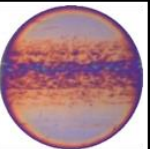

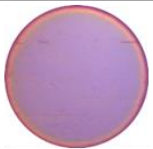


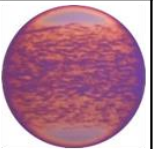
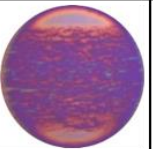
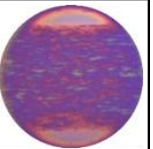
Test Time, minutes	0	10	20	30	40	50	60
Dispersant D 1.00%							
Dispersant D 0.50%							

Table A1-5 MTM-SLIM interference images for ZDDP tribofilms formed in presence of Dispersant E.


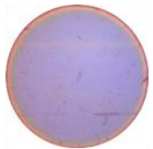
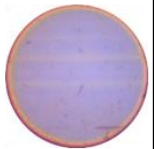
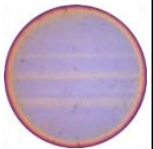
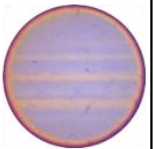
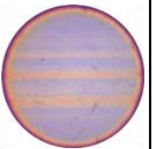
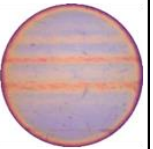



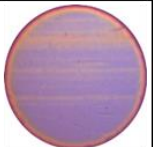
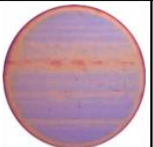
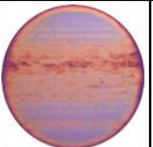
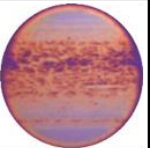
Test Time, minutes	0	10	20	30	40	50	60
Dispersant E 1.00%							
Dispersant E 0.50%							

Table A1-5 MTM-SLIM interference images for ZDDP tribofilms formed in presence of PIB.


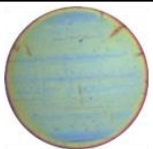

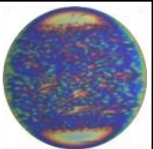
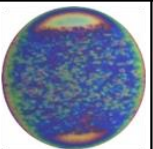
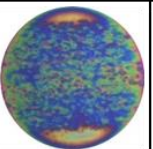
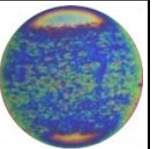

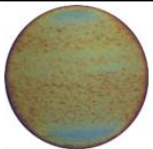
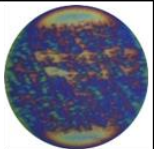
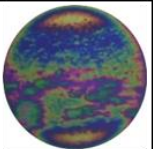
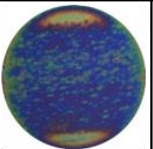
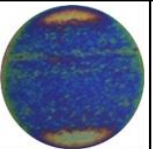
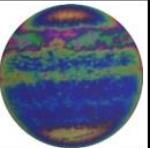
Test Time, minutes	0	10	20	30	40	50	60
PIB 1.00%							
PIB 0.50%							

Table A1-6 MTM-SLIM interference images for ZDDP tribofilms formed in presence of PIBSA.

Test Time, minutes	0	10	20	30	40	50	60
PIBSA 1.00%							
PIBSA 0.75%							
PIBSA 0.50%							
PIBSA 0.25%							

Table A1-7 MTM-SLIM interference images for ZDDP tribofilms formed in presence of PIB diacid.

Test Time, minutes	0	10	20	30	40	50	60
PIB DIACID 0.25%							
PIB DIACID 0.10%							

Appendix 2

SEM-EDX images of ZDDP tribofilms used to obtain elemental composition.

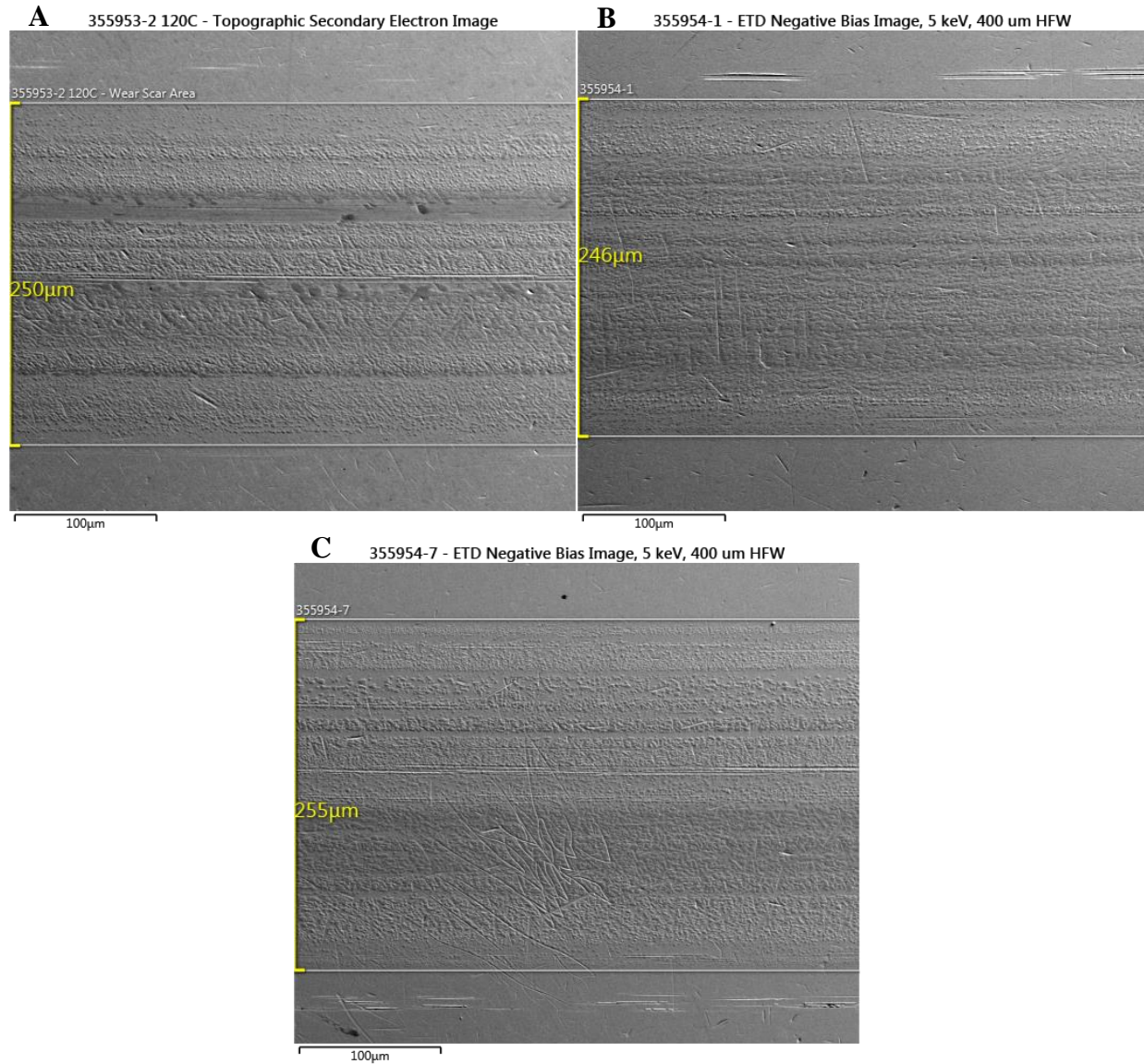


Figure A2 - 1 SEM-EDX images of ZDDP tribofilms formed in presence of (A) 1.00% Dispersant A, (B) 0.50% Dispersant A, and (C) 0.25% Dispersant A.

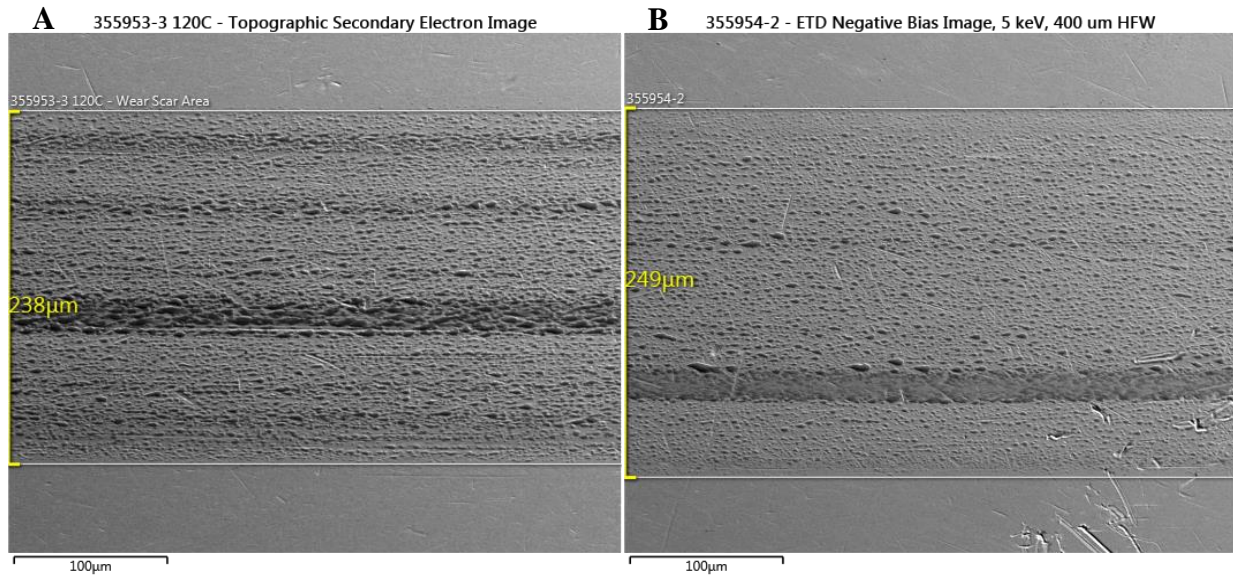


Figure A2 - 2 SEM-EDX images of ZDDP tribofilms formed in presence of (A) 1.00% Dispersant B and (B) 0.50% Dispersant B.

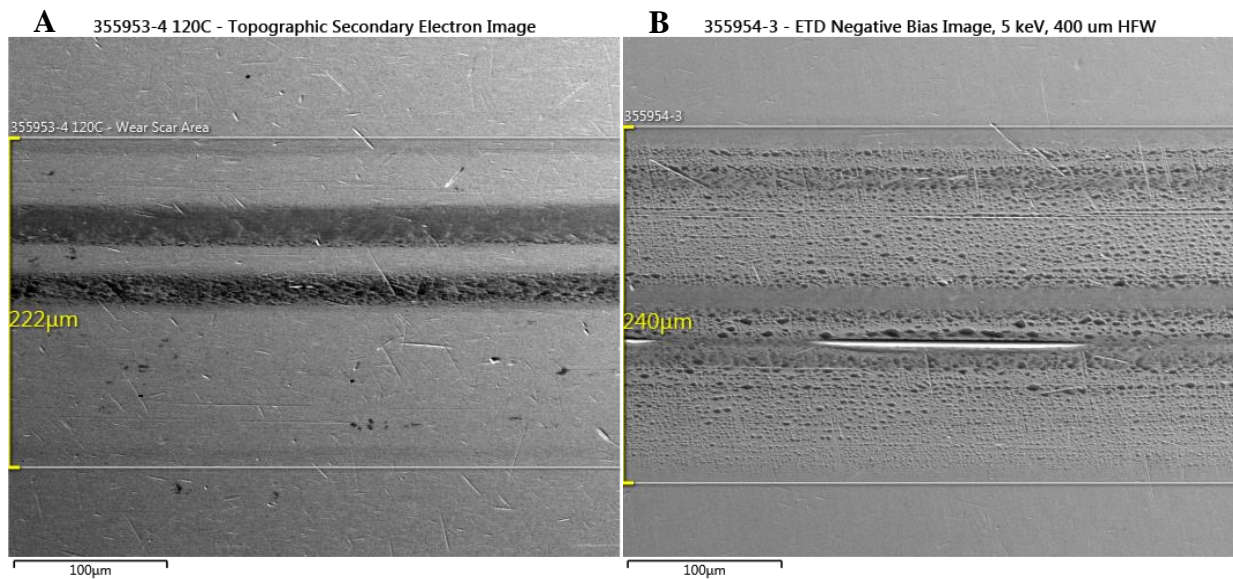


Figure A2 - 3 SEM-EDX images of ZDDP tribofilms formed in presence of (A) 1.00% Dispersant C and (B) 0.50% Dispersant C.

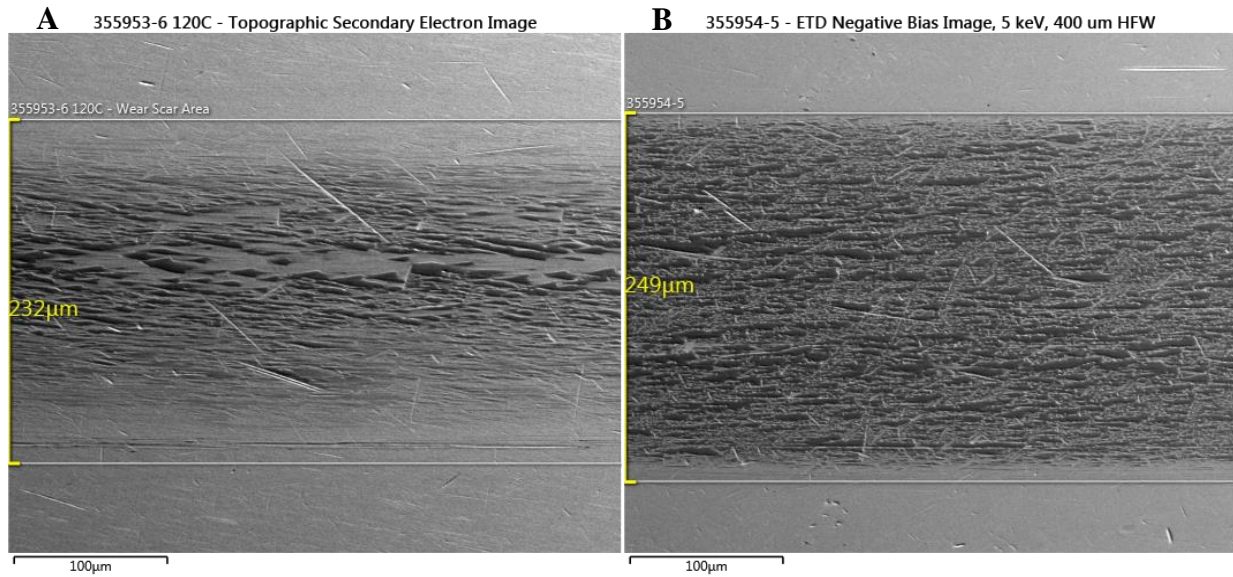


Figure A2 - 4 SEM-EDX images of ZDDP tribofilms formed in presence of (A) 1.00% Dispersant D and (B) 0.50% Dispersant D.

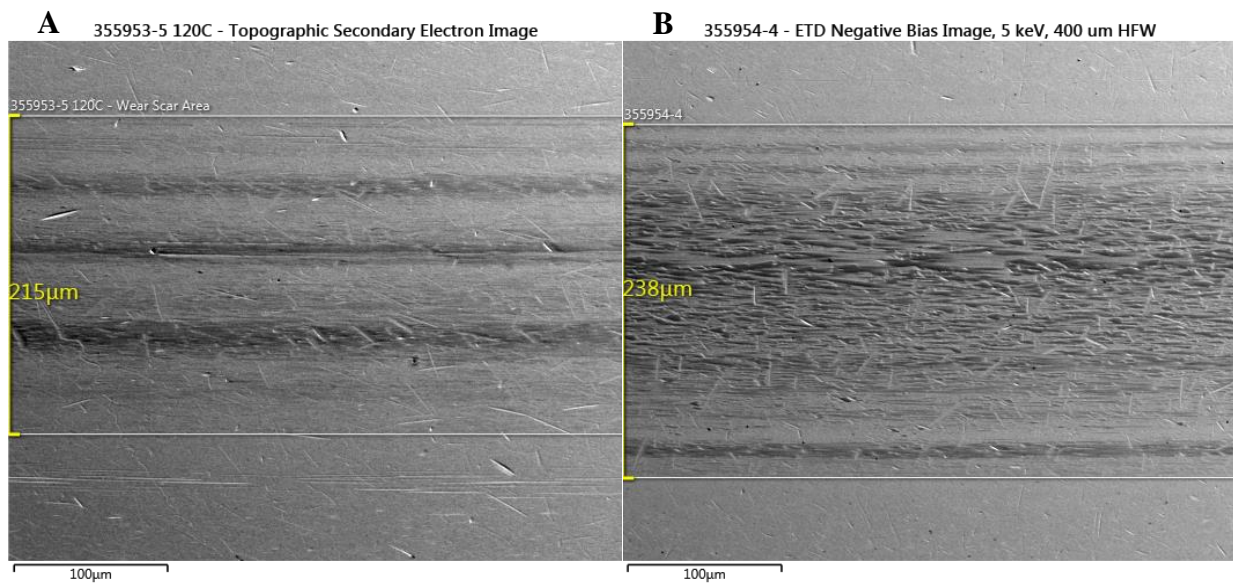


Figure A2 - 5 SEM-EDX images of ZDDP tribofilms formed in presence of (A) 1.00% Dispersant E and (B) 0.50% Dispersant E.

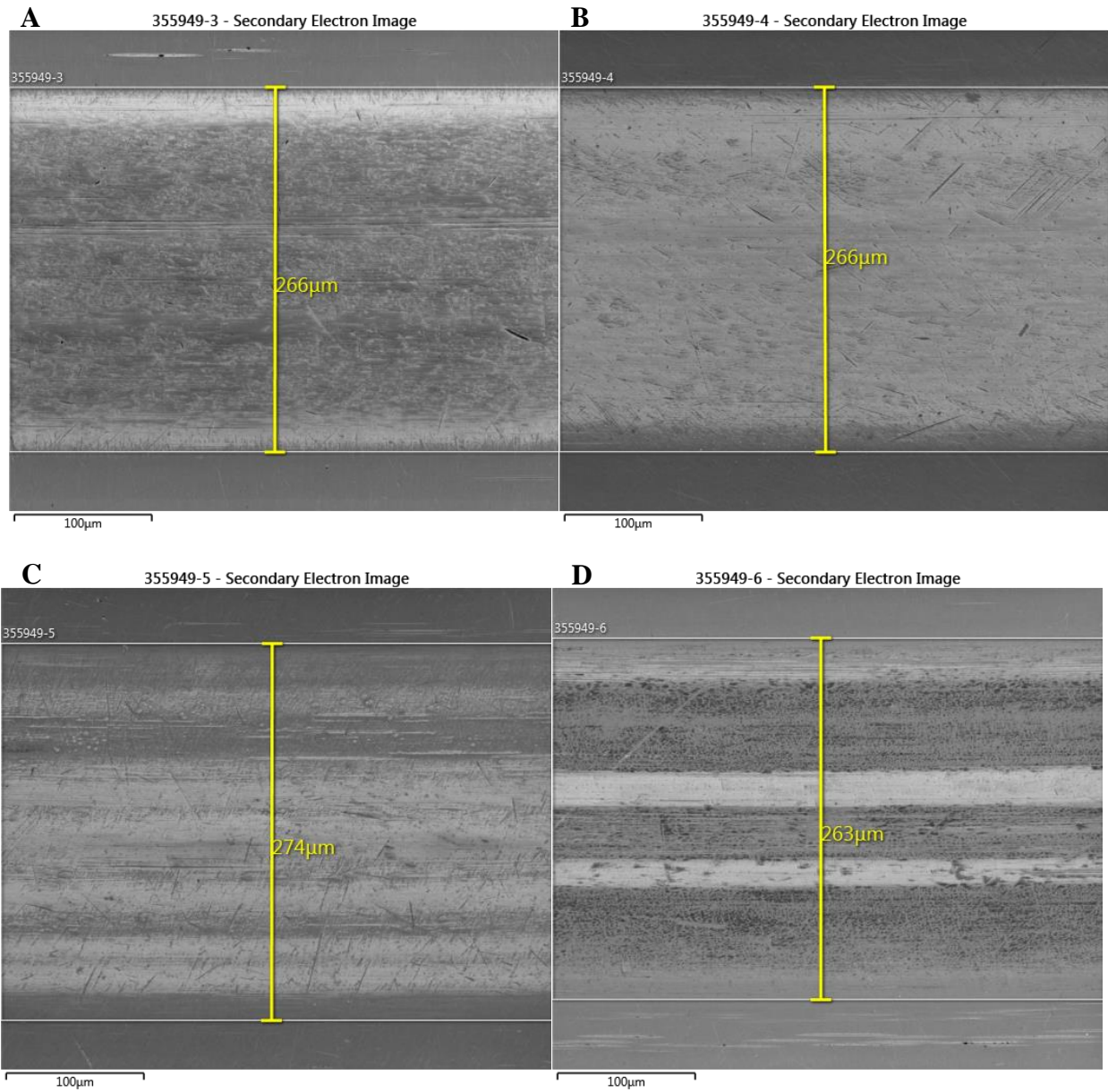


Figure A2 - 6 SEM-EDX images of ZDDP tribofilms formed in presence of (A) 0.25% PIBSA, (B) 0.50% PIBSA, (C) 0.75% PIBSA, and (D) 1.00% PIBSA.

Appendix 3

Appendix 3

SEM-EDX elemental composition and spectra of ZDDP tribofilms.

Table A3- 1 SEM-EDX elemental composition of ZDDP tribofilms

Sample Description	C atom %	N atom %	O atom %	Si atom %	P atom %	S atom %	Na atom %	Ca atom %	Fe atom %	Zn atom %	Total
No Dispersant	9.32	0.82	29.40	0.10	7.96	5.84	0.00	0.00	29.36	17.19	99.99
No Dispersant	9.30	0.66	26.65	0.13	7.62	6.76	0.00	0.00	32.46	16.43	100.01
Dispersant A 1.00 wt.%	8.53	0.00	6.25	0.25	1.10	7.34	0.00	0.00	64.89	11.63	99.99
Dispersant A 0.50 wt.%	8.63	0.00	5.53	0.28	0.82	7.30	0.00	0.00	66.08	11.36	100.00
Dispersant A 0.25 wt.%	9.23	0.00	6.32	0.28	1.06	7.23	0.00	0.00	64.57	11.31	100.00
Dispersant B 1.00 wt.%	9.44	1.17	10.27	0.21	2.40	4.66	0.00	0.00	62.62	9.23	100.00
Dispersant B 0.50 wt.%	9.51	1.54	14.83	0.19	3.60	5.30	0.00	0.00	53.04	12.00	100.01
Dispersant C 1.00 wt.%	9.89	1.41	11.37	0.25	2.68	3.80	0.00	0.00	62.43	8.17	100.00
Dispersant C 0.50 wt.%	8.89	0.00	6.03	0.34	0.87	0.91	0.00	0.00	80.94	2.01	99.99
Dispersant D 1.00 wt.%	7.83	1.56	28.25	0.13	7.78	4.96	0.00	0.00	33.71	15.77	99.99
Dispersant D 0.50 wt.%	7.26	0.00	16.71	0.27	4.05	2.90	0.00	0.00	58.64	10.17	100.00
Dispersant E 1.00 wt.%	7.26	0.00	16.09	0.23	3.88	2.67	0.00	0.00	60.36	9.51	100.00
Dispersant E 0.50 wt.%	8.36	0.00	8.91	0.33	1.83	0.86	0.00	0.00	76.09	3.63	100.01
PIBSA 0.25 wt.%	6.43	0.00	27.12	0.15	7.19	3.66	3.48	0.26	37.96	13.74	99.99

PIBSA 0.50 wt.%	7.16	0.00	14.90	0.24	3.40	1.70	1.72	0.25	63.73	6.89	99.99
PIBSA 0.75 wt.%	8.61	0.00	7.27	0.34	1.17	0.62	0.66	0.00	78.86	2.46	99.99
PIBSA 1.00 wt.%	11.69	0.00	6.45	0.33	0.64	0.34	0.39	0.24	78.53	1.39	100.00
Removal Dispersant A	10.67	0.00	15.79	0.62	3.67	3.01	0.00	0.21	59.07	6.96	100.00
Removal Dispersant C	10.34	0.00	20.42	0.52	5.20	4.06	0.00	0.32	49.78	9.36	100.00
Removal Dispersant D	9.24	0.00	16.44	0.48	3.72	2.97	0.00	0.19	59.43	7.50	99.97
Removal PIBSA	9.49	0.00	21.69	0.43	5.58	3.90	0.00	0.15	49.20	9.56	100.00

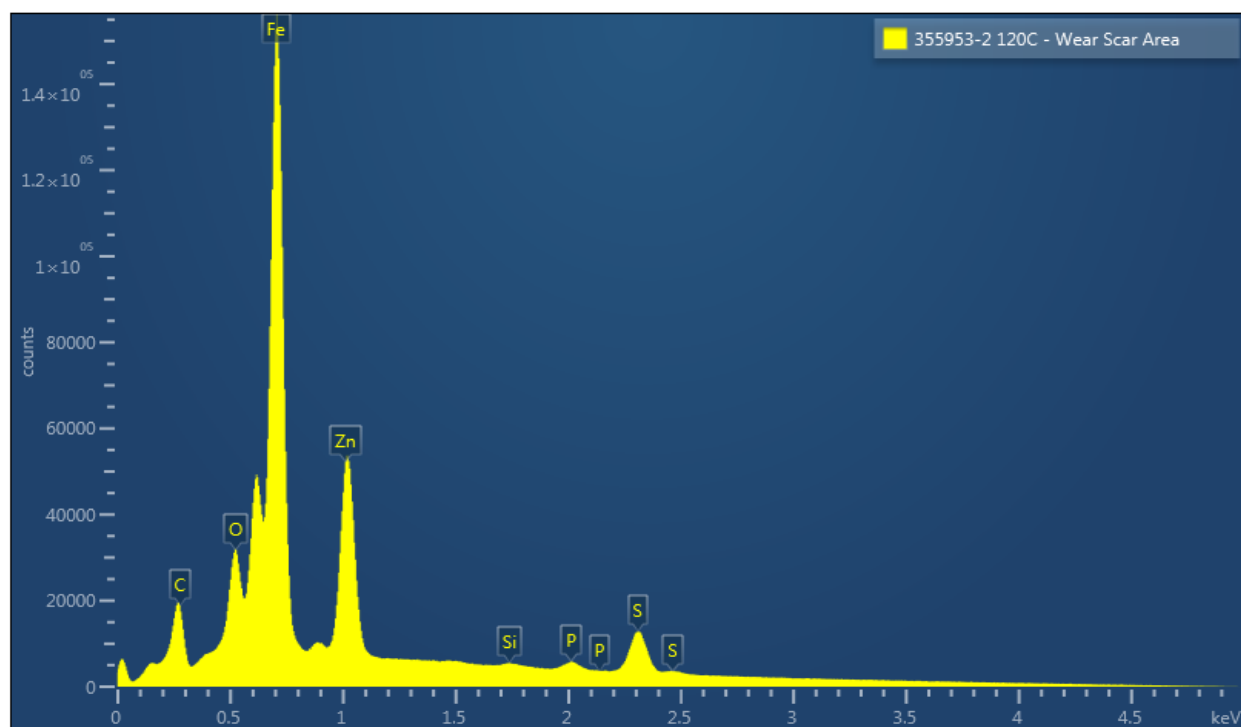


Figure A3 - 1 SEM-EDX spectra of ZDDP tribofilm formed in presence of 1.00 wt.% Dispersant A.

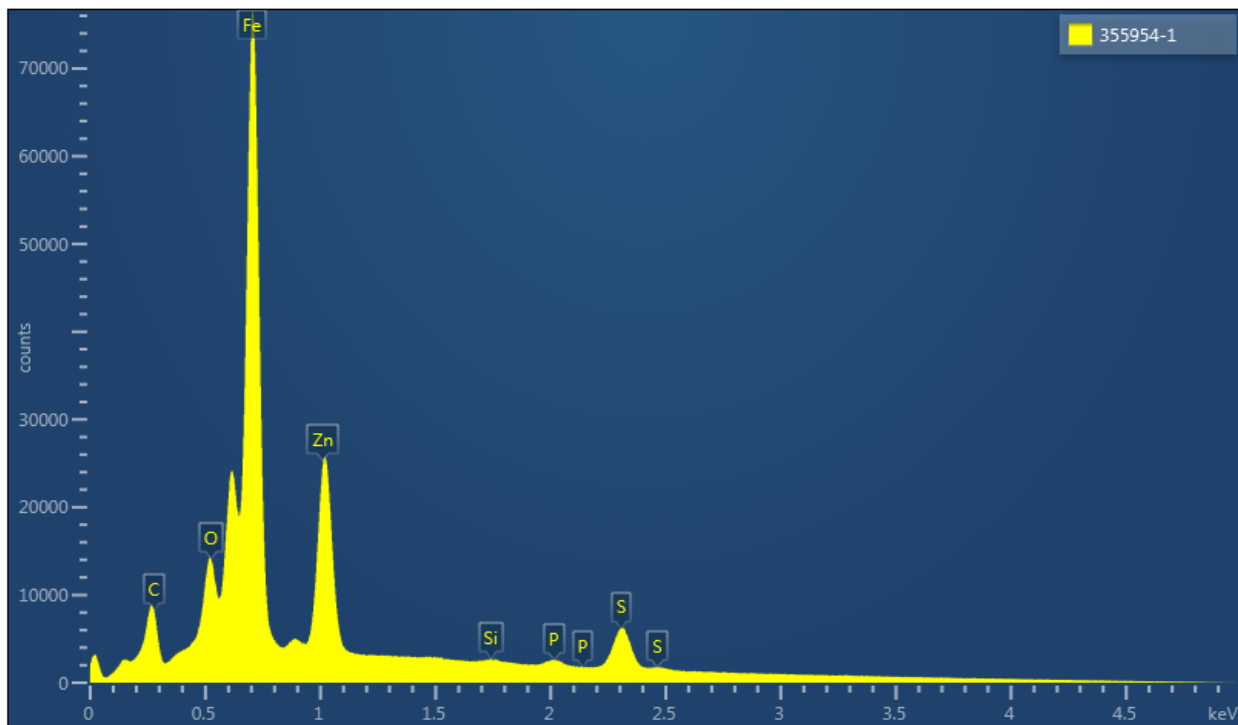


Figure A3 - 2 SEM-EDX spectra of ZDDP tribofilm formed in presence of 0.50 wt.% Dispersant A.

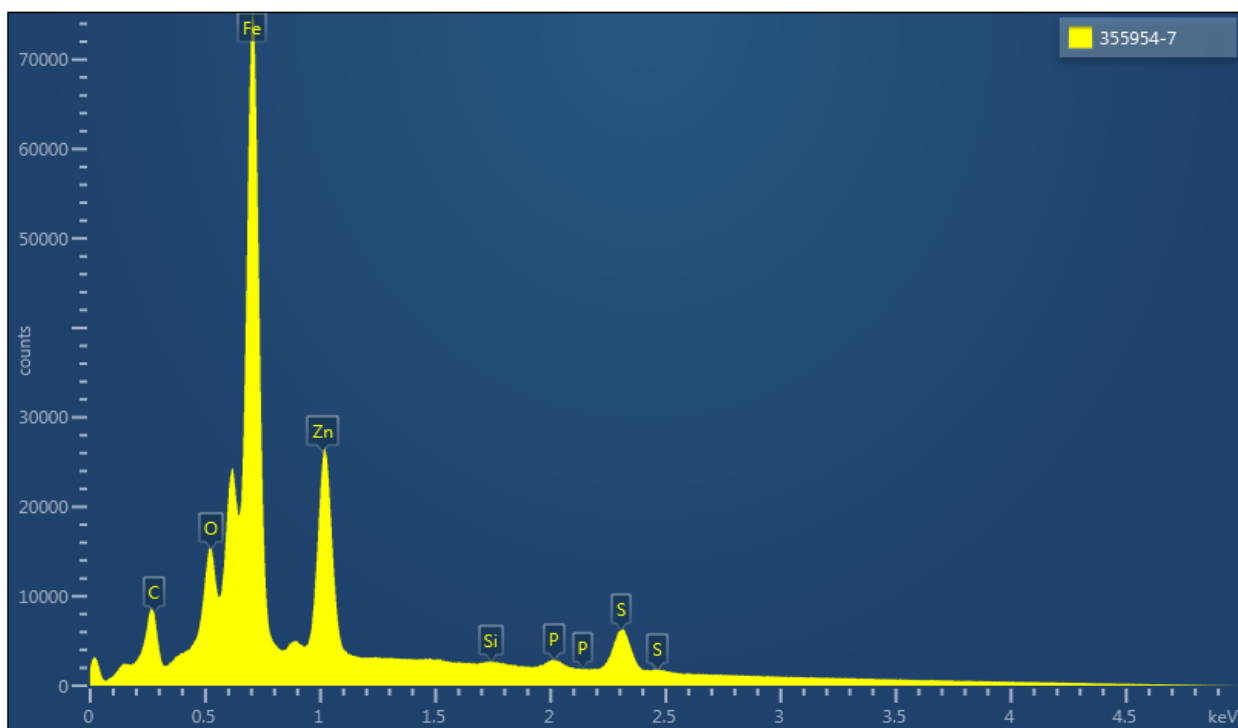


Figure A3 - 3 SEM-EDX spectra of ZDDP tribofilm formed in presence of 0.25 wt.% Dispersant A.

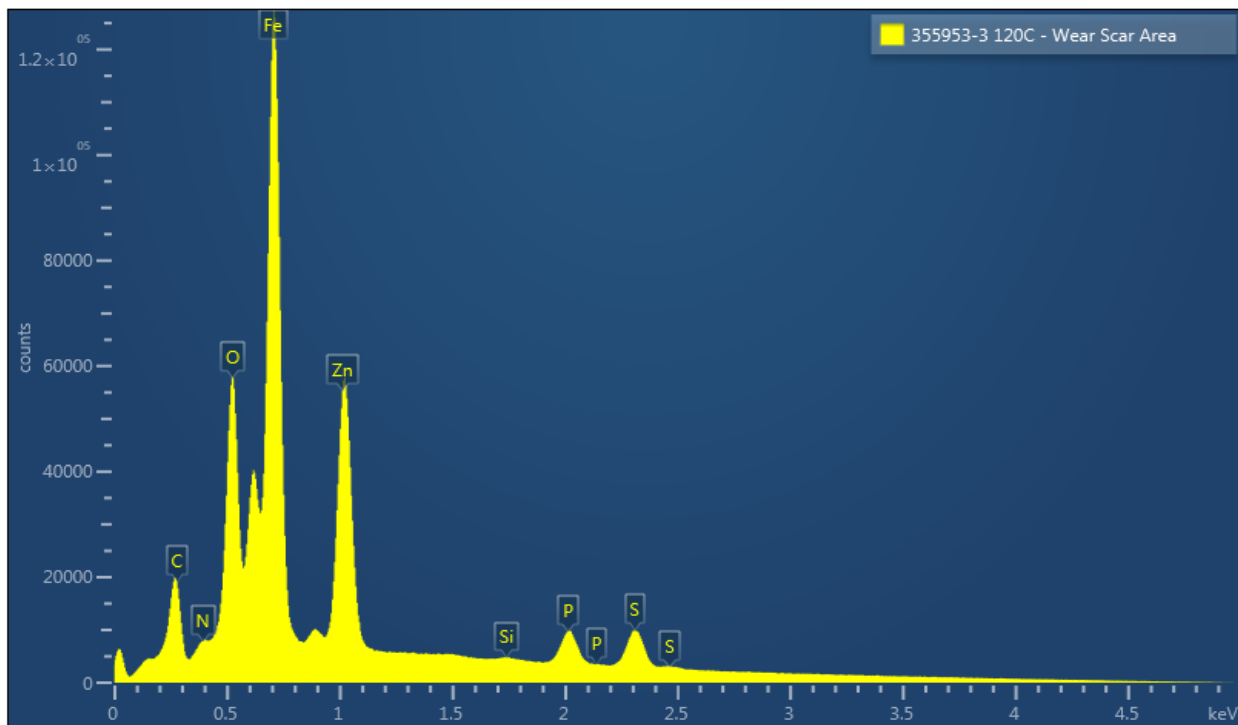


Figure A3 - 4 SEM-EDX spectra of ZDDP tribofilm formed in presence of 1.00 wt.% Dispersant B.

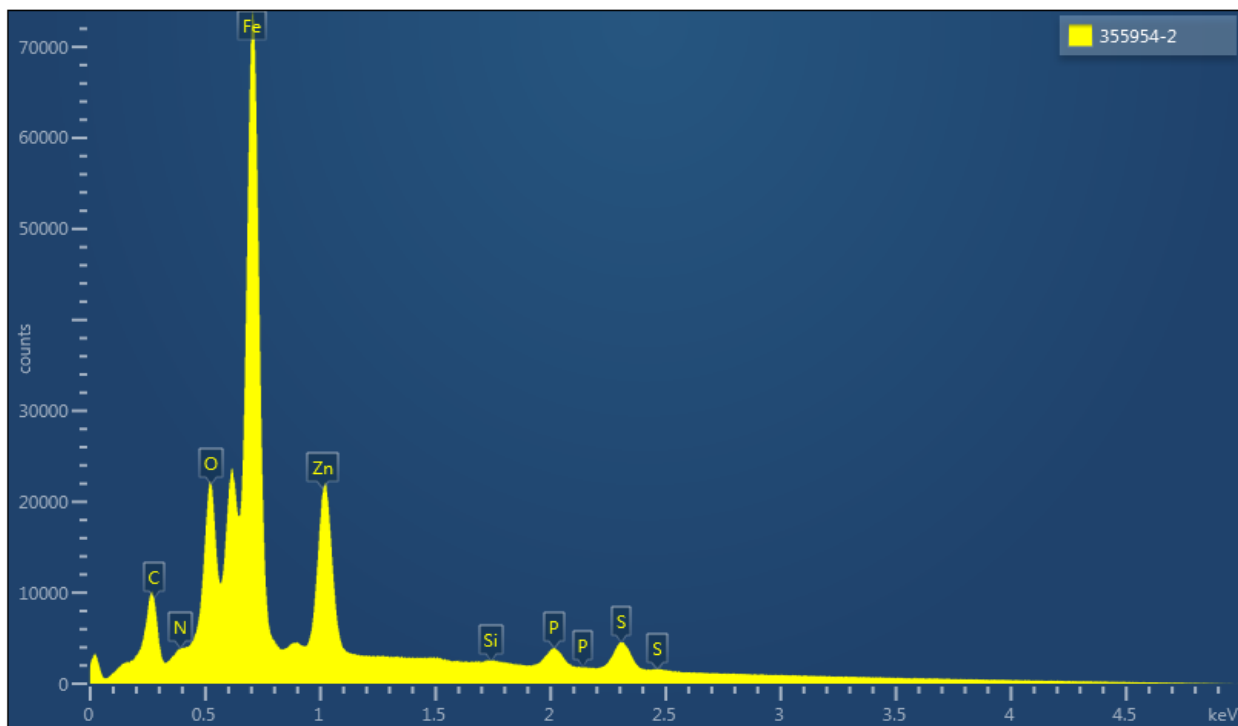


Figure A3 - 5 SEM-EDX spectra of ZDDP tribofilm formed in presence of 0.50 wt.% Dispersant B.

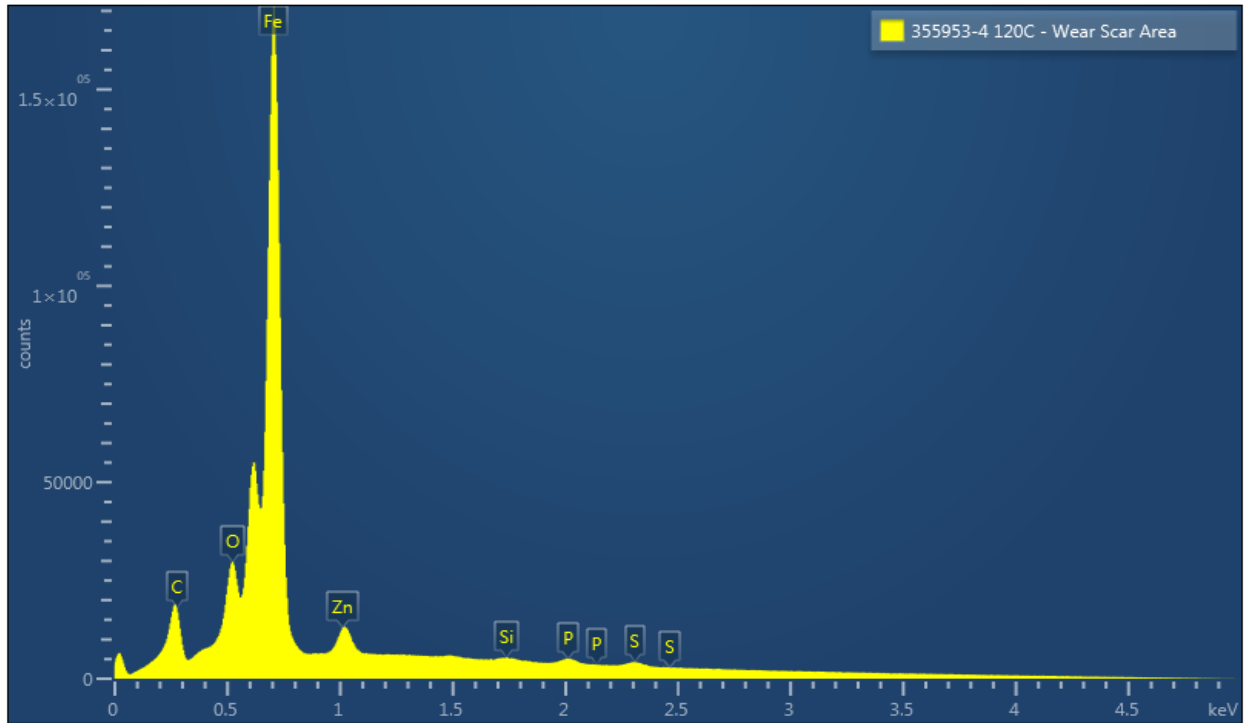


Figure A3- 6 SEM-EDX spectra of ZDDP tribofilm formed in presence of 1.00 wt.% Dispersant C.

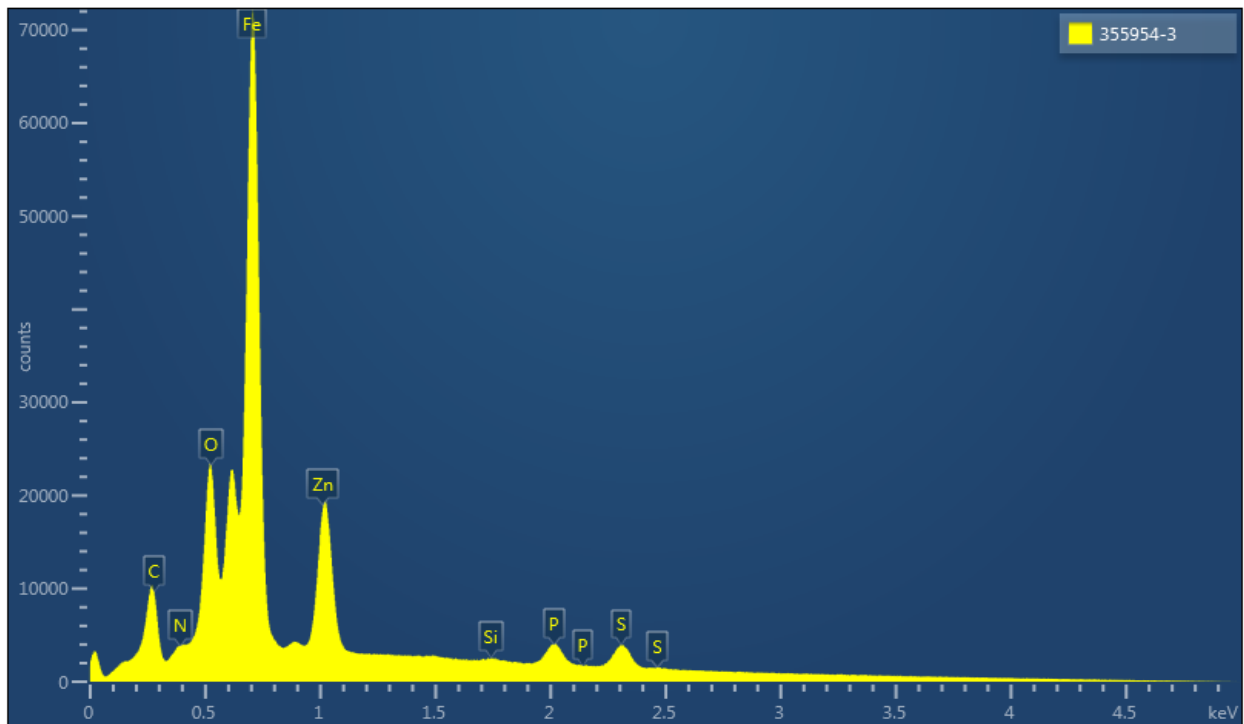


Figure A3- 7 SEM-EDX spectra of ZDDP tribofilm formed in presence of 0.50 wt.% Dispersant C.

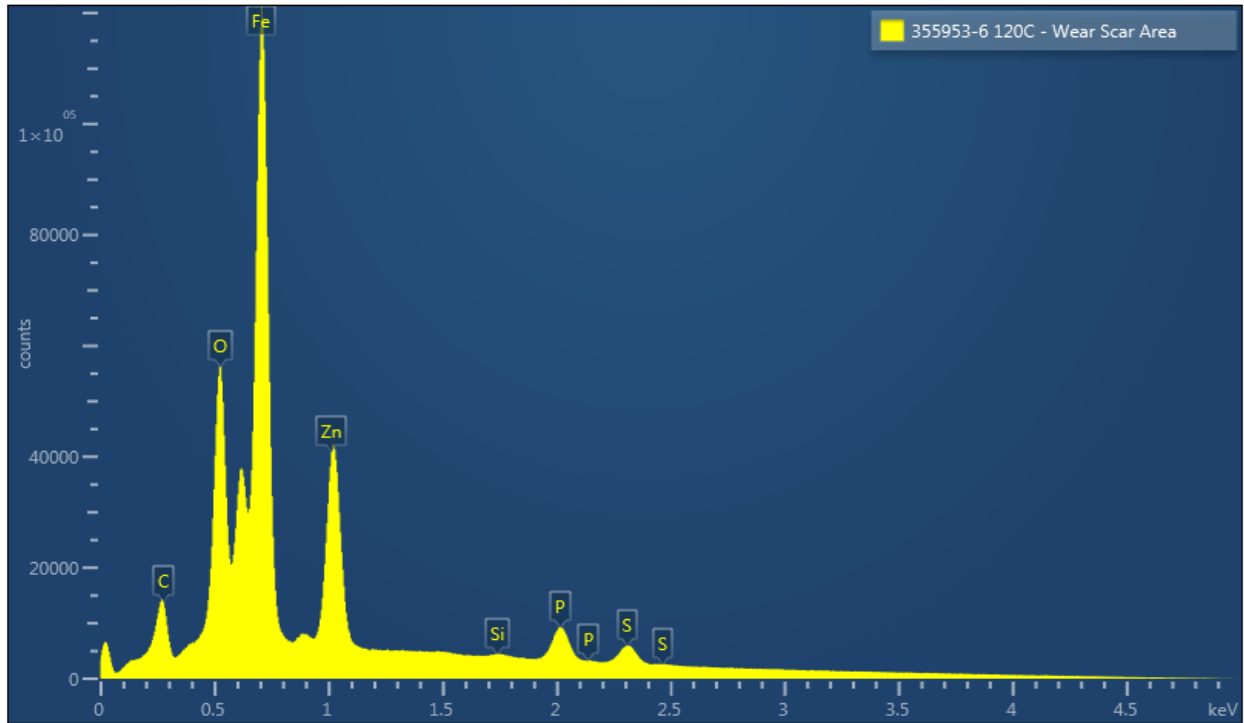


Figure A3- 8 SEM-EDX spectra of ZDDP tribofilm formed in presence of 1.00 wt.% Dispersant D.

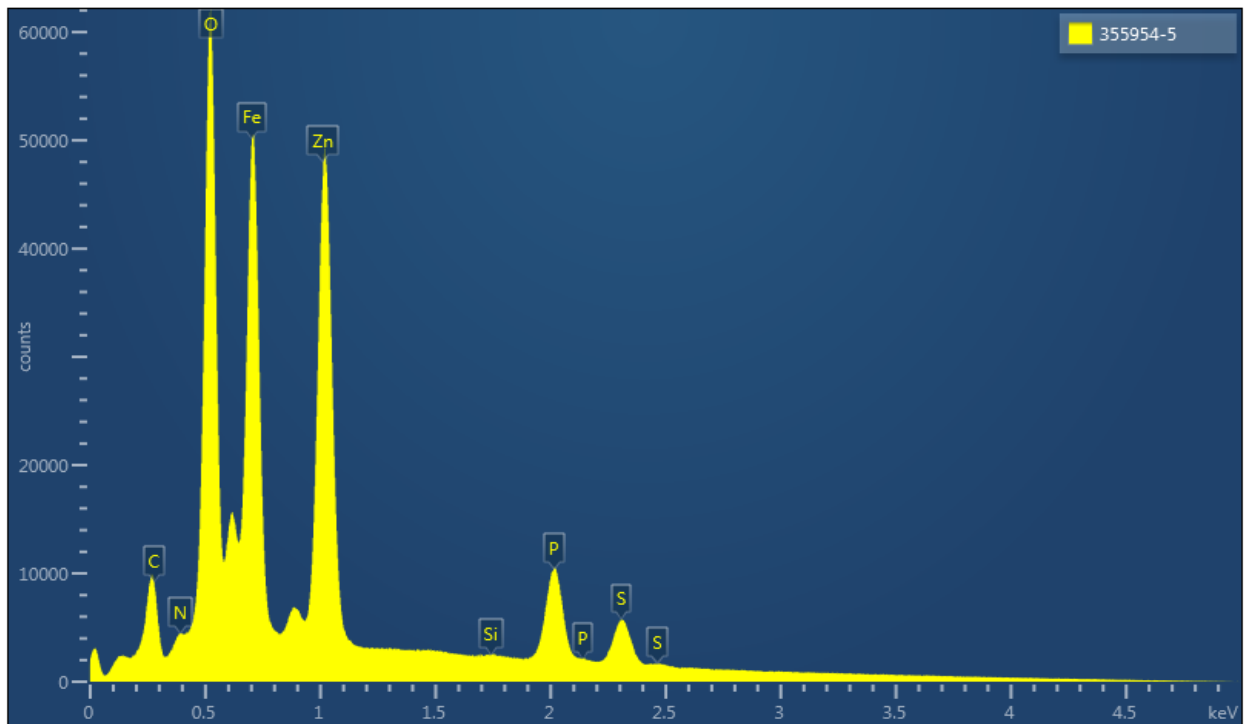


Figure A3- 9 SEM-EDX spectra of ZDDP tribofilm formed in presence of 0.50 wt.% Dispersant D.

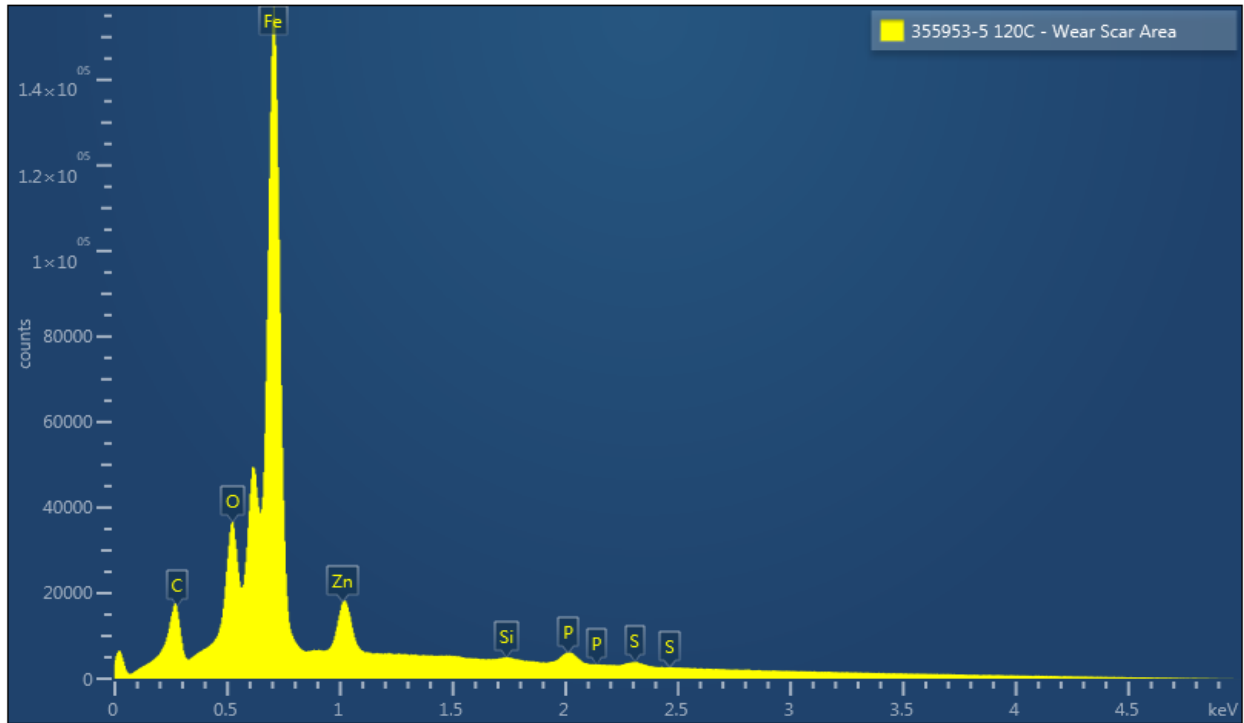


Figure A3- 10 SEM-EDX spectra of ZDDP tribofilm formed in presence of 1.00 wt.% Dispersant E.

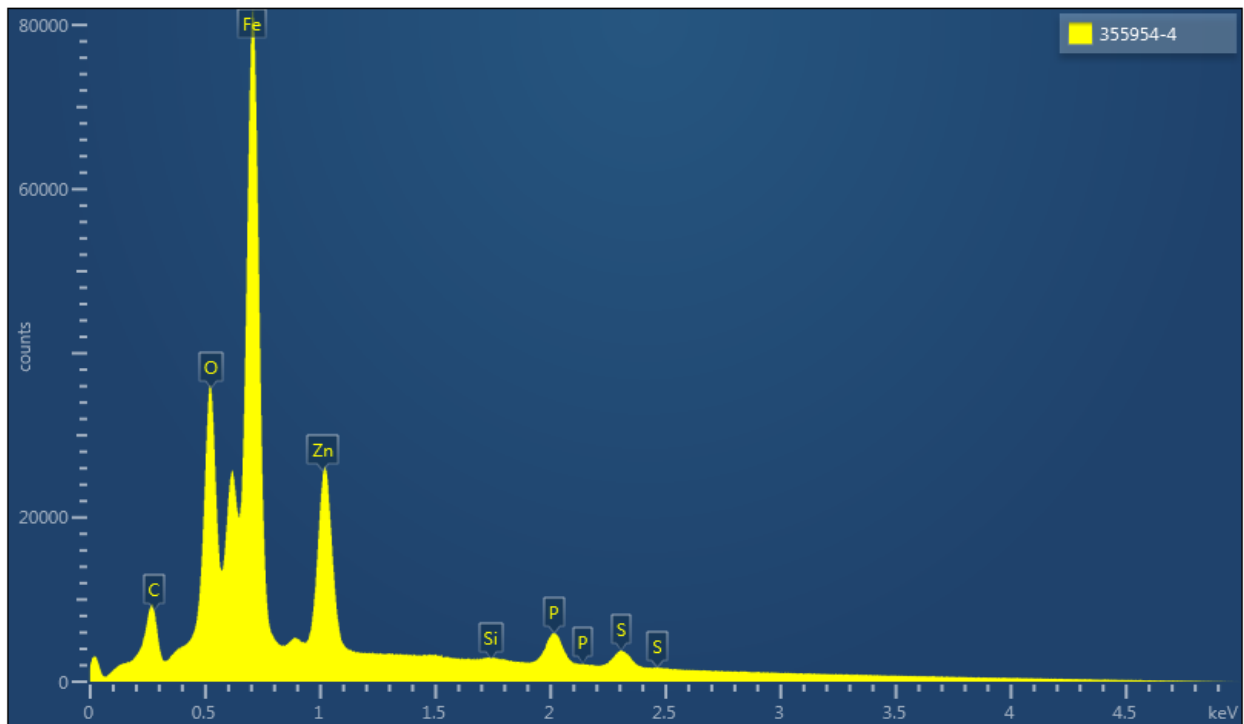


Figure A3- 11 SEM-EDX spectra of ZDDP tribofilm formed in presence of 0.50 wt.% Dispersant E.

Appendix 4

IR spectra of Dispersant A structures polyamide, mixed amide/imide, and imide forms.

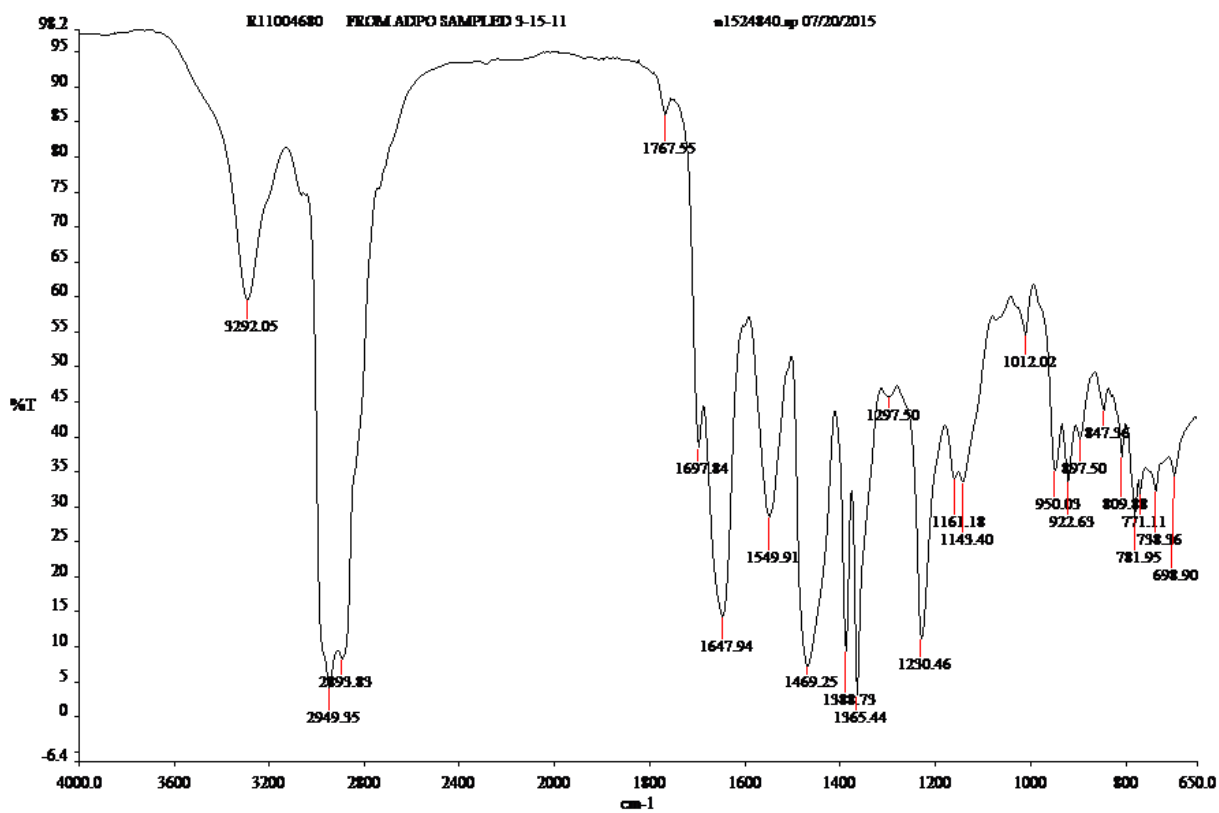


Figure A4 - 1 IR-HATR spectra of Dispersant A polyamide form.

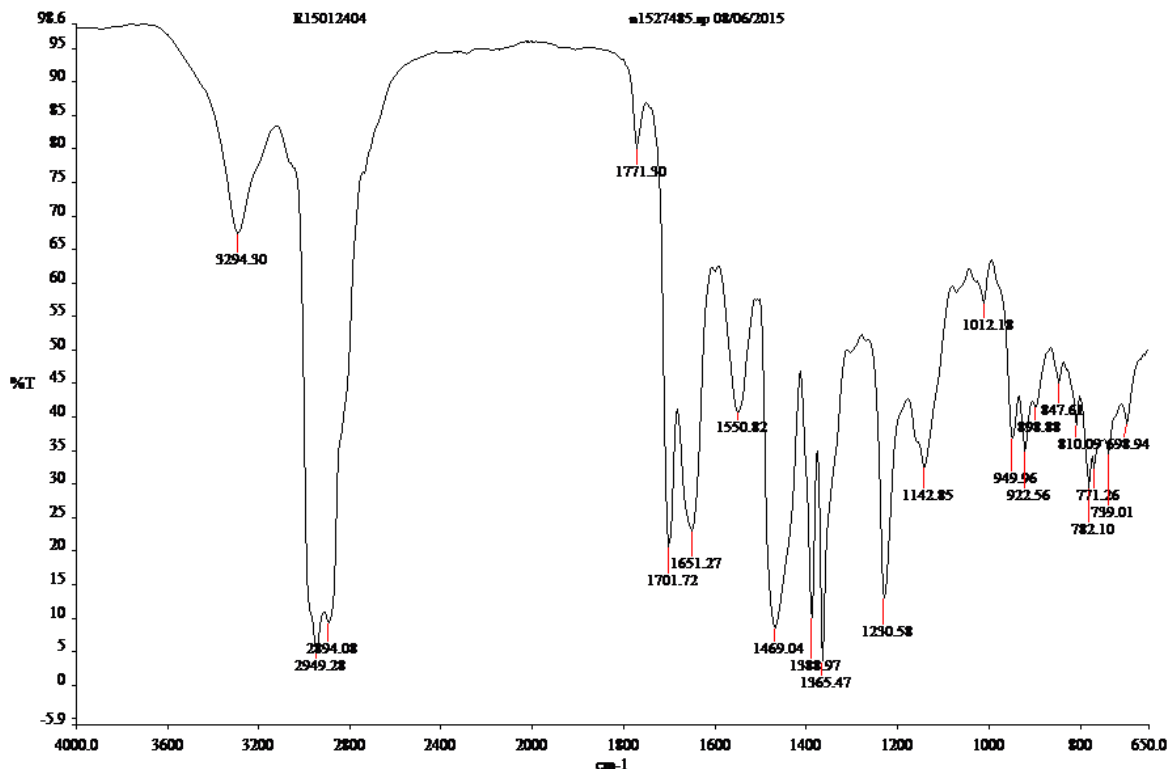


Figure A4 - 2 IR-HATR of Dispersant A mixed polyamide and imide forms.

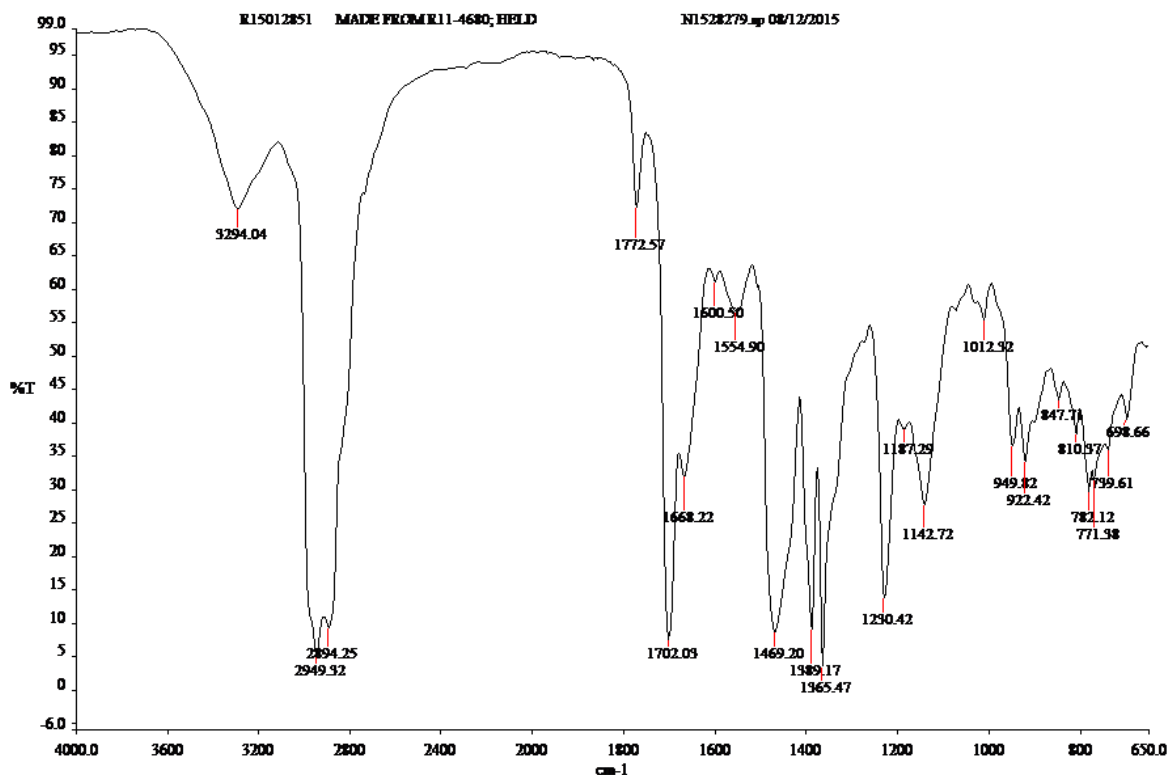


Figure A4 - 3 IR-HATR of Dispersant A imide form.

Appendix 5

³¹P-NMR spectra of ZDDP and dispersant blends in base oil.

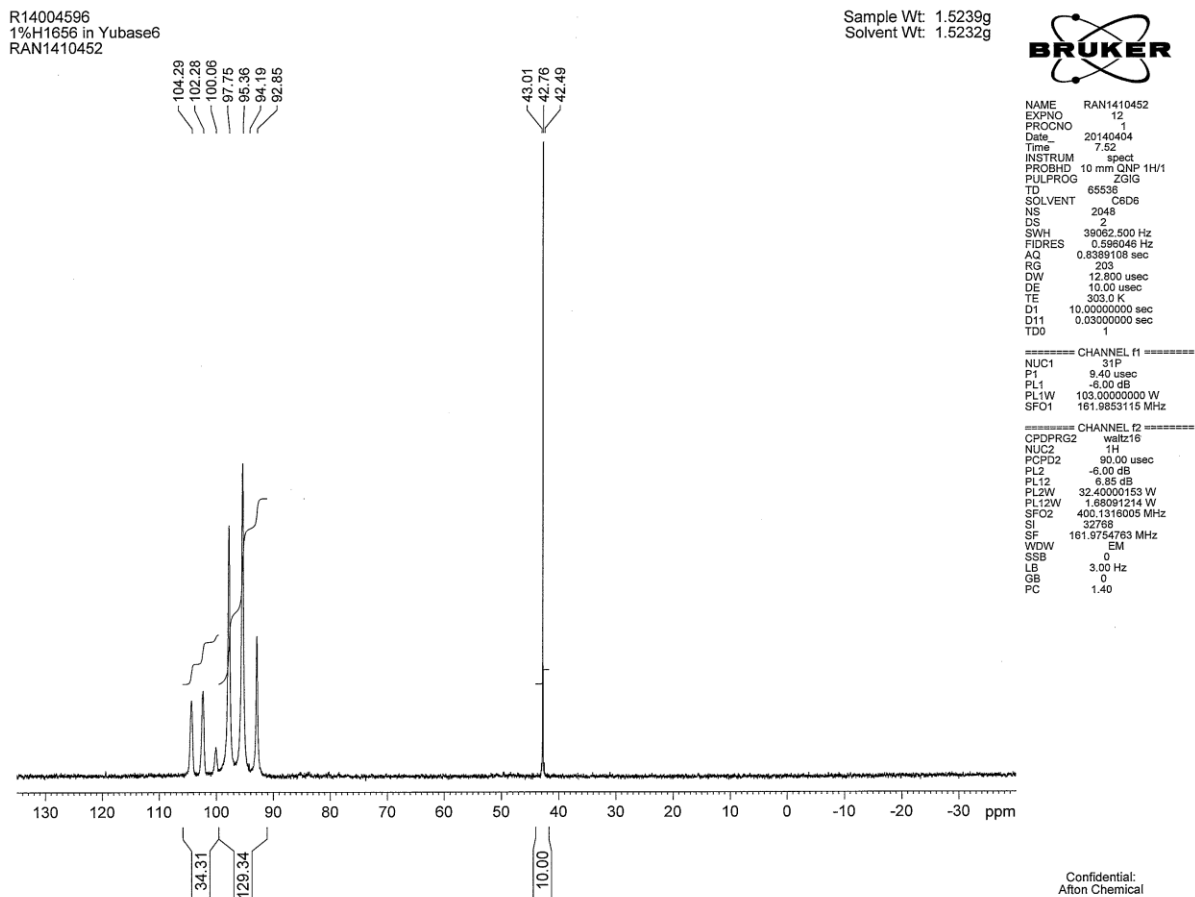
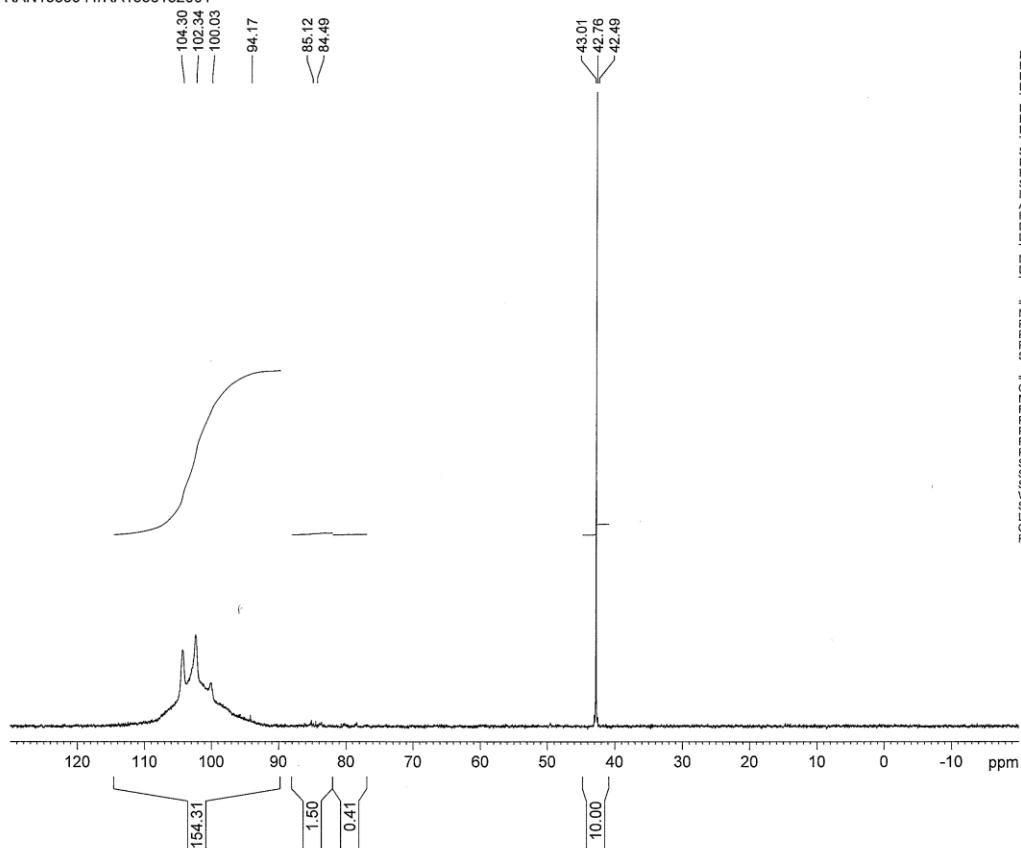


Figure A5 - 1 ³¹P-NMR spectra of 1.00 wt.% ZDDP in base oil.

R15018656
 1% X12888 + 1% H1656 in base oil
 RAN1539941/RA1538132001

Sample Wt: 1.5013g
 Solvent Wt: 1.5002g



```

NAME RAN1539941
EXPNO 12
PROCNO 1
Date_ 20151113
Time 18.44
INSTRUM spect
PROBHD 10 mm QNP 1H/1
PULPROG zgpgv2
TD 65536
SOLVENT C6D6
NS 2048
DS 2
SWH 39062.500 Hz
FIDRES 0.596046 Hz
AQ 0.8389108 sec
RG 203
DW 12.800 usec
DE 10.00 usec
TE 303.0 K
D1 10.00000000 sec
D11 0.03000000 sec
TD0 1

===== CHANNEL f1 =====
NUC1 31P
P1 9.40 usec
PL1 -6.00 dB
PL1W 103.00000000 W
SFO1 161.9853115 MHz

===== CHANNEL f2 =====
CPDPRG2 waltz16
NUC2 1H
PCPD2 90.00 usec
PL2 -6.00 dB
PL12 6.85 dB
PL2W 32.40000153 W
PL12W 1.88091214 W
SFO2 400.1316005 MHz
SI 32768
SF 161.9754785 MHz
WDW EM
SSB 0
LB 3.00 Hz
GB 0
PC 1.40
  
```

Confidential:
 Afton Chemical

Figure A5 - 2 ³¹P-NMR spectra of 1.00 wt.% ZDDP and 1.00 wt.% Dispersant A polyamide in base oil.

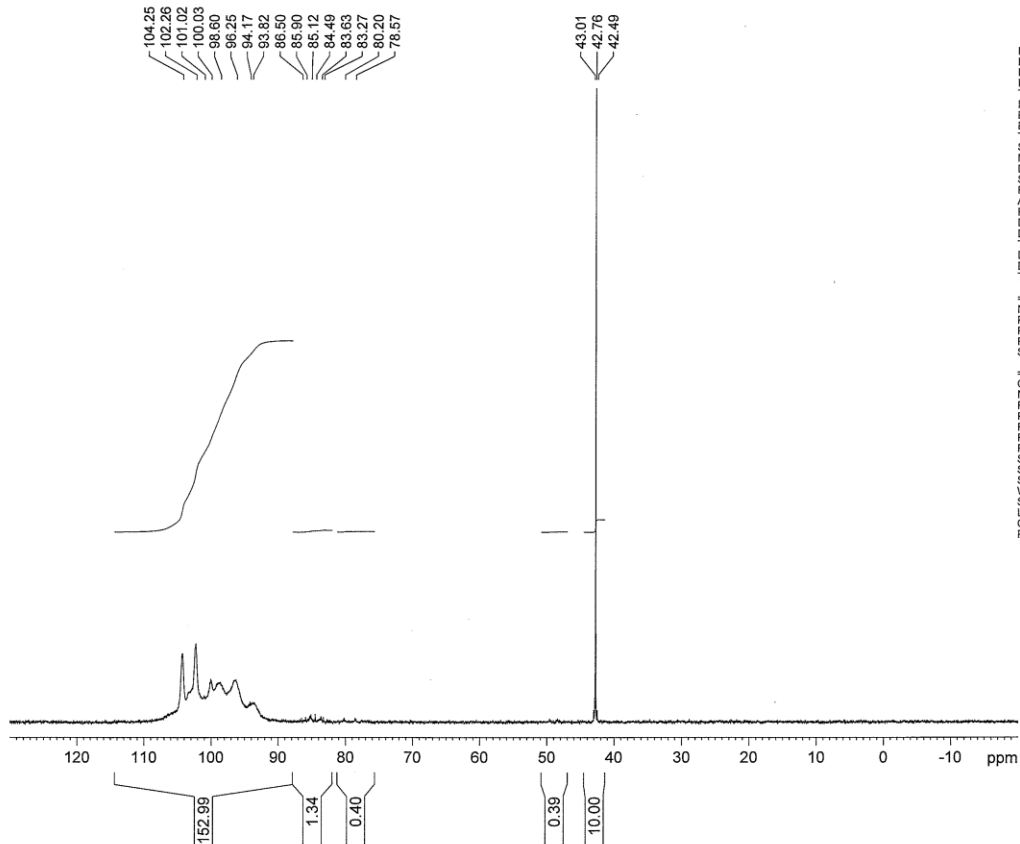
R15018657
 1% D10R + 1% H1656 in base oil
 RAN1539942/RA1538133001

Sample Wt: 1.5103g
 Solvent Wt: 1.5099g



NAME RAN1539942
 EXPNO 12
 PROCNO 1
 Date_ 20151114
 Time 1.00
 INSTRUM spect
 PROBHD 10 mm QNP 1H/1
 PULPROG zgpgv2
 TD 65536
 SOLVENT C6D6
 NS 2048
 DS 2
 SWH 39062.500 Hz
 FIDRES 0.596046 Hz
 AQ 0.8389108 sec
 RG 210
 DW 12.800 usec
 DE 10.00 usec
 TE 303.0 K
 D1 10.00000000 sec
 D11 0.03000000 sec
 TDD 1

===== CHANNEL f1 =====
 NUC1 31P
 P1 9.40 usec
 PL1 -6.00 dB
 PL1W 103.00000000 W
 SFO1 161.9853115 MHz
 ===== CHANNEL f2 =====
 CPDPRG2 waltz16
 NUC2 1H
 PCPD2 90.00 usec
 PL2 -6.00 dB
 PL12 6.85 dB
 PL2W 32.40000153 W
 PL12W 1.68091214 W
 SFO2 400.1316005 MHz
 SI 32768
 SF 161.9754786 MHz
 WDWW EM
 SSB 0
 LB 3.00 Hz
 GB 0
 PC 1.40



Confidential:
 Afton Chemical

Figure A5 - 3 ³¹P-NMR spectra of 1.00 wt.% ZDDP and 1.00 wt.% Dispersant B in base oil.

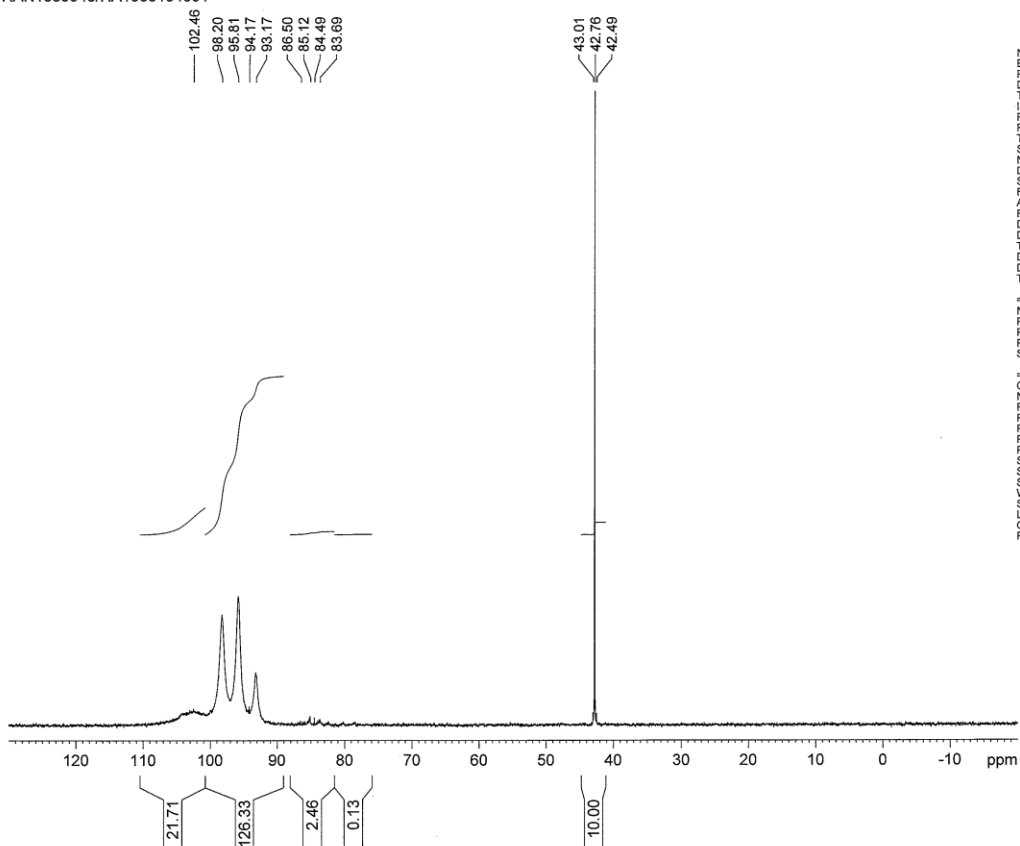
R15018658
 1% H1932X + 1% H1656 in base oil
 RAN1539943/RA1538134001

Sample Wt: 1.5039g
 Solvent Wt: 1.5041g



NAME RAN1539943
 EXPNO 12
 PROCNO 1
 Date 20151114
 Time 7.15
 INSTRUM spect
 PROBHD 10 mm QNP 1H/1
 PULPROG zgpgv2
 TD 65536
 SOLVENT C6D6
 NS 2048
 DS 2
 SWH 39082.500 Hz
 FIDRES 0.596046 Hz
 AQ 0.8389108 sec
 RG 203
 DW 12.800 usec
 DE 10.00 usec
 TE 303.0 K
 D1 10.0000000 sec
 D11 0.0300000 sec
 TDD 1

===== CHANNEL f1 =====
 NUC1 31P
 P1 9.40 usec
 PL1 -6.00 dB
 PL1W 103.00000000 W
 SFO1 161.9853115 MHz
 ===== CHANNEL f2 =====
 CPDPRG2 waltz16
 NUC2 1H
 PCPD2 90.00 usec
 PL2 -6.00 dB
 PL12 6.85 dB
 PL2W 32.40000153 W
 PL12W 1.68091214 W
 SFO2 400.1316005 MHz
 SI 32768
 SF 161.9754784 MHz
 WDW EM
 SSB 0
 LB 3.00 Hz
 GB 0
 PC 1.40



Confidential:
 Afton Chemical

Figure A5 - 4 ³¹P-NMR spectra of 1.00 wt.% ZDDP and 1.00 wt.% Dispersant C in base oil.

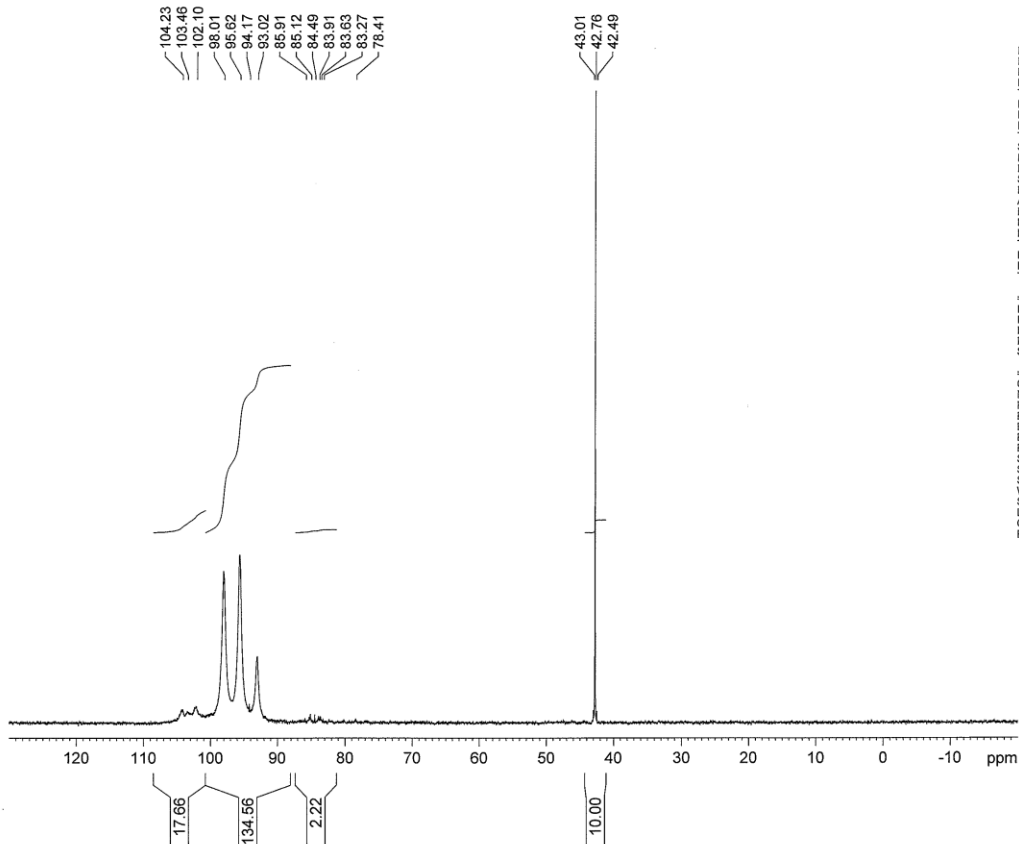
R15018659
 1% X15476 + 1% H1656 in base oil
 RAN1539944/RA1538135001

Sample Wt: 1.5097g
 Solvent Wt: 1.5113g



NAME RAN1539944
 EXPNO 12
 PROCNO 1
 Date_ 20151114
 Time 13.31
 INSTRUM spect
 PROBHD 10 mm QNP 1H/1
 PULPROG zgpgv2
 TD 65536
 SOLVENT C6D6
 NS 2048
 DS 2
 SWH 39082.500 Hz
 FIDRES 0.596046 Hz
 AQ 0.8389108 sec
 RG 203
 DW 12.800 usec
 DE 10.00 usec
 TE 303.0 K
 D1 10.0000000 sec
 D11 0.0300000 sec
 TDD 1

===== CHANNEL f1 =====
 NUC1 31P
 P1 9.40 usec
 PL1 -6.00 dB
 PL1W 103.0000000 W
 SFO1 161.9853115 MHz
 ===== CHANNEL f2 =====
 CPDPRG2 waltz16
 NUC2 1H
 PCPD2 90.00 usec
 PL2 -6.00 dB
 PL12 6.85 dB
 PL2W 32.40000153 W
 PL12W 1.68091214 W
 SFO2 400.1316005 MHz
 SI 32768
 SF 161.9754783 MHz
 WDWW EM
 SSB 0
 LB 3.00 Hz
 GB 0
 PC 1.40



Confidential:
 Afton Chemical

Figure A5 - 5 ³¹P-NMR spectra of 1.00 wt.% ZDDP and 1.00 wt.% Dispersant D in base oil.

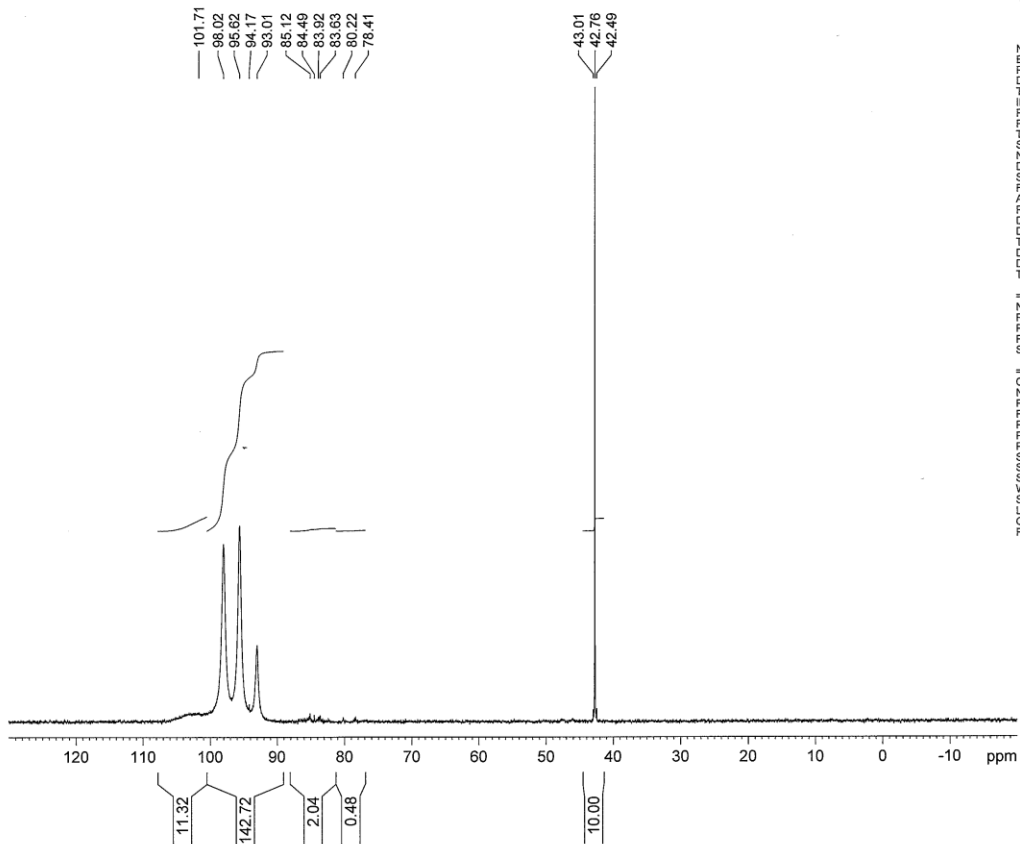
R15018660
 1% PEHA + 1% H1656 in base oil
 RAN1539945/RA1538136001

Sample Wt: 1.5069g
 Solvent Wt: 1.5059g



NAME RAN1539945
 EXPNO 12
 PROCNO 1
 Date_ 20151114
 Time 19.46
 INSTRUM spect
 PROBHD 10 mm QNP 1H/1
 PULPROG zgpgv2
 TD 65536
 SOLVENT C6D6
 NS 2048
 DS 2
 SWH 39082.500 Hz
 FIDRES 0.596046 Hz
 AQ 0.8389108 sec
 RG 203
 DW 12.800 usec
 DE 10.00 usec
 TE 303.0 K
 D1 10.0000000 sec
 D11 0.0300000 sec
 TDD 1

===== CHANNEL f1 =====
 NUC1 31P
 P1 9.40 usec
 PL1 -6.00 dB
 PL1W 103.0000000 W
 SFO1 161.9853115 MHz
 ===== CHANNEL f2 =====
 CPDPRG2 waltz16
 NUC2 1H
 PCPD2 90.00 usec
 PL2 -6.00 dB
 PL12 6.85 dB
 PL2W 32.40000153 W
 PL12W 1.68091214 W
 SFO2 400.1316005 MHz
 SI 32768
 SF 161.9754782 MHz
 WDWW EM
 SSB 0
 LB 3.00 Hz
 GB 0
 PC 1.40



Confidential:
 Afton Chemical

Figure A5 - 6 ³¹P-NMR spectra of 1.00 wt.% ZDDP and 1.00 wt.% Dispersant E in base oil.

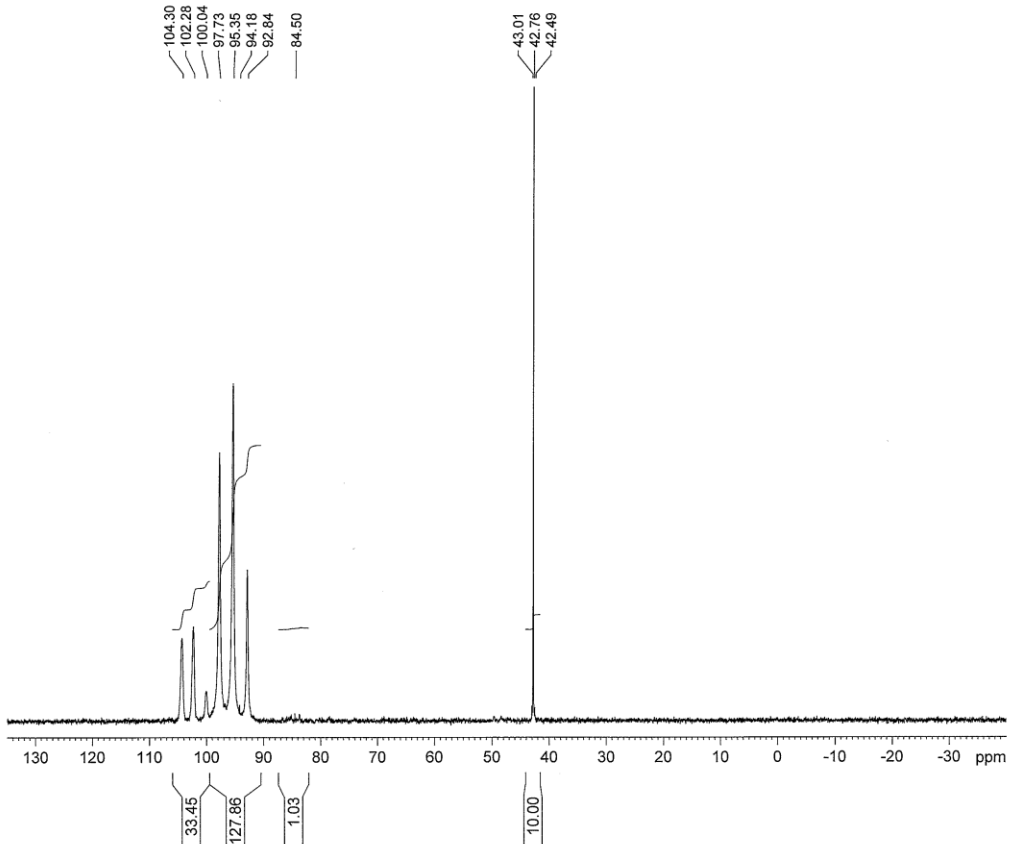
R14004597
 1%H1656 + 1%PIB in Yubase6
 RAN1410453

Sample Wt: 1.6597g
 Solvent Wt: 1.6591g



NAME RAN1410453
 EXPNO 12
 PROCNO 1
 Date_ 20140404
 Time 14.08
 INSTRUM spect
 PROBHD 10 mm QNP 1H/1
 PULPROG zgpg30
 TD 65536
 SOLVENT CRD6
 NS 2048
 DS 2
 SWH 39062.500 Hz
 FIDRES 0.596046 Hz
 AQ 0.8389108 sec
 RG 203
 DW 12.800 usec
 DE 10.00 usec
 TE 303.0 K
 D1 10.00000000 sec
 D11 0.03000000 sec
 TDD 1

===== CHANNEL f1 =====
 NUC1 31P
 P1 9.40 usec
 PL1 -6.00 dB
 PL1W 103.00000000 W
 SFO1 161.9853115 MHz
 ===== CHANNEL f2 =====
 CPDPRG2 waltz16
 NUC2 1H
 PCPD2 90.00 usec
 PL2 -6.00 dB
 PL12 6.85 dB
 PL2W 32.4000153 W
 PL12W 1.68081214 W
 SFO2 400.1316005 MHz
 SI 32768
 SF 161.9754770 MHz
 WDW EM
 SSB 0
 LB 3.00 Hz
 GB 0
 PC 1.40

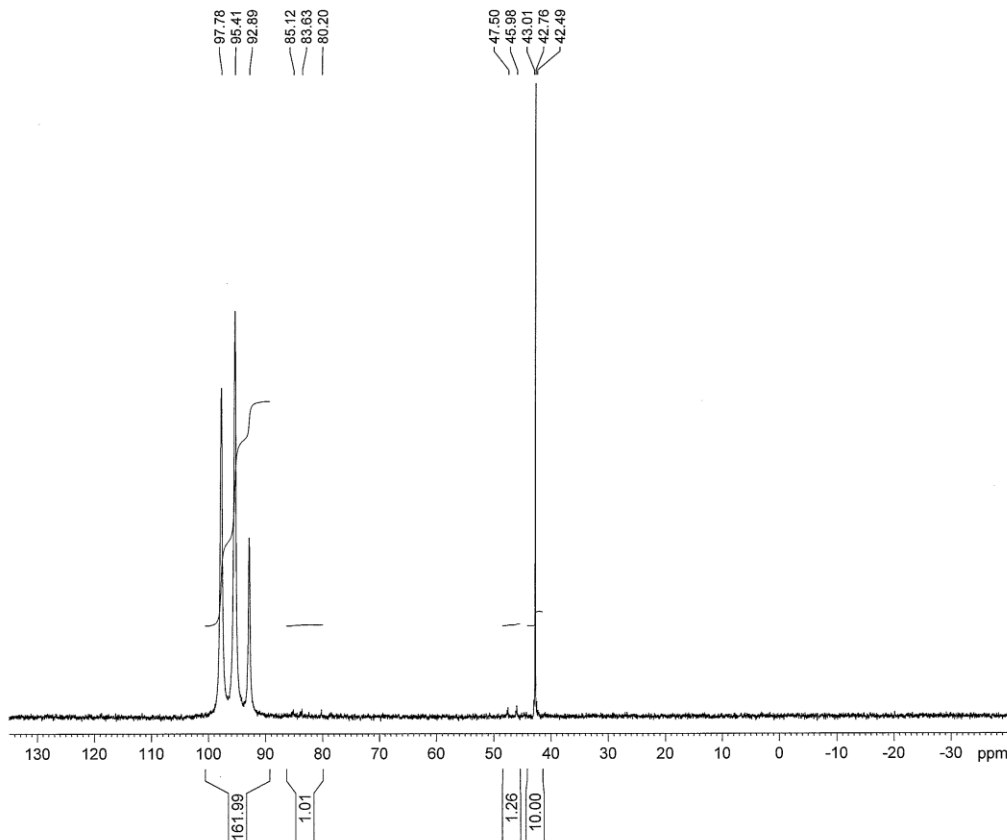


Confidential:
 Afton Chemical

Figure A5 - 7 ³¹P-NMR spectra of 1.00 wt.% ZDDP and 1.00 wt.% PIB in base oil.

R14004598
 1%H1656 + 1%PIBSA in Yubase6
 RAN1410454

Sample Wt: 1.5955g
 Solvent Wt: 1.5980g



```

NAME RAN1410454
EXPNO 12
PROCNO 1
Date_ 20140404
Time 20.24
INSTRUM spect
PROBHD 10 mm QNP 1H/1
PULPROG zgpg30
TD 65536
SOLVENT CRD6
NS 2048
DS 2
SWH 39062.500 Hz
FIDRES 0.598046 Hz
AQ 0.8389108 sec
RG 203
DW 12.800 usec
DE 10.00 usec
TE 303.0 K
D1 10.00000000 sec
D11 0.03000000 sec
TD0 1

===== CHANNEL f1 =====
NUC1 31P
P1 9.40 usec
PL1 -6.00 dB
PL1W 103.00000000 W
SFO1 161.9853115 MHz

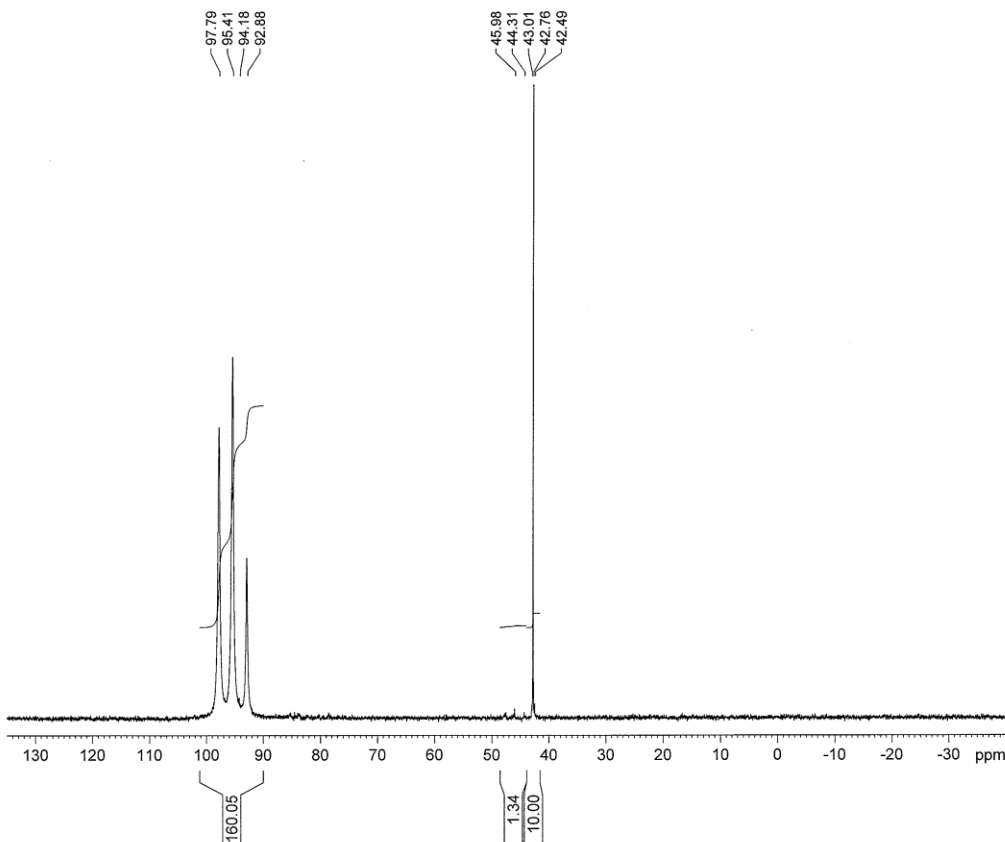
===== CHANNEL f2 =====
CPDPRG2 waltz16
NUC2 1H
PCPD2 60.00 usec
PL2 -6.00 dB
PL12 6.85 dB
PL2W 32.40000153 W
PL12W 1.68091214 W
SFO2 400.1316005 MHz
SI 32768
SF 161.9754776 MHz
WDW EM
SSB 0
LB 3.00 Hz
GB 0
PC 1.40
  
```

Confidential.
 Afton Chemical

Figure A5 - 8 ³¹P-NMR spectra of 1.00 wt.% ZDDP and 1.00 wt.% PIBSA in base oil.

R14004599
 1%H1656 + 1%PIBSdiacid in Yubase6
 RAN1410455

Sample Wt: 1.6278g
 Solvent Wt: 1.6277g



```

NAME RAN1410455
EXPNO 12
PROCNO 1
Date_ 20140405
Time 2.40
INSTRUM spect
PROBHD 10 mm QNP 1H/1
PULPROG zgpg30
TD 65536
SOLVENT CRD6
NS 2048
DS 2
SWH 39062.500 Hz
FIDRES 0.596046 Hz
AQ 0.8389108 sec
RG 203
DW 12.800 usec
DE 10.00 usec
TE 303.0 K
D1 10.00000000 sec
D11 0.03000000 sec
TDO 1

===== CHANNEL f1 =====
NUC1 31P
P1 9.40 usec
PL1 -6.00 dB
PL1W 103.00000000 W
SFO1 161.9853115 MHz

===== CHANNEL f2 =====
CPDPRG2 waltz16
NUC2 1H
PCPD2 60.00 usec
PL2 -6.00 dB
PL2 6.85 dB
PL2W 32.4000153 W
PL12W 1.68091214 W
SFO2 400.1316005 MHz
SI 32768
SF 161.9754774 MHz
WDW EM
SSB 0
LB 3.00 Hz
GB 0
PC 1.40
  
```

Confidential:
 Afton Chemical

Figure A5 - 9 ³¹P-NMR spectra of 1.00 wt.% ZDDP and 1.00 wt.% PIB di-acid in base oil.

Appendix 6

Investigation of PIBSA effects on changing ZDDP structures. ZDDP's were blended at 1.00 wt.% with 0.50 wt.% in base oil and tested in the MTM-SLIM under standard operating conditions over one hour. ZDDPs A and C were primary ZDDPs, ZDDP B was the mixed ZDDP used in testing for our project, and ZDDP D was a secondary ZDDP.

